North West Shelf Ocean Bottom Seismometer Data Processing Report: AGSO Survey 168, Line 4, Petrel Sub-Basin

by

P. Petkovic and T. Fomin

AGSO Record 1997/47

AGSO

AUSTRALIAN GEOLOGICAL SURVEY ORGANISATION

North West Shelf

Ocean Bottom Seismometer Data Processing Report:

AGSO Survey 168, Line 4,

Petrel Sub-Basin

by

P. Petkovic and T. Fomin

Record 1997/47

October 1997

DEPARTMENT OF PRIMARY INDUSTRIES AND ENERGY

Minister for Primary Industries and Energy: Hon. J. Anderson, M.P.
Minister for Resources and Energy: Senator the Hon. W.R. Parer
Secretary: Paul Barratt

AUSTRALIAN GEOLOGICAL SURVEY ORGANISATION

Executive Director: Neil Williams

ISSN: 1039-0073
ISBN: 0 642 27312 1

Contents

Figures

Tables

Objectives of the Refraction Programme

AGSO's regional deep crustal reflection seismic programme over the North West Shelf (1990-present) has provided researchers with excellent quality data for interpretation of basin history and structure. To add velocity control to these data, in order to resolve questions relating to margin evolution, AGSO conducted a refraction survey (Survey168) on the North West Shelf with the following objectives:

- obtain P-wave velocities along five transects representing the major structural elements of the Shelf, so that depth conversion of the reflection profiles can be better constrained,

- identify the base of the sedimentary section, particularly in the deepest section where this cannot be identified in the reflection profiles,

- identify major intra-crustal boundaries, and particularly the crust-mantle boundary so that changes in crustal thickness can be mapped,

- provide detailed velocities within certain key features along the transects where this will allow better identification, such as the presence of volcanics,

- record S-wave velocities which will be used to better identify the petrology, and

- by using onshore recorders as well as the OBSs, link the offshore crustal structure with the onshore structure.

To address these objectives RV *Rig Seismic* was used to acquire refraction and other geophysical data during December 1995 and January 1996. A total of 2827 km of data were acquired along five separate transects across the entire North West Shelf region. All transects coincided with previously shot deep crustal reflection profiles. Table 1 lists the correspondence between Survey 168 line name and the previously shot reflection line name.

Figure 1 and Figure 2 show the location of Lines 168/401 and 168/501 refraction recording stations, on a background of the AGSO deep crustal seismic grid.

Ninety one ocean-bottom seismometers (OBS) were deployed and successfully retrieved during the 37 days of surveying. In addition, 16 land recording stations were deployed during the course of the survey (Lukaszyk and Soames, in prep.).

Table 1 - Correspondence between Survey 168 and earlier reflection line names

Survey 168 Line	Length (km)	Number of Stations	Reflection Line	Area
168/101	240.0	7	128/08 (1994)	Carnarvon Basin
168/102	230.5	5	128/08 (1994)	Carnarvon Basin
168/103	274.1	10	101/10 (1991)	Carnarvon Basin
168/201	340.8	12	120/01 (1993)	Canning Basin
168/202A	95.3	2	120/02 (1993)	Canning Basin
168/202B	57.1	0	-	
168/202C	236.8	9	120/01 (1993)	Canning Basin
168/301	314.9	8	128/01 (1994)	Browse Basin
168/302	352.6	13	119/06 (1993)	Browse Basin
168/401	348.5	15	100/03 (1991)	Petrel Sub-basin
168/501	336.1	10	98/03 (1990)	Vulcan Sub-basin
Total	2826.7	91		

Figure 1 - Lines 168/401, 501

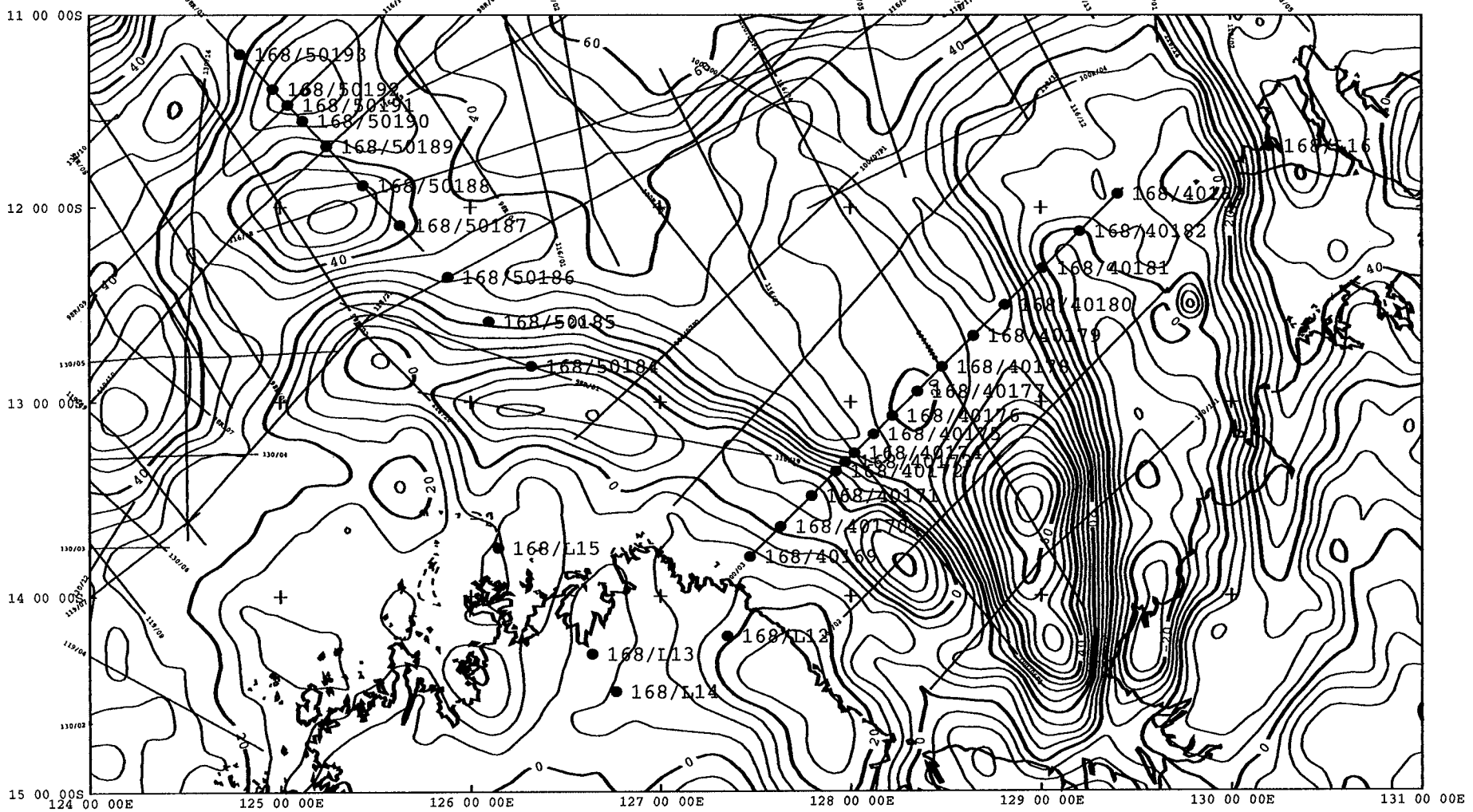

MERCATOR PROJECTION
AUSTRALIAN NATIONAL SPHEROID
EQUATORIAL ORIGIN OF TRUE SCALE. CENTRAL MERIDIAN 127 30 00E

AGSO deep seismic lines from surveys 98,100,116,118,122
OBS locations shown along lines 98/03 and 100/03

Bouguer anomaly contour interval 5 mgal

Figure 2 - Lines 168/401, 501

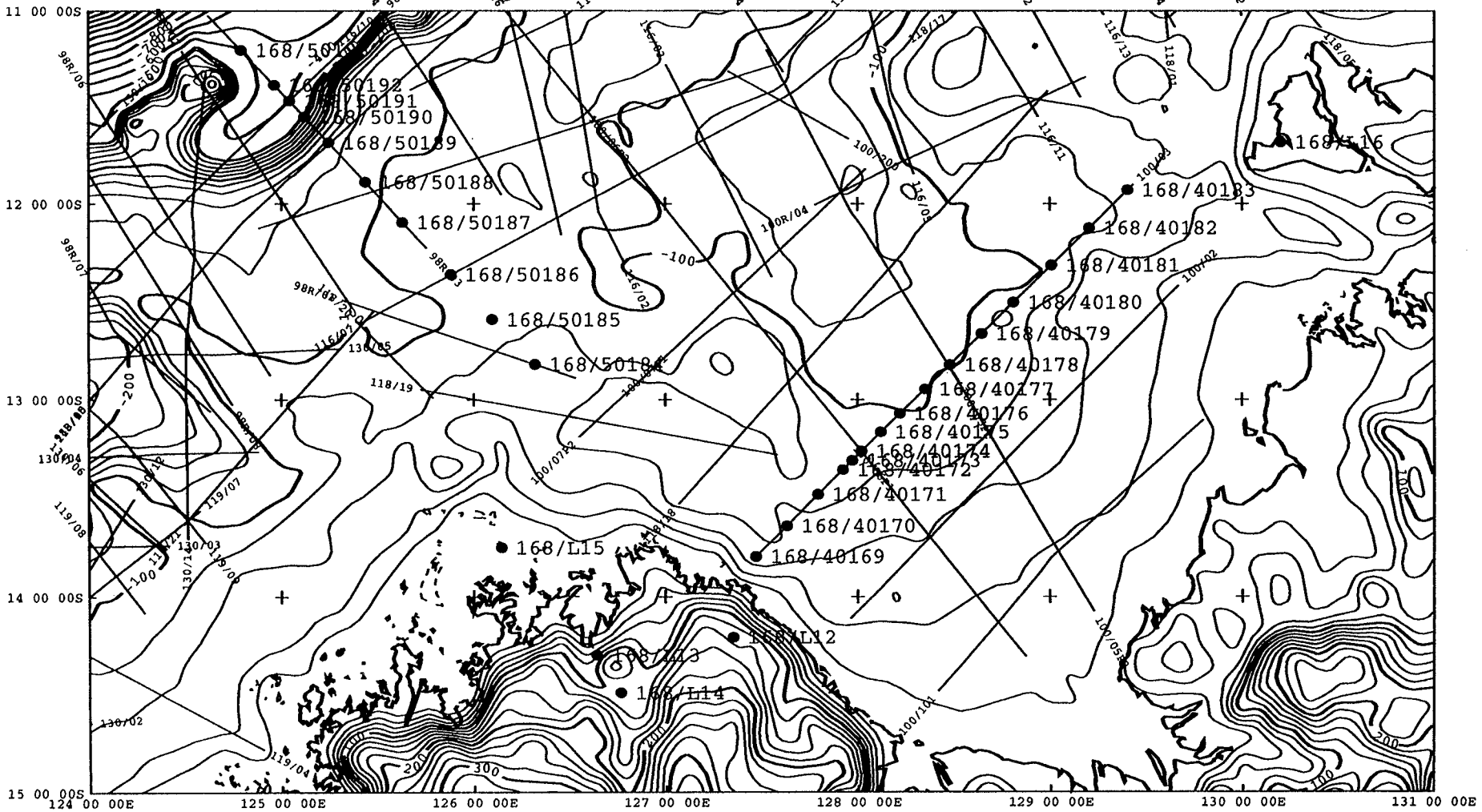

0 40 80 120 160 200

KILOMETRES

MERCATOR PROJECTION
AUSTRALIAN NATIONAL SPHEROID
EQUATORIAL ORIGIN OF TRUE SCALE. CENTRAL MERIDIAN 127 30 00E

AGSO deep seismic lines from surveys 98,100,116,118,122
OBS locations shown along lines 98/03 and 100/03
Topography contour interval 20m

Data Acquisition

For a detailed account of the acquisition, see Collins and Lee (in prep.). This report gives information on the Ocean Bottom Seismometer (OBS) construction, its method of deployment and retrieval, and the onshore seismic recorders.

Seismic Configuration and Recording Parameters

The seismic source was *Rig Seismic*'s entire thirty-two sleeve air gun array (4800 in^3 and 2000 psi air pressure). Shot spacing was 100m. A single channel streamer was towed for water depth control. Data were recorded continuously by OBS units manufactured by the University of Texas Institute for Geophysics (UTIG) and National Taiwan Ocean University (NTOU). These units had 3 internal geophones recording horizontal and vertical components, and the UTIG units also had an external hydrophone.

Non-seismic Data

Navigation was by differential GPS, and measurements of the Earth's gravity field and the depth of water, were carried out simultaneously.

Navigation data were of high quality, with the primary dGPS navigation system being used more than 95% of the time for all lines. The accuracy of the positions was better than 5 m (See Table 2). Gravity and water depth data are good quality for the duration of the survey.

Table 2 - Summary of the inter-shot distance variations

	first shot	last shot	shots	± 2%	± 5%	± 10%	SD
				(%)	(%)	(%)	(m)
whole			28225	12.0	1.3	0.5	
L101	100	2501	2402	23.2	2.5	0.5	2.7
L102	100	2395	2296	17.1	1.7	1.0	3.2
L103	100	2835	2736	10.4	2.7	1.7	4.8
L201	102	3505	3404	8.2	0.6	0.1	1.3
L202A	100	1054	955	7.3	0.0	0.0	1.2
L202B	1155	1724	570	6.2	0.4	0.2	1.8
L202C	3318	5674	2357	15.7	3.7	1.8	2.7
L301	100	3248	3149	6.7	0.0	0.0	1.0
L303	100	3626	3527	15.8	0.8	0.2	1.6
L401	100	3581	3482	9.0	0.9	0.3	1.4
L501	100	3456	3357	8.8	0.6	0.0	1.3

The 2% column gives the percentage of shots where the intershot distance was +/- 2% of the nominal distance of 100 m. For example, for Line 202C, 1.8% of shots were between 90 and 110 m from the previous shot.

The SD column is the standard deviation of the inter-shot distances from the nominal distance of 100m for each line.

Refraction Data

The refraction data are of variable quality, being subject to several types of noise of unresolved origins. The Petrel data are generally of good quality in the central OBS units, while the units on the flanks of the line have poor data recovery. The data have been processed using bandpass filter and gain control to enhance arrivals. F-K filtering has been moderately successful in resolving signal buried in noise (See section on F-K filtering later in this report).

Water Temperature Measurements

A water temperature recorder was included inside the sphere of some of the OBS units, in order to measure the operating temperatures, which have a direct bearing on instrument clock drift. Table 3 is a list of the instruments for which the bottom temperature was recorded, and these data are depicted graphically in Figure 3 and Figure 4.

Table 3 - Operating temperature inside the OBS

OBS	Depth (m)	Temperature (° C)
3	4723	1.1
7	1850	2.7
14	1105	4.6 to 5.0
22	43	26.3
30	156	20.6 to 21.3
34	1246	3.9 to 4.3
42	5685	1.1 to 1.5
53	2418	1.5 to 2.3
63	91	22.7 to 23.4
71	72	22.0 to 27.7
76	99	26.6 to 27.0
88	103	24.5 to 24.8
93	382	9.1 to 9.5

Figure 3 - Temperature vs Water Depth

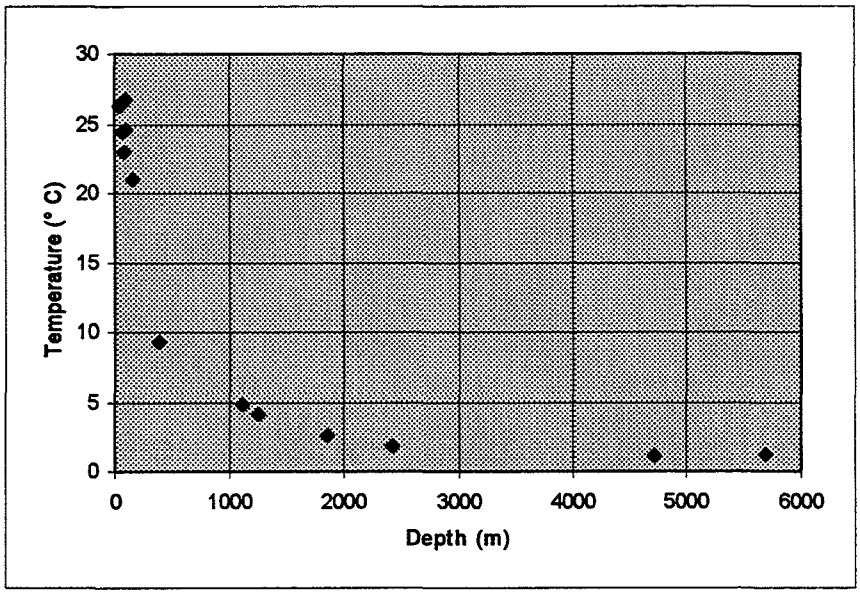

Figure 4 - Temperature vs Water Depth

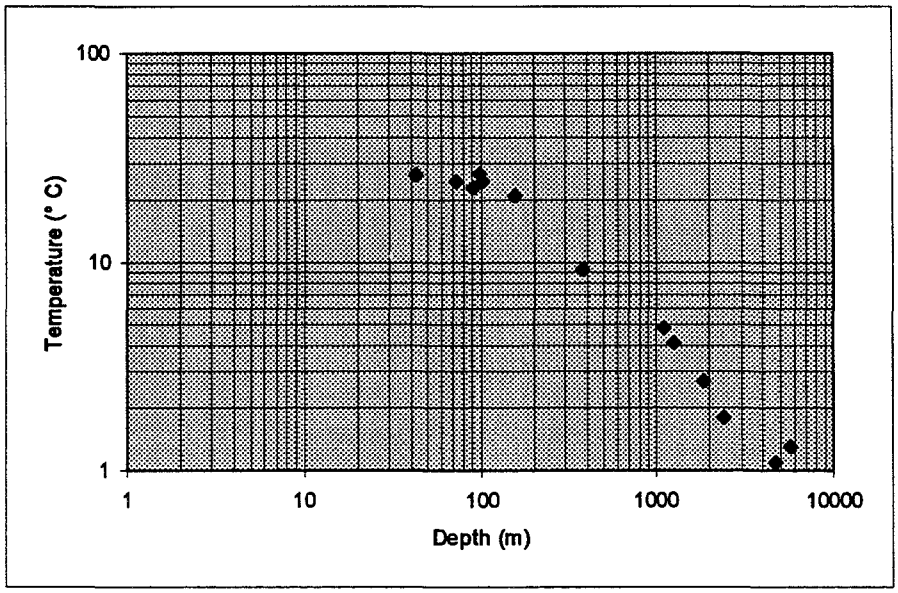

Processing to SEG-Y Stage

Stage one of the data processing takes the data file as recorded in the OBS to a standard SEG-Y format. The software used for this purpose is OBSTOOL, developed specifically for processing these type of data. See Christeson (1995) for a detailed description of the processing scheme. OBSTOOL presents a graphical user interface on a Unix platform, and allows the user to run a series of programs which perform various tasks, described below. Various input data are required, and these are contained in Floppy disks 1 to 3, included as **Error! Reference source not found.** with this report. The disk contents are:

'Nakamura' format shot times (shottm.*),
AGSO UKOOA format navigation file (*.uko),
OBSTOOL format navigation files for each line (*.nav),
OBS clock calibration files (cc.*)

Essentially, the stages are as follows:

Data Entry

Navigation Data

Prepare a shot file consisting of shot time, position and bathymetry, in OBSTOOL specified format (Christeson, 1995, p1). Program MERT (Appendix 1) is used for this purpose. In the following descriptions, LLL signifies the line number, 101, 102, and so on.

Program: mert

Input	shottm.LLL	s168uks.asc
Output	LLL.nav	

shottm.LLL

This is the 'Nakamura' format shot times file, in *local time*:

```
014:11:53:42.984013700
014:11:54:10.974063300
014:11:54:38.943976200
014:11:55:06.673785400
014:11:55:34.963679900
014:11:56:03.113624700
```

which are Julian day:hour:minute:second

s168uks.asc

This is the AGSO UKOOA format file containing the position for each shot. See Appendix 2 for format description.

LLL.nav

This is the OBSTOOL format shot file:

A	B	C	D	E	F	G	H	I
118	96	14	20	15	19.970	-11.684222	129.649075	59
119	96	14	20	15	48.390	-11.684836	129.648400	60
120	96	14	20	16	16.550	-11.685450	129.647742	61
121	96	14	20	16	45.240	-11.686128	129.647122	61
122	96	14	20	17	13.360	-11.686803	129.646514	60
123	96	14	20	17	42.270	-11.687458	129.645867	61
124	96	14	20	18	10.360	-11.688114	129.645242	61

Where:
A - shot number
B - year
C - Julian day
D - hour
E - minute
F - second
G - latitude
H - longitude
I - water depth

and time is *local time*.

Clock Calibration Data

Have available the OBS clock calibration files (cc.xx) . An example follows:

OBS Time	GPS Time
T779601111312001	011:05:12:00.213545300
T779601111313001	011:05:13:00.213804900
T779601111314001	011:05:14:00.214060200
T779601112315001	011:15:15:00.364207500
T779601112316001	011:15:16:00.364455000

where the last record indicates:

	OBS Time (Local)	GPS Time (GMT)	
T77	time record for station 77		
96	year		
01	month		
11	day	011	Julian day
23	hour	15	hour
16	minute	16	minute
001	tenths of second	00.364455	second

Deployment Data

Have available the time intervals over which acquisition took place (Table 4), OBS deployment location (Table 5), water depth (Table 5), and water velocity. The water depths in Table 5 assume a speed of sound in sea water of 1500 m/s.

Table 4 - OBS Recording intervals (Local Time)

Line	Start	End
168/101	20 08:00:00	21 08:00:00
168/102	22 19:30:00	23 16:30:00
168/103	25 17:00:00	26 19:00:00
168/201	30 09:00:00	31 15:30:00
168/202C	02 15:30:00	04 01:00:00
168/202A	02 15:30:00	04 01:00:00
168/301	06 19:30:00	07 22:30:00
168/302	09 20:00:00	11 04:00:00
168/401	14 20:00:00	16 02:30:00
168/501	18 22:00:00	20 04:00:00

Table 5 - OBS Deployment Locations

Traverse Number	Shot Number	OBS Number	CPU	LatD	LatM	LonD	LonM	Water Depth (m)	Coincident Reflection Traverse	Shot Number
168/100	2501	EOL101		-17	05.151	111	45.379	-4838		
168/101	2201	01	698	-17	13.291	111	59.997	-4968	128/08	1000
168/101	1801	02	717	-17	24.158	112	19.581	-4790	128/08	1800
168/101	1486	03	750	-17	32.707	112	34.977	-4723	128/08	2400
168/101	1100	04	751	-17	43.167	112	53.843	-3483	128/08	3200
168/101	810	05	752	-17	50.603	113	07.449	-2306	128/08	3780
168/101	711	06	753	-17	53.679	113	12.904	-1804	128/08	4200
168/101	600	07	754	-17	56.714	113	18.366	-1850	128/08	4600
168/101	100	SOL101		-18	10.301	113	42.899	-1758		
168/102	2403	EOL102		-18	00.757	113	25.640	-1840		
168/102	2151	08	755	-18	07.527	113	37.983	-1818	128/08	5000
168/102	1750	09	756	-18	18.471	113	57.638	-1549	128/08	5800
168/102	1351	10	757	-18	29.311	114	17.315	-1428	128/08	6600
168/102	951	11	769	-18	40.160	114	37.026	-1745	128/08	7400
168/102	550	12	759	-18	51.191	114	56.735	-1734	128/08	8200
168/102	100	SOL102		-19	03.233	115	18.947	-1456		
168/103	2841	EOL103		-18	22.078	115	26.800	-1622		
168/103	2539	13	760	-18	34.241	115	38.332	-1497	101/10	-
168/103	2237	14	761	-18	46.495	115	49.641	-1105	101/10	-
168/103	1932	15	762	-18	58.572	116	01.509	-411	101/10	3550
168/103	1705	16	698	-19	07.813	116	10.160	-298	101/10	3100
168/103	1396	17	717	-19	20.048	116	22.170	-147	101/10	2500
168/103	1441	18	750	-19	31.722	116	34.252	-80	101/10	1900
168/103	1289	19	751	-19	37.401	116	40.592	-54	101/10	1600
168/103	798	20	752	-19	42.657	116	46.641	-64	101/10	1300
168/103	501	21	753	-19	53.352	116	59.346	-62	101/10	700
168/103	203	22	754	-20	04.299	117	11.946	-43	101/10	103
168/103	100	SOL103		-20	07.950	117	16.351	-88		
168/201	3505	EOL201		-19	32.093	120	16.763	-31		
168/201	3183	23	755	-19	17.942	120	06.180	-54	120/01	200
168/201	2997	24	756	-19	09.852	119	59.859	-64	120/01	570
168/201	2732	25	757	-18	58.320	119	50.867	-68	120/01	1100
168/201	2468	26	769	-18	46.823	119	41.904	-102	120/01	1630
168/201	2235	27	759	-18	36.615	119	33.942	-109	120/01	2100
168/201	1984	28	760	-18	25.730	119	25.491	-123	120/01	2600
168/201	1771	29	752	-18	16.413	119	18.231	-148	120/01	3030
168/201	1586	30	762	-18	08.696	119	11.526	-156	120/01	3400
168/201	1387	31	698	-18	00.377	119	04.319	-187	120/01	3800
168/201	1086	32	717	-17	47.832	118	53.473	-319	120/01	4400
168/201	739	33	750	-17	32.851	118	41.517	-486	120/01	5100
168/201	389	34	751	-17	17.249	118	30.366	-1246	120/01	5800
168/201	100	SOL201		-17	04.376	118	21.215	-1567		
168/202C	5064	EOL204		-17	23.955	118	35.169	-835		
168/202C	4640	35	752	-17	04.975	118	21.605	-1561	120/01	6350
168/202C	4365	36	761	-16	52.685	118	12.894	-1912	120/01	6900
168/202C	4115	37	753	-16	41.526	118	04.961	-2536	120/01	7400
168/202C	3967	38	754	-16	34.873	118	00.228	-2911	120/01	7700
168/202C	3832	39	755	-16	28.845	117	55.944	-5269	120/01	7970
168/202C	3591	40	756	-16	18.218	117	48.346	-5678	120/01	8450

168/202C	3352	41	757	-16	07.416	117	40.773	-5686	120/01	8930
168/202C	3153	42	769	-15	58.503	117	34.459	-5685	120/01	9330
168/202C	2954	44	760	-15	49.676	117	28.026	-5688	120/01	
168/202C	3318	SOL204		-15	38.289	117	20.105	-5677		170
168/202B	1726	EOL203		-15	38.289	117	20.001	-5673		9730
168/202B	1155	SOL203		-16	07.844	117	10.928	-5681		
168/202A	1054	EOL202		-16	08.402	117	10.707	-5684		
168/202A	801	43	759	-16	02.990	117	23.720	-5680	120/02	
168/202A	401	45	762	-15	54.276	117	44.333	-5681	120/02	950
168/202A	100	SOL202		-15	47.672	117	59.695	-5681		
168/301	3248	EOL301		-12	15.392	118	49.753	-5198		
168/301	2849	46	698	-12	29.034	119	06.833	-5127	128/01	6400
168/301	2499	47	717	-12	40.517	119	22.220	-4887	128/01	5700
168/301	2149	48	750	-12	51.982	119	37.620	-3778	128/01	5000
168/301	1849	49	751	-13	01.817	119	50.831	-2109	128/01	4400
168/301	1550	50	761	-13	11.648	120	04.047	-1730	128/01	3800
168/301	1249	51	753	-13	21.489	120	17.281	-2674	128/01	3200
168/301	900	52	754	-13	32.959	120	32.709	-2331	128/01	2500
168/301	500	53	755	-13	46.073	120	50.372	-2481	128/01	1700
168/301	100	SOL301		-13	59.189	121	08.052	-2407		
168/302	3626	EOL302		-13	44.419	120	48.137	-2505		
168/302	3225	54	756	-13	57.570	121	05.829	-2436	128/01	1000
168/302	3001	55	757	-14	04.931	121	15.788	-2339	128/01	550
168/302	2798	56	769	-14	11.838	121	24.573	-2108		600
168/302	2573	57	759	-14	20.118	121	33.756	-978	119/06	1050
168/302	2398	58	HT-8	-14	26.560	121	40.882	-530	119/06	1400
168/302	2248	59	760	-14	32.033	121	47.042	-372	119/06	1700
168/302	1949	61	762	-14	43.015	121	59.344	-260	119/06	2000
168/302	1799	62	HT-5	-14	48.493	122	05.510	-194	119/06	2300
168/302	1624	63	717	-14	54.921	122	12.698	-91	119/06	2600
168/302	1245	65	750	-15	08.792	122	28.276	-86	119/06	2900
168/302	1049	66	751	-15	15.968	122	36.356	-85	119/06	3300
168/302	750	67	761	-15	26.916	122	48.672	-85	119/06	3700
168/302	399	68	752	-15	39.753	123	03.125	-58	119/06	4100
168/302	100	SOL302		-15	50.536	123	15.659	-58	119/06	4700
168/401	3581	EOL401		-13	53.257	127	22.942	-46	119/06	5400
168/401	3445	69	753	-13	47.923	127	28.190	-77	100/003	200
168/401	3198	70	754	-13	38.528	127	37.885	-82	100/003	700
168/401	2951	71	755	-13	29.054	127	47.604	-72	100/003	1200
168/401	2754	72	756	-13	21.518	127	55.354	-90	100/003	1600
168/401	2680	73	757	-13	18.713	127	58.244	-90	100/003	1750
168/401	2606	74	HT-7	-13	15.888	128	01.162	-88	100/003	1900
168/401	2453	75	769	-13	10.013	128	07.186	-95	100/003	2200
168/401	2303	76	HT-5	-13	04.330	128	13.134	-99	100/003	2500
168/401	2103	77	759	-12	56.741	128	21.023	-97	100/003	2900
168/401	1904	78	760	-12	49.166	128	28.846	-98	100/003	3300
168/401	1653	79	761	-12	39.645	128	38.748	-100	100/003	3800
168/401	1401	80	762	-12	30.075	128	48.651	-96	100/003	4300
168/401	1102	81	717	-12	18.719	129	00.436	-88	100/003	4900
168/401	802	82	750	-12	07.296	129	12.254	-85	100/003	5500
168/401	499	83	751	-11	55.765	129	24.173	-67	100/003	6100
168/401	100	SOL401		-11	40.392	129	39.603	-54		
168/501	-	EOL501		-13	07.043	126	37.076			
168/501	2742	84	752	-12	48.956	126	19.330	-64	98/01	600

168/501	2391	85	753	-12	35.229	126	05.879	-79	-	-
168/501	2045	86	754	-12	21.474	125	52.916	-73	116/07	7100
168/501	1643	87	755	-12	05.500	125	37.828	-83	98/03	3200
168/501	1334	88	756	-11	53.269	125	26.229	-103	98/03	2600
168/501	1028	89	757	-11	41.114	125	14.734	-116	98/03	2000
168/501	828	90	HT-8	-11	33.174	125	07.197	-290	98/03	1600
168/501	703	91	769	-11	28.234	125	02.513	-398	98/03	1350
168/501	578	92	HT-5	-11	23.265	124	57.800	-441	98/03	1100
168/501	303	93	760	-11	12.366	124	47.495	-382	98/03	550
168/501	-	SOL501		-11	04.326	124	39.894	-		

Clock Drift Characteristics

The crystal oscillators inside each OBS exhibited frequency dependence on temperature. Clock drift rates are measured before deployment, but the temperature may be quite different at the water bottom. Furthermore, during their acquisition period the OBS internal temperature may rise by up to 1° C. UTIG supplied laboratory determined crystal calibration curves to allow corrections to variations in clock drift due to these temperature variations. Figure 5 and Figure 6 show that, for all crystals, the variation at low temperatures is greater than at high temperatures. Table 5 gives the CPU number used for each station.

Table 6 - Serial numbers of UTIG OBS units

Chassis	Preamp	A/D Converter	CPU	Memory	SCSI
92-7	208	8004	698	118	218
93-4	217	659	717	127	225
94-6	236	8068	750	154	S1
94-7	237	8007	751	155	S2
94-8	238	8008	752	156	S3
94-9	239	8056	753	157	S4
94-10	240	8057	754	158	S5
94-11	241	8058	755	159	S6
94-12	242	8069	756	160	S7
94-13	243	8071	757	161	S8
94-14	244	8061	769	162	S9
94-15	245	8070	759	163	S10
94-16	246	8072	760	164	S11
94-17	247	8064	761	165	S12
94-18	248	8065	762	166	S13

Figure 5: RTC Crystal Calibration A

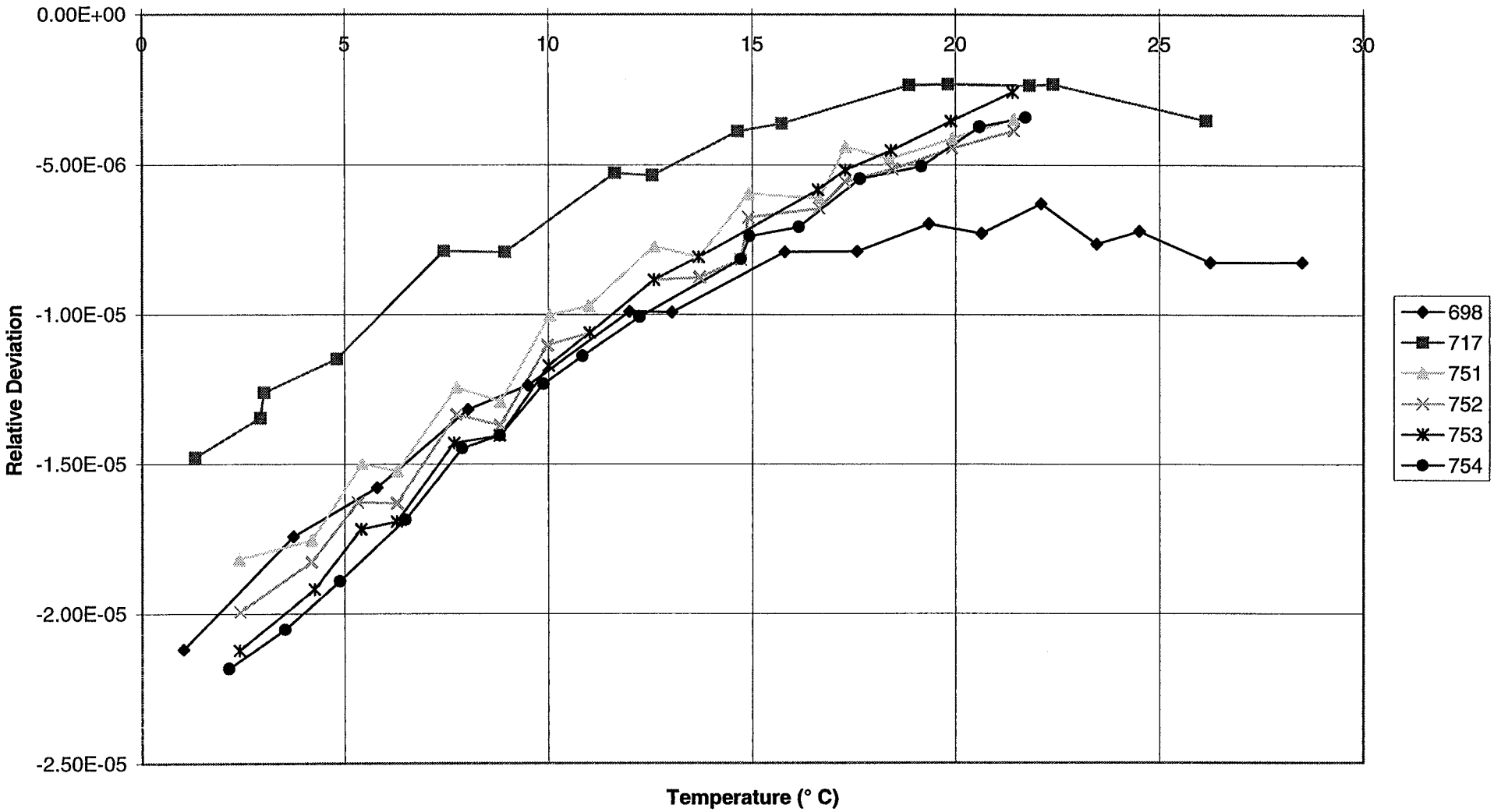

Figure 6: RTC Crystal Calibration B

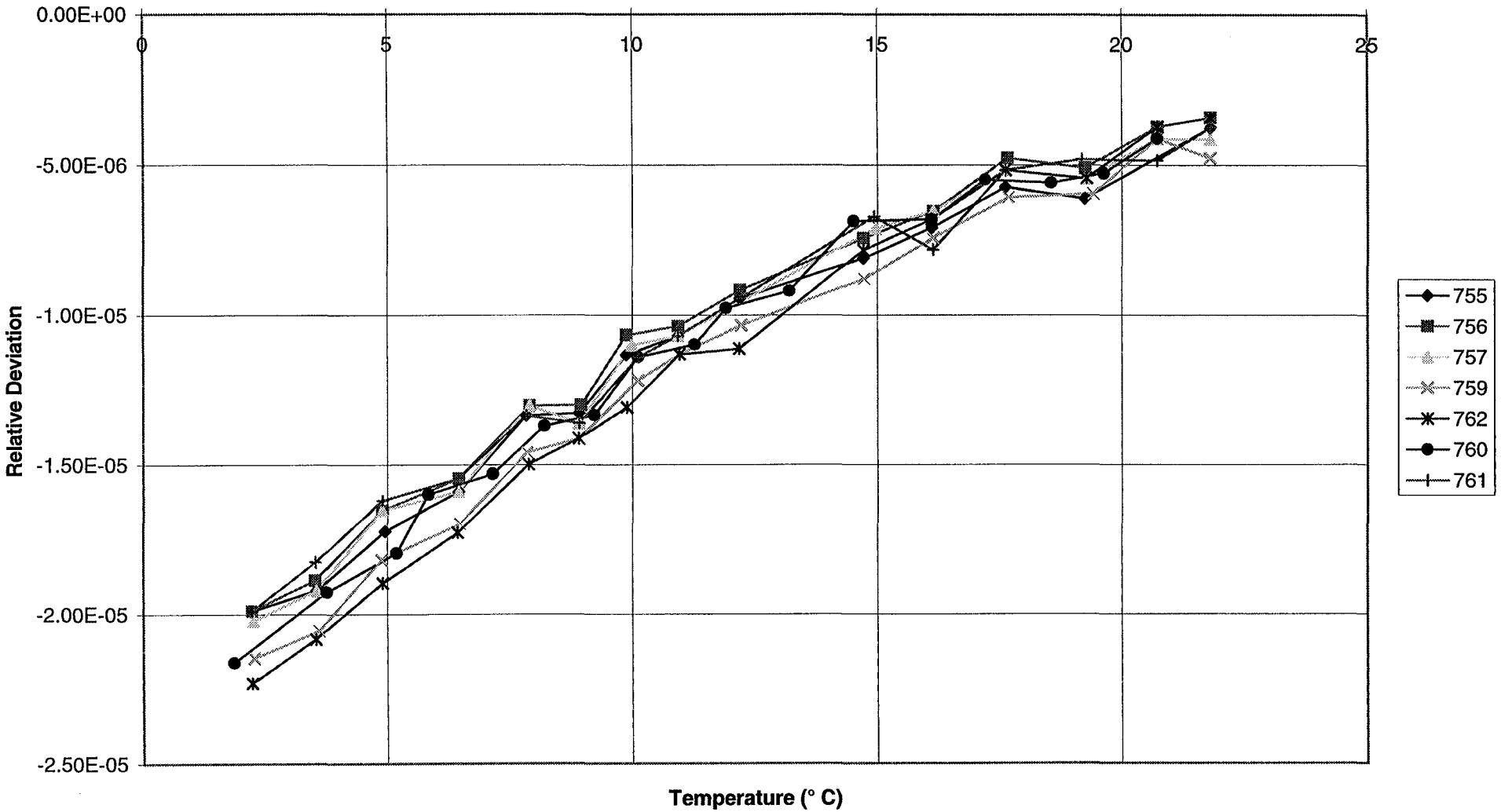

Raw OBS Data

The OBS data were written in raw OBS floating point format, and after retrieval, was converted to a "raw SEG-Y format" using OBSTOOL. Both files were written to 8mm Exabyte tape (one file per tape) and lodged with the MPSR Database as field data. The files are of the order 100-200 Mb in size. The file naming convention used by OBSTOOL is followed throughout the processing for this stage, and these conventions will be presented with the description of each step. In the file names that follow, xx will be used to denote the OBS station number, as given in column 3 of Table 5.

The sizes of raw SEG-Y data files is given in Table 7.

Table 7 - SEG-Y file sizes

Station	raw SEG-Y (bytes)	final SEG-Y (bytes)	Channels	Type
69	205612560	279212304	4	UTIG
70	205612560	274458000	4	UTIG
71	205612560	274781840	4	UTIG
72	205612560	279779472	4	UTIG
73	205612560	275510480	4	UTIG
74	157996560	206573040	3	NTOU
75	206142480	274862800	4	UTIG
76	159597840	193032480	3	NTOU
77	205612560	279941520	4	UTIG
78	205612560	265069568	4	UTIG
79	205612560	280346640	4	UTIG
80	205612560	280346640	4	UTIG
81	205612560	273243600	4	UTIG
82	205612560	273729360	4	UTIG
83	205612560	271300560	4	UTIG

Conversion to 'raw SEG-Y'

The conversion from raw OBS floating point format to raw SEG-Y format was done using OBSTOOL, as were all subsequent processing steps to the generation of a final SEG-Y file. A sampling rate correction is performed during the conversion, to correct for a byte shift which occurs every time data is written to disk. This hardware bug affects most 8088 OBS's with SCSI tape or disk, and the software corrects for the byte shift if it detects an occurrence of it.

In creating the raw SEG-Y file, the program assumes that the number of channels is constant for the entire file, and determines the number of traces required to break the file into approximately equal parts. The raw SEG-Y file remains in 16-bit floating point format. The headers are extracted in two files.

Program: raw2segy

Input	obsdata.xx				
Output	obsdata.xx.log	obsdata.xx.corr	hdrlist.xx	hdrint.xx	obsdata.xx.segy

obsdata.xx.log

This is the master log file to which OBSTOOL appends pertinent parameters each time the program is executed.

The following was logged for station 77:

```
Tue Jan 16 18:31:54 1996
  Program raw2segy version  1.30 run

  input obs file: /export/mpsr/obs-11/raw168/line401/obsdata.77
  output segy file: /export/mpsr/obs-12/rawsegy/obsdata.77.segy
  Skipped   4 test records.
  input is being byte-shift adjusted

First record            3 at 014 20:00:00
  Segy file parameters:
    OBS QADC3 samples (Non-standard SEGY!)
    number of samples/trace:  8160
    number of records/trace:  16
    number of bytes/trace:  16560
  Traces written :    12448

  Sample interval corr. written to /export/mpsr/obs-11/logs/obsdata.77.corr
    obs  comps s.i.    res cnt  corr (ns)
     77    4     4        98         6

     Assumed  s_int: .003997000
   Corrected  s_int: .003997401
Last  record          391 at 014 02:29:26

  Header times written to /export/mpsr/obs-11/logs/hdrint.77
```

obsdata.xx.corr (correction file incl. sampling rate correction)

Example for station 77:

```
     SAMP
             77     4      4      98     6
```

station number, comps, sample interval (ms), residual count, correction (ns)

hdrlist.xx (raw header information)

An excerpt from station 77 is:

```
   128 0300 8080 8f04 6200 7760 010e 1400 0006
   256 0400 8080 8f04 6200 7760 010e 1404 2b05
   384 0500 8080 8f04 6200 7760 010e 1409 1a04
   512 0600 8080 8f04 6200 7760 010e 140e 0903
   640 0700 8080 8f04 6200 7760 010e 1412 3403
   768 0800 8080 8f04 6200 7760 010e 1417 2302
   896 0900 8080 8f04 6200 7760 010e 141c 1201
```

Cols 2:7 are the block number; then follows 16 bytes arranged as 8(x,2(a2))

Format is given in Table 8.

Table 8 - Format of file hdrlist.xx

Byte	Contents
1,2	byte swapped record number
3	block number within record
4	number of blocks within record
5	active channels (f = all channels active)
6	sample rate (ms)
7	residual count (time offset) see Christeson, 1995, p 20
8	not used
9	station code
10	year
11	month
12	day
13	hour
14	minute
15	second
16	tenth of second

hdrint.xx (interpreted header information)

First few records from station 77 are:

```
Station 77      Year 1996
 block rec mo dy hr mn   sec    dt,s    tx,s
   128   3  1 14 20  0   0.6
   256   4  1 14 20  4 43.5   282.9 21.950
   384   5  1 14 20  9 26.4   282.9 21.950
   512   6  1 14 20 14  9.3   282.9 21.950
   640   7  1 14 20 18 52.3   283.0 22.050
   768   8  1 14 20 23 35.2   282.9 21.950
```

The format is given in Table 9.

Table 9 - Format of file hdrint.xx

columns	format	contents
02:06	i5	block
08:10	i3	rec
12:13	i2	month
15:16	i2	day
18:19	i2	hour
21:22	i2	minute
24:27	f4.1	second
29:34	f5.1	dt (s) between consecutive records
36:41	f6.3	tx (s)

obsdata.xx.segy

This is the raw SEG-Y file as recorded in the field and cannot be viewed using Focus.

Initial Clock Correction

The clock drift rate is estimated during this step. The data from cc.xx are entered manually into OBSTOOL. Note that the example given by Christeson (1995, p3) uses GMT for OBS time, whereas the OBS times for survey 168 are local time for all stations.

The variation in OBS clock drift from standard time is largely dependent on temperature. The difference between clock time and standard time can only be measured while the OBS is on deck, and so an estimate of the drift rate during data acquisition is based on laboratory measurements of the relationship of drift rate and temperature (see Christeson, 1995, p22). The difference between drift rates at "sleeping-on-the-floor" temperature and operating temperature, dcdw, is estimated from these data (Figure 5, Figure 6) and input to OBSTOOL.

Figure 7 - OBS clock drift rate pre-deployment and during data acquisition

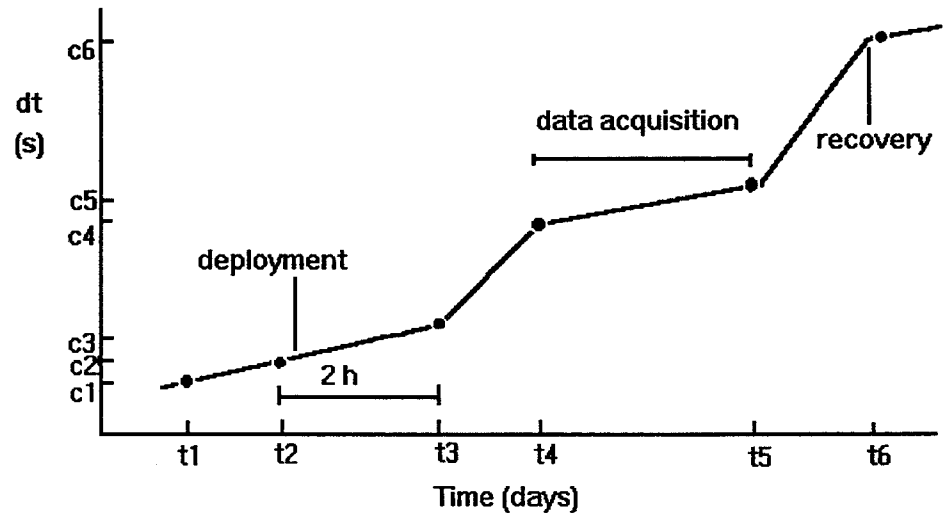

Figure 7 (not drawn to scale) depicts the values supplied to OBSTOOL and the typical drift variation in an instrument deployed on a cold ocean floor. c1 and c2 are the diffrences between OBS time and UTC at t1 and t2 , and the OBS is deployed shortly after t2. The drift rate is then extrapolated to t3, 2 hours after t2. While the OBS is on the ocean floor, which may be ~4° C, the drift rate increases. During data acquisition, the instumentation warms up by ~1° C and the drift rate falls. CLOCKCORR computes the amount of drift rate change from the values c1, c2, c6 and dcdw supplied by the user.

Program: clockcorr

Input	cc.xx (manual)			
Output	obsdata.xx.log	obsdata.xx.corr	obsdata.xx.clock.dat	obsclock.xx

obsdata.xx.log

The following example from station 77 was appended to the log file:

```
Wed Mar 13 14:52:20 1996
  Program clockcorr version  1.20 run
  Input clock calibration data file obsclock.77
  Output clock correction file obsdata.77.corr
      time (day)     corr
         0.0000    1.032   t1
         0.0368    1.044   t2
         0.1201    1.072   t3
         0.8049    1.280   t4
         2.0785    1.667   t5
         2.7181    1.861   t6
```

obsdata.xx.corr

The following is appended to the file, already created by the previous process (eg from station 77):

```
CLOCK
  96  14 20  0   1.280   0.30346
```

which is: year, day, hour, minute, correction, drift rate

obsclock.xx

This file contains the clock calibration times entered by the user from the files cc.*.

```
96 14 00 41 0 1.032187
96 14 01 34 0 1.044455
96 14 03 45 0
96 14 20 00 0
96 16 02 34 0
96 16 17 55 0 1.8608152
0
```

obsdata.xx.clock.dat

This file contains the clock calibration times entered by the user from the files cc.*, and the clock corrections at these times. Time t2 is immediately prior to deployment, and t6 is after retreval.

```
      821752860. - time in seconds of t1
         0.0000    1.032   t1
         0.0368    1.044   t2
         0.1278    1.075   t3
  1 data acquisition periods
         0.8049    1.280   t4
         2.0785    1.667   t5
         2.7181    1.861   t6
  0. dcdw
```

Create Water Wave Subset

In this step, a subset is extracted from the raw SEG-Y file (created earlier) in preparation for computing the OBS location using the direct water wave. Only the shots nearest the OBS are needed, where the direct water wave arrives ahead of all other arrivals.

Program: getwwdata

Input	hdrlist.xx	obsdata.xx.segy	LLL.nav	obsloc.dat
Output	obsdata.xx.log	shot_file.xx.ww	obsdata.xx.segy.ww	

obsdata.xx.log

The following example from station 77 was appended to the file:

```
Wed Mar 13 18:44:00 1996
  Program getwwdata version  1.20 run on
  /d/agso/u/ppetkovi/401/obsdata.77.segy
  Input shot file /d/mpsr/obs-11/logs/401.nav
  OBS   77  -12.94568   128.35038
    14 shots within  0.70 km of obs written to /d/mpsr/obs-
11/logs/401.nav.77.ww
  Input OBS data file /d/agso/u/ppetkovi/401/obsdata.77.segy
  Clock correction read from /d/mpsr/obs-11/logs/obsdata.77.corr
   # yr day hr mn   corr  drift rate
   1 96 14 20  0   1.280   0.304
     52 traces written to /d/mpsr/obs-11/ww/obsdata.77.segy.ww
   min bias:     -198.524   avg bias:       -5.603   max bias:      159.349
```

LLL.nav.xx.ww

This is a subset of the navigation file, in the same format. LLL is the line number 101, 102 and so on.

obsdata.xx.segy.ww

This is the SEG-Y subset file.

Pick water Wave Arrivals

The water wave arrival times are picked in order to compute the OBS location by inversion in the next step. Arrivals can be picked automatically, and then adjusted according to assessment of the data display. Christeson (1995, p5) describes the method used.

Note that after editing of the pick file, the output file has the same name as the input file (obsdata.xx.arr) and that the only way to restore the automatic picks is to run ARRPICK again.

In the case of the Petrel line where the waters are only 60-100 m deep (see Figure 2), the critical distance for generation of headwaves at the water bottom is approximately 100m. Hence one might expect refracted arrivals to overtake direct wave arrivals almost immediately. However, the first strong refractions come from some ~200 m deeper, and hence we can confidently pick the water wave arrivals out to at least 500m from the source. Appendix 3 is a collection of plots for results of the arrival picking.

The algorithm used by ARRPICK is described by Christeson (1995, p16) as follows:

Let the set of samples from the nominated channel be $P_1, P_2, P_3, \ldots, P_n$

and let the absolute value of first differences be:

$$D_k = | P_k - P_{k-1}| \text{ for } k = 2, 3, \ldots, n$$

Compute the running mean of D_k:

$$A_k = \left(\sum_{k-m}^{k+m} Dj\right) / (2m + 1) \qquad \text{where m is small.}$$

Then repeat the following block for all samples:

Let T_R be the relative threshold and T_A be the absolute threshold supplied by the user. Then a trigger condition occurs when:

$$P_k - P_{k-1} > A_k * T_R \qquad \text{and} \qquad P_k - P_{k-1} > T_R$$

assuming that water wave first motion is positive, as is the case in the hydrophone.

The first zero crossing after the trigger is sought, and the travel time to this point is computed. The data near the trigger are saved for later computation of the duration of this first pulse, so that the correct travel time can be computed. The horizontal polarisations are as follows:

Let the set of samples from the vertical component be $V_1, V_2, V_3, \ldots, V_n$
and the set of samples from the horizontal component be $H_1, H_2, H_3, \ldots, H_n$

Let $\Delta H = H_k - H_{k-1}$ for k = 2, 3, . . . , n and
$\Delta V = V_k - V_{k-1}$ for k = 2, 3, . . . , n

For each horizontal channel, calculate:

$$S_{HH} = \sum_{1}^{10} (\Delta H * \Delta H), \quad \text{and} \quad S_{HV} = \sum_{1}^{10} (\Delta H * \Delta V)$$

For each horizontal component, *i*, let

$$A_i = +\sqrt{S_{HH}} \quad \text{if } S_{HV} > 0, \quad \text{and} \quad A_i = -\sqrt{S_{HH}} \quad \text{if } S_{HV} < 0$$

If A_1 is the radial component and A_2 is the transverse component, then the horizontal polarisation is equal to:

$$\tan^{-1}\left(\frac{A_2}{A_1}\right)$$

Now compute the duration of the first positive pulse in the water wave arrival, and subtract this from the travel time computed above. This gives the correct travel time for the onset of the water wave arrival.

Program: arrpick

Input	obsdata.xx.corr	obsdata.xx.segy.ww	
Output	obsdata.xx.log	wwtta.xx	obsdata.xx.arr

obsdata.xx.log

The following example from station 77 is appended to the file:

```
Thu Mar 14 18:24:11 1996
  Program arrpick  1.10 run on
  /d/mpsr/obs-11/ww/obsdata.77.segy.ww
    4 channels,   750 samples, si =     3.99700 ms
  Input correction file /d/mpsr/obs-11/logs/obsdata.77.corr
   Sampling interval correction     6.00000 usec
  Relative threshold     30.0000
  Absolute threshold     2.00000
  10 potential water wave picks were
    output to /d/mpsr/obs-11/logs/obsdata.77.arr
```

wwtta.xx

This is the arrival time pick file formatted for input to inversion programs. The following is wwtta.77 :

```
  2098  0.391  252.89  -12.94206   128.35411  821878520.9660
  2099  0.329  247.06  -12.94269   128.35347  821878548.7270
  2100  0.264  336.22  -12.94336   128.35283  821878576.6660
  2101  0.203  334.87  -12.94400   128.35217  821878604.4070
  2102  0.140  224.50  -12.94464   128.35153  821878632.4270
  2103  0.087  312.11  -12.94525   128.35086  821878660.0750
  2105  0.070  288.31  -12.94653   128.34953  821878715.4970
```

obsdata.xx.arr

This is the arrival time pick file formatted for plotting. The following is obsdata.77.arr:

```
-578    0.39124       2098   92     0
-477    0.32908       2099   96     0
-374    0.264         2100   97     0
-273    0.203         2101   101    0
-172    0.13992       2102   108    0
-71     0.086922      2103   112    0
133     0.069529      2105   116    0
235     0.12023       2106   120    0
336     0.184         2107   121    0
437     0.243         2108   125    0
539     0.30601       2109   132    0
```

After automatically picking the arrival times for the direct water wave, the display program is used to edit the arrivals if necessary. After editing, the obsdata.xx.arr file is overwritten when <s> is pressed in the plot window.

Program: xpltsegy

Input	obsdata.xx.segy.ww	obsdata.xx.arr
Output		obsdata.xx.arr

When the <Done> button is pressed in the above procedure, program ARR_FINAL is executed, in which the water wave travel times and horizontal polarisations are written to files formatted for input into the OBS location programs.

Program: arr_final

Input	obsdata.xx.segy.ww	obsdata.xx.arr		
Output	obsdata.xx.log	wwtta_az.xx	wwtta_orig.xx	wwtta.xx

obsdata.xx.log

The following was appended to the log file for station 77:

```
Thu Mar 14 19:09:38 1996
  Program arr_final version  1.10 run on
  /d/mpsr/obs-11/ww/obsdata.77.segy.ww
    4 channels,    0 samples, si =     3.99700 ms
  Input correction file /d/mpsr/obs-11/logs/obsdata.77.corr
   Sampling interval correction     6.00000 usec
  11 recomputed water wave picks were
    output to /d/mpsr/obs-11/logs/wwtta.77
```

wwtta_az.xx

This file has the same format as wwtta.xx

wwtta_orig.xx

This file has the same format as wwtta.xx

Invert for OBS Location and Orientation

OBSTOOL has several inversion programs for computing combinations of OBS position, orientation, clock correction, and speed of sound. For each program there is a companion program to plot the results.

Because of shallow water along the entire line, there were few water wave first arrivals (Appendix 3), and inversion for all parameters was not successful. The best results were achieved when inverting for position (Appendix 4) and clock correction (Appendix 5) only. Inverting for orientation gave mostly spurious results with large residual errors (Appendix 6). The travel times to the OBS in its position before and after inversion are given in Appendix 7.

Programs: obsloc *ext*, (where *ext* = llv, llc, llcv, ll)

Input	wwtta.xx	
Output	obsloc *ext*	obsdata.xx.log

For line 168/401, the most reliable results were obtained with llc, the inversion for position and clock correction. The log file output for station 77 was:

```
Sun Mar 24 20:07:55 1996
  Program obsloc_llc version  1.20 run
  Input water wave travel time file wwtta.77
  Shot depth   15.0
  Initial Position, clock correction (sec)
    -12.94568  128.35038 -0.010
  Final Position, clock correction (sec)
    -12.94568  128.34977 -0.014
  Change from initial x,y   -66 m,     1 m
  Initial Mean Error  0.028 sec
  Final Mean Error    0.002 sec
  1 closest approaches
  shot clcorr      time (sec)    arrivals
  2103 -0.014  821878660.0750     1,     11
    11 input travel times
   22 iterations
  Damping parameter     5.0
```

Programs: obsloc *ext*, (where *ext* = llcaz, cvaz, az)

Input	wwtta.az.xx	
Output	obsloc *ext*	obsdata.xx.log

Following the inversion for position, the inversion for azimuth was executed, with the following appended to the log file for station 77. The inversions for orientation were not successful for the Petrel line (See Appendix 6), with few direct arrivals available.

```
Wed Mar 20 14:14:58 1996
  Program obsloc_az version  1.00 run
  Input water wave travel time file
logs/wwtta_az.77
  Initial azimuth     0.0 Final azimuth  185.4
  Initial Mean Error   57.866 deg
  Final Mean Error     57.412 deg
```

Then plot the inversion results:

Programs: plot_*ext*, (where *ext* = ll, llcv, llc, llv, llcaz, cvaz, az)

Input	obsloc_*ext*
Output	display (see Appendices 4-7)

Evaluate plots, then update the OBS location file with the inversion results, and create closest approach file.

Final Clock Correction

In this step, the secondary clock correction determined via inversion is added to the initial clock correction for each time in the closest approach file. (Shot delay was not computed. If it was computed, it would be subtracted from the sum of the initial and secondary clock corrections.) The final clock correction and drift rate during the data acquisition period is determined from a line of best fit to the individual clock corrections.

Program: clockcorr_final

Input	cl_app.xx.dat	
Output	obsdata.xx.corr	obsdata.xx.log

obsdata.xx.log

The following is an example of additions to the log file:

```
Sun Mar 24 20:13:32 1996
  Program clockcorr_final version  1.10 run
  shot delay set to 0.0 sec, would have been   0.004 sec
  Mean secondary clock correction -0.014 sec
  Clock corrections at    1 closest approaches
    shot    corr
    2103  -0.014
      time (day)    corr
         0.0000    1.032   t1
         0.0368    1.044   t2
         0.1278    1.075   t3
         0.8049    1.280   t4
         1.4560    1.464
         2.0785    1.667   t5
         2.7181    1.861   t6
                      Initial          Final
  clock correction    1.280  sec      1.276  sec
     drift rate       0.30346 sec/dy    0.30329 sec/dy
```

obsdata.xx.corr

The program appends shot delay and final clock correction to this file, which in the case of station 77 becomes:

```
SAMP
  77   4   4   98   6
CLOCK
  96   14 20   0    1.280    0.30346
SDELAY
  0.000
CLOCK_FINAL
  96   14 20   0    1.276    0.30329
```

Final SEG-Y File

The final SEG-Y file created by OBSTOOL is standard format. The header values are given by Christeson, 1995, p17 and are reproduced here in Table 11 and Table 12.

Program: final_segy

Input	obsdata.xx.segy	LLL.nav	obsdata.xx.corr	
Output	obsdata.xx.segy.final	obsdata.xx.log	ebc_head	ehdrfile

The parameters supplied to FINAL_SEGY are given in Table 10:

Table 10 - Parameters used for creating final SEG-Y file

obs number	xx	
output file extension	final	output is: obsdata.xx.segy.final
shot file	LLL.nav	
line number	168/LLL	
output number of channels	4	or 3 for NTOU instruments
advance window opening (s)	0	the time trace starts before shot time
window shift rate (km/s)	8	ie the reduction velocity required
length of time window (s)	20	
shot depth (m)	15	for SEG-Y header
anti-alias frequency (Hz)	62.5	for SEG-Y header
azimuth for sign calculation	-90	+ve distances for shooting towards obs
turn-on mute length (s)	1.5	mute period after recording starts
Delay type	16-bit	
rotate horizontals	yes	
change EBCDIC header	yes	

Table 11 - SEG-Y Trace Header

byte	length	parameter
1	4	sequence number
5	4	sequence number
9	4	shot number
17	4	shot number
21	4	shot number
25	4	shot number
29	2	trace id code (1 = seismic data)
31	2	number of vertically summed traces (= 1)
33	2	number of horizontally stacked traces (= 1)
35	2	data use (1 = production)
37	4	shot-receiver distance (+ve shooting towards OBS)
41	4	receiver elevation (-ve below S.L.)
49	4	depth of airgun
61	4	water depth below shot
69	2	scalar to be applied to depths in bytes 41-86 (= 1)
71	2	scalar to be applied to coordinates in bytes 73-83 (= –100)
73	4	shot longitude
77	4	shot latitude
81	4	OBS longitude
85	4	OBS latitude
89	2	coordinate units (= 2, seconds of arc)
109	2	delay between shot time and first sample (ms)
115	2	number of samples
117	2	sample interval (μs)
119	2	gain type of OBS (= 3, floating point)
141	2	alias filter frequency
143	2	alias filter slope (= 2)
217	4	azimuth of shot (degrees * 100)
235	2	component ID (negative if unrotated) 1 - horizontal component #1 2 - vertical component 3 - pressure (hydrophone) 4 - horizontal component #2
237	2	OBS station number
239	2	number of non-zero samples in trace

Table 12 - Binary Reel Header

byte	length	parameter
3201	4	OBS station number
3205	4	line number
3213	2	number of output channels (= 4 or 3)
3217	2	sample interval (μs)
3221	2	number of output samples per trace
3225	2	output format (1= IBM floating point)
3261	4	number of traces in file
3265	4	orientation of OBS channel H1 from N (degrees * 100)

obsdata.xx.log

Information appended, for example for station 77:

```
Sun Mar 24 20:17:08 1996
  Program final_segy version  1.30 run on
  shotfile logs/401.nav
  datafile /d/agso/u/ppetkovi/401/obsdata.77.segy
  Final clock correction read from logs/obsdata.77.corr
   # yr day hr mn   corr  drift rate
   1 96 14 20  0   1.276   0.303
  Job No.   77
  Line No.   168
  Number of output channels   4
  Advance window opening    0.000 sec
  Window shift rate    8.000 km/sec
  Minimum trace length   20.000 sec
  OBS depth    100.0000 m
  Air gun depth     15.0000 m
  OBS lat & long in deg.    -12.94568   128.34977
  Alias filter frequency   62.500 Hz
  Shot Delay =    0.000 sec
  Ranges have standard SEGY signs.
  Turn on mute time =    1.500 sec.
  Rotate horizontals
  H1 direction (deg. from N)     200.00000000000

  First data in range at trace     46 shot        100
   INFO: shot    104 was muted   0.000 to   1.499
ERROR: delay overflow at shot   104  45786
   INFO: shot    114 was muted   0.000 to   1.499
ERROR: delay overflow at shot   114  45737
   INFO: shot    124 was muted   0.000 to   1.499
ERROR: delay overflow at shot   124  44719
                                     .
                                     .
                                     .
   INFO: shot   3557 was muted   0.000 to   1.499
   INFO: shot   3567 was muted   0.000 to   1.499
ERROR: delay overflow at shot   3567  37280
   INFO: shot   3577 was muted   4.633 to  20.001
   INFO: shot   3578 was muted   0.000 to   1.499
  Last  data in range at trace   3501 shot       3581
  Processed   3482 shots
  Output   13820 traces to fsy/obsdata.77.segy.final
```

obsdata.xx.segy.final

This is the final product from Stage 1 processing. This file can be further processed, in OBSTOOL or DISCO/FOCUS. It was found convenient to use OBSTOOL to split the file into individual channels, and use the vertical channel (channel 1) for P-wave picks.

ebc_head

This file is the template for the first 15 lines of the SEG-Y header. The ASCII version is given below.

ehdrfile

The ASCII version of the SEG-Y header:

```
Shooting Ship: Rig Seismic
Source Size: 4800 ci
Chief Scientist(s)/Institution(s): C. Collins, C.S. Lee

Data Processor(s):  P.Petkovic

Area Information: Line 168/401, NWS Australia
Station 70

Horizontals rotated, OBS Orientation 320.9 degrees
Horizontals rotated, OBS Orientation 320.9 degrees
Sample Rate Correction: -10 nannoseconds
Shot Delay of 0.000 seconds applied.
Clock Correction at Time (yr, julian day, hour, minute) 96  14 20  0
  is 1.135 seconds, Drift Rate 0.19898 seconds/day
Processing History:
  Program raw2segy version  1.30 run
  Program clockcorr version  1.20 run
  Program getwwdata version  1.20 run on
  Program getwwdata version  1.30 run on
  Program arrpick  1.10 run on
  Program arrpick  1.20 run on
  Program arr_final version  1.10 run on
  Program arr_final version  1.20 run on
  Program obsloc_llc version  1.20 run
  Program obsloc_llcaz version  1.20 run
  Program obsloc_llcv version  1.00 run
  Program obsloc_llv version  1.00 run
  Program obsloc_llcvaz version  1.00 run
  Program obsloc_az version  1.00 run
  Program clockcorr_final version  1.10 run
```

Processing of SEG-Y Data

The second stage of processing aimed at displaying the SEG-Y data in a form suitable for interpretation. The DISCO/FOCUS software was used throughout this stage of the processing.

The most significant enhancement was achieved by applying a bandpass filter followed by trace amplitude equalisation. Other techniques, including trace stacking and velocity filtering, yielded some further improvements in those parts of the section where the signal to noise ratio was poor. Figure 8 shows the extent of data recovery after these basic processing steps were applied.

Noise and Data Loss

The OBS data were affected by several types of noise and data loss.

Acquisition Losses

Firstly, 10% of traces were muted during acquisition at times when the data were being written to disk. Every 10th trace is muted to avoid recording the noise from the disk drive motor.

Broad Band Noise

Secondly, the data are masked by several types of broad-band and monotonic noise on all channels. These result in a further ~50% loss, as is seen in Figure 8 which shows those parts of the records that can be interpreted after bandpass filtering. One interesting feature to note in this figure is that during shots 500 to 1100 (about 60 km or 5 hours) there is loss of signal on all OBS stations. This loss is attributed to broad band high amplitude noise of unknown origin. Various hypotheses have been put forward, including drilling rig noise and local geology bottom conditions at the shot locations.

Figure 9c shows the amplitude spectrum during this period on OBS 77, compared to the background noise (Figure 9a), and amplitude spectrum during signal reception (Figure 9b).

Figure 8 - OBS Data Recovery after Bandpass Filter

The dashed lines indicate regions of data recovery, while the blank areas indicate regions of low signal to noise ratio. The shot interval is 100m. Total length of traverse is ~350km.

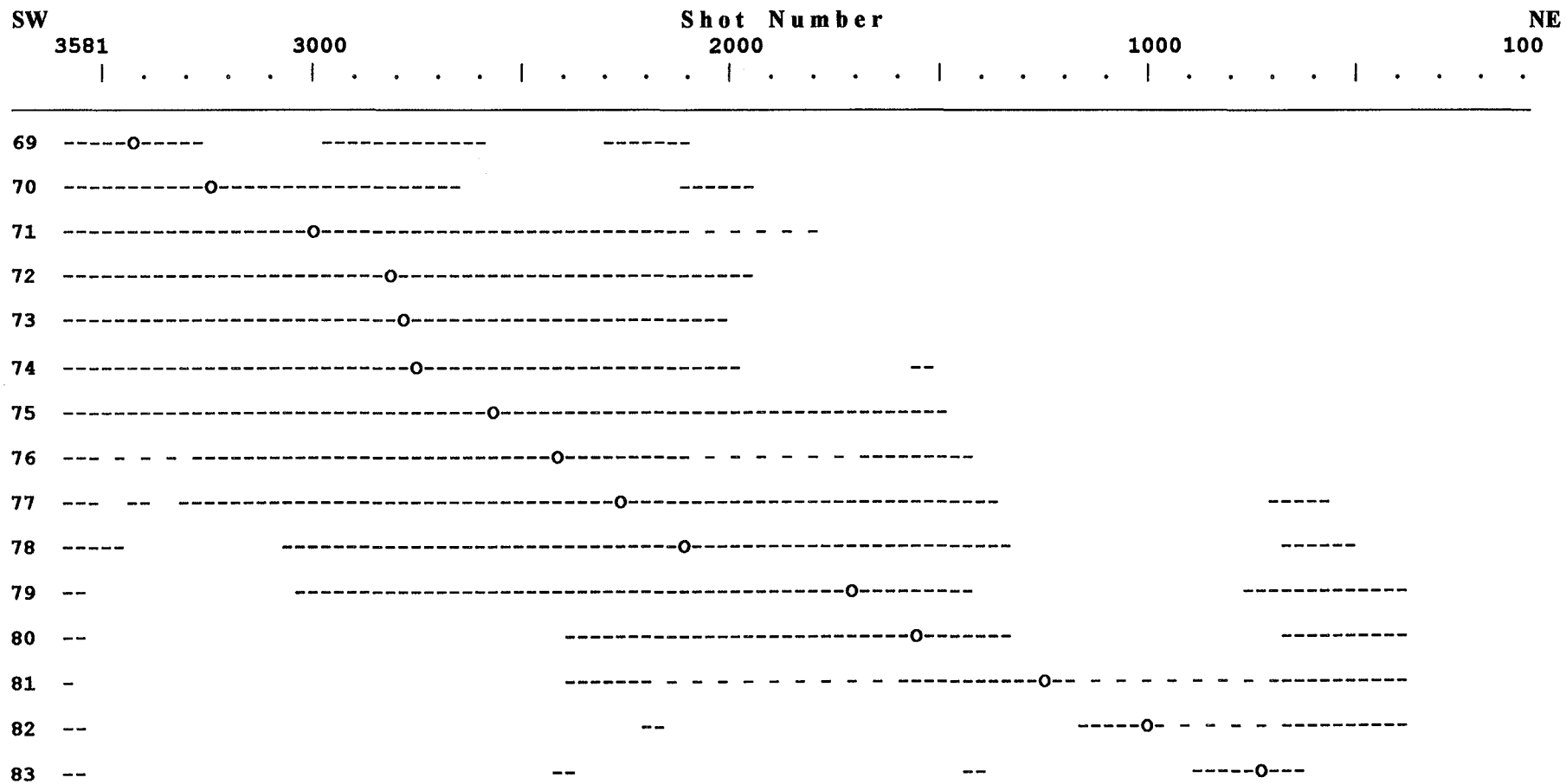

Mean Spectral Analysis

Figure 9

Amplitude Spectra for 168/401.77

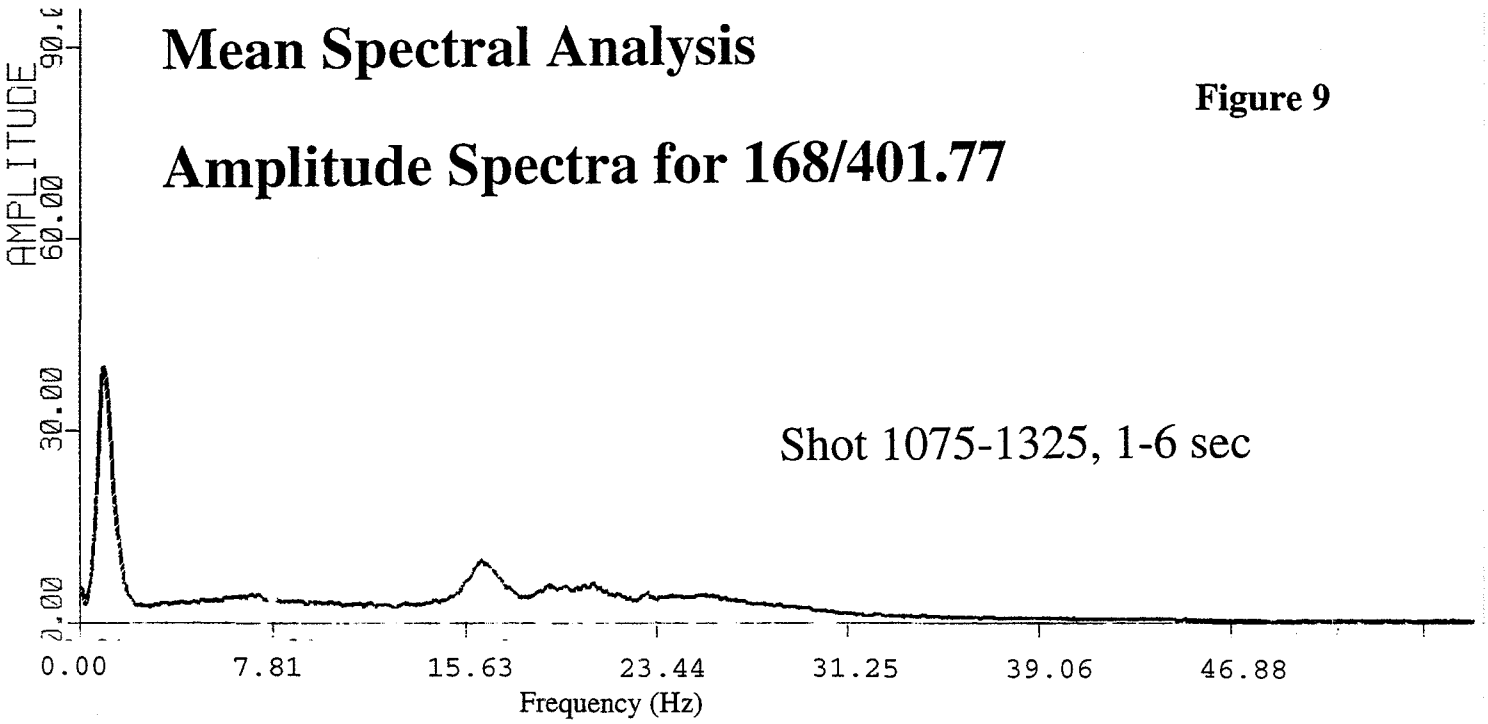

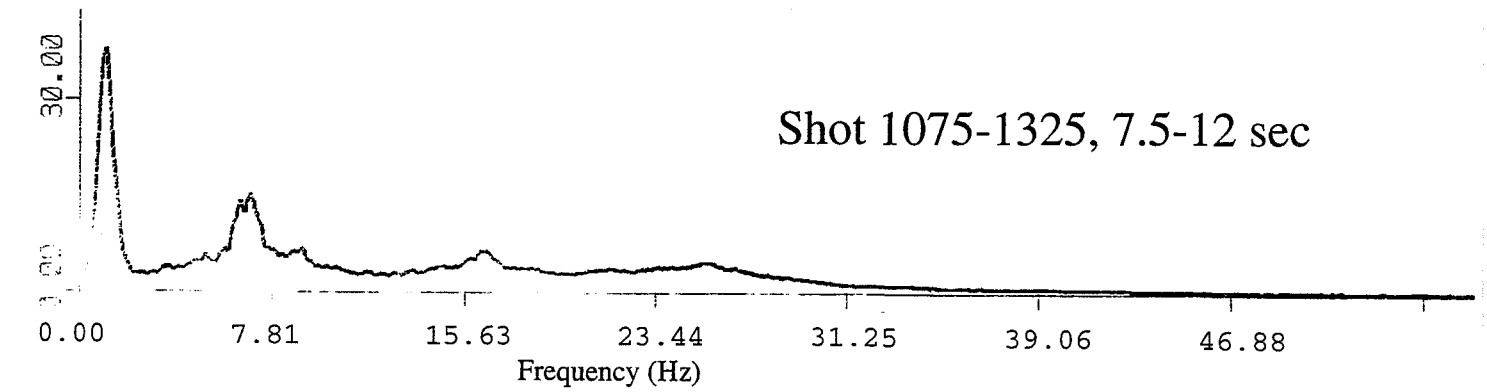

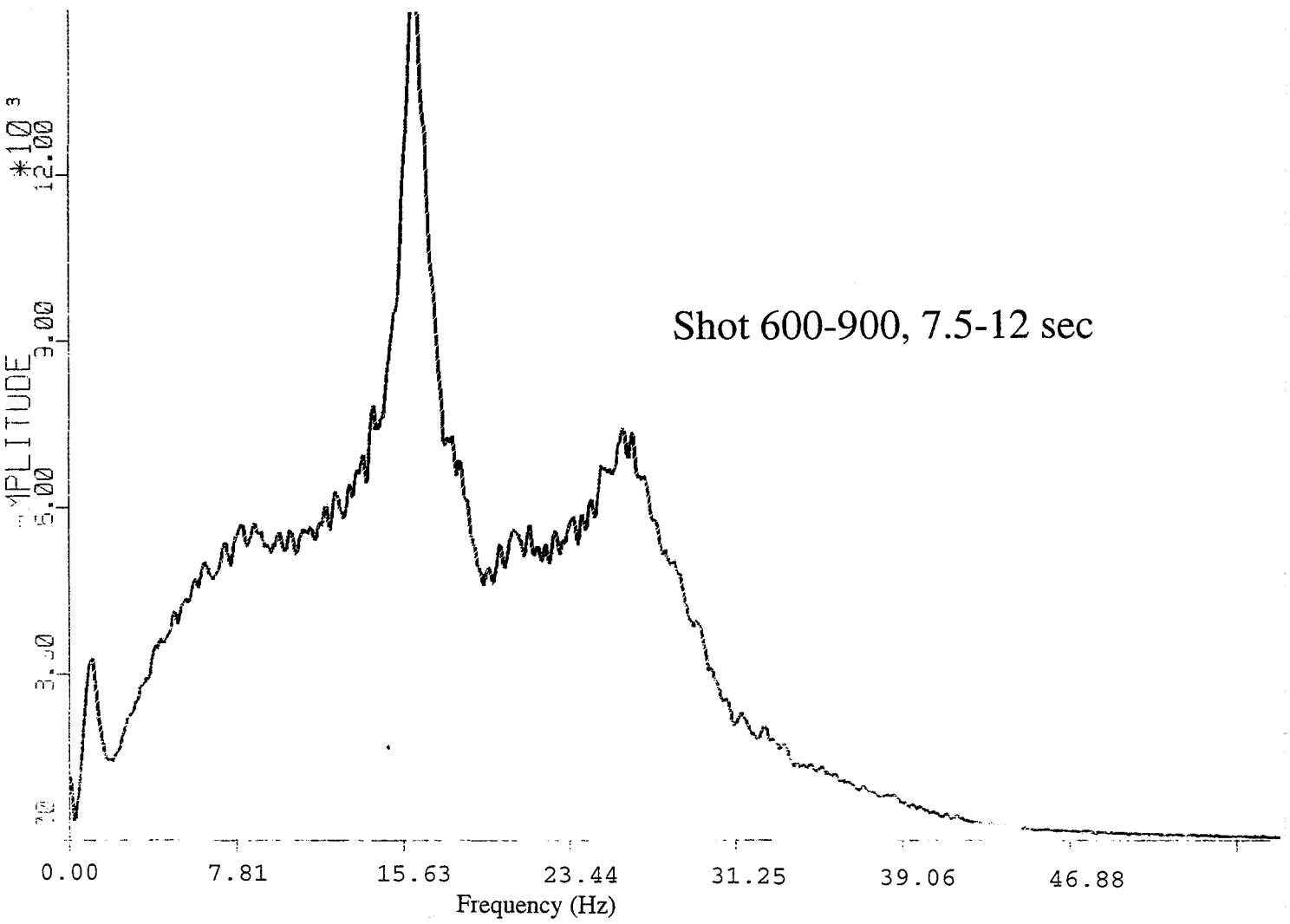

Figure 9a shows the wave noise at ~2 Hz and some small activity at ~16 Hz. Figure 9b is identical except that the source energy is coming in at ~6 Hz. Figure 9c then shows a noise amplitude at least 4 times that of the signal over a broad band and especially strong at ~16 Hz.

A typical DISCO job segment for the spectral analysis is given below:

```
*CALL    SPECTRM shot     seqno    HAMM     20
SPECTRA  AMPLIT  OFF      MNONLY                          OFF
METHOD   FFT
PLOTX    LIN     8        10       0        80
PLOTY    LIN     5        3000     0        15000
TGATES   INT
600      1       7500     12000
900      1       7500     12000
```

Water Wave Noise

This type of noise is more of a problem for the deep OBSs on other lines. There was no attempt to apply processing techniques to remove the water wave noise from 168/401. It is also very broad, and often the signal can be seen going through it.

Monochromatic Noise

Noise areas where there is no discernable signal, and the noise seems to be very 'monochromatic' at a frequency similar to the signal frequency (6-9 Hz). These noise areas often start and terminate abruptly, and in some cases seem to repeat at semi-regular intervals. The noise may be coherent across several traces, giving the noise a patterned appearance. Its source appears to be instrumental, although there are other suggestions, such as:

- rocking of the anchor frame for a precariously landed OBS, and
- oil rig operation

A notch filter was applied in an attempt to suppress this type of noise, but was unsuccessful due to the proximity of the signal at this frequency.

Interpolation Across Muted Traces

The OBSTOOL log file identified traces which were muted traces while data was being written to disk with partial success. Program MUTED was used to read this log file and write a DISCO 'PATCH' job segment to interpolate across the muted traces. This segment was the second stage of the DISCO job sequence, following the data input stage. See Appendix 9 for a listing of a typical DISCO job. **Error! Reference source not found.** contains all the DISCO jobs used in the enhancement and display of the data.

A typical DISCO job segment for this stage is given below:

```
**------ READ SEG-Y DATA ------------------------------------------
-
*CALL   GIN     12000   4       1       cdp     INCR    SEGY
TAPEOPT
/tapefile="/export/mpsr/nsp0/s168/401/obsdata.77.segy.final.c1"
DENSITY 6250
REEL    sgydisk 100     3581
LIST
**
** ---- PATCH MUTED TRACES BY COMPUTING MEAN ------------------------
-
*CALL   PATCH           SHOT    10
TRACES
0       1499    104     103     105     104     103
0       1499    114     113     115     114     113
1111    12000   144     143     145     144     143
6919    12000   154     153     155     154     153
0       1499    155     154     156     155     154
.
.
.
```

Frequency Filter

Spectral analysis of the data, visual inspection of the raw record and various tests confirmed that the signal frequency is approximately 6-7 Hz. Figure 9 shows an amplitude spectrum test over several traces in noise only and signal areas of the record for station 77. At the low end of the spectrum, the wave noise is at ~2 Hz, while at the high end, no useful contribution to the signal occurs above ~12 Hz.

For plotting of the data for digitisation, we used a minimum phase bandpass filter of 5 - 10 Hz attenuating gradually at the low end at 24 dB/octave and at the high end at 40 dB/octave.

A typical DISCO job segment for this stage is given below:

```
*CALL   FILTER  shot                            MINIMUM
KEYDEF  1
BANDSL  BP      OCTSL
1               5       24      10      40
```

Trace Stacking

DISCO allows several methods of summing traces, and tests were performed to find an optimum stack to improve signal to noise ratio. These tests included:

- running triangular tapered mean stack from 3 to 40 traces,
- Nth root stack for N = 2, 3, 4,
- median stack, and
- mean followed by median stack

In particular, the target area was the region of high noise from shots 500-1000, in an attempt to reveal the continuity of deep crustal refractors across this range of shots.

None of the methods were especially useful over this problem region. For plotting of the data for digitisation, the 'mildest' stacking process (3 trace tapered mean) was used at far offsets where the 8 km/s time scale reduction resulted in near zero-slope events.

A typical DISCO job segment for this stage is given below:

```
*IF
RANGE    shot     100      1140
*CALL    RUNMIX   3
WEIGHTS
1        2        1
*RESET
**
*IF
RANGE    shot     3080     3581
*CALL    RUNMIX   3
WEIGHTS
1        2        1
*RESET
```

Trace Equalisation

AGC was used to equalise trace amplitudes for plotting.

A typical DISCO job segment for this stage is given below:

```
*CALL    AGC      1500
```

F-K Filter

The data recorded on the Petrel line are mostly of a very high quality. Occasionally noise bands appear in the data which interrupt smooth correlation of seismic phases. The origin of this noise remains poorly understood. Noisy bands in the data seem to correlate with specific real time intervals rather than with location of an OBS or seismic properties near sources. The noise varies in frequency composition and amplitude which suggests its different origin, but no reasonable explanation of the nature of this noise has been suggested so far.

On the other hand the direct water wave and other low-velocity waves are serious obstacles for tracking reflections at offsets close to the source. These waves have higher amplitudes compared to the primary reflections.

Thus there are at least 2 separate tasks in attempting to improve data quality:

- To reduce the noise level within the occasional noise bands on the basis of frequency and apparent velocity analysis. Spatial and time distribution of the noisy bands must be also taken into consideration.

- To reduce the level of low-velocity arrivals masking the primary reflections at close offsets thus improving the tracking of the primary reflections. This in turn will provide reflection travel times at small offsets. The possible correlation of near-vertical and wide-angle reflections will determine the origin of the reflections at large (more than ~5 s) times.

Improving signal/noise ratio within noisy bands

Several types of noise were identified after analysis of the noisy bands performed for all 15 OBSs on the Petrel line. A module of the DISCO commercial seismic processing package, FKANALYZ, was used to analyse frequency and velocity composition of the noisy bands. This module performs FK-analysis of the data as a result of a double Fourier transform, along frequency and wave number variables. Analysis can be performed for any time and spatial window requested by the user. The result can be plotted as a two-dimensional (frequency and wave number) distribution of the seismic energy (Figure 10). Analysed time frequencies vary from 0 to Nyquist frequency. Note that in Figure 10 frequency axis is limited to 18 Hz. Spatial frequencies are represented by wave numbers which vary from the negative to positive Nyquist wave number.

The relationship between the parameters involved is defined by:

$$V = F/K$$

where V = apparent velocity, F = frequency and K = wave number.

Figure 10

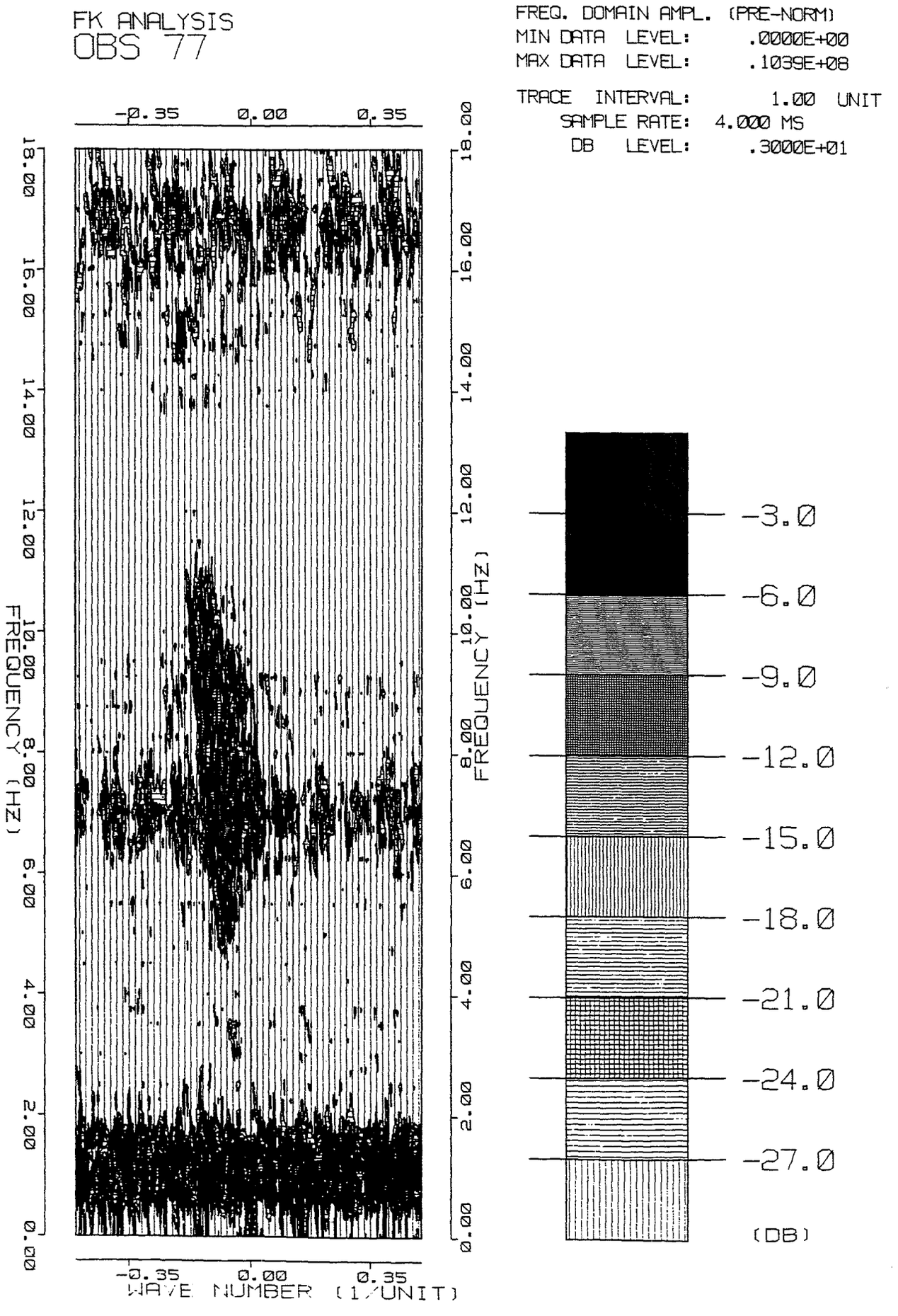
FK ANALYSIS
OBS 77
CDP RANGE: 1100 - 1260
TIME RANGE: 18000 - 22000 MS
FREQ. DOMAIN AMPL. (PRE-NORM)
MIN DATA LEVEL: .0000E+00
MAX DATA LEVEL: .1039E+08
TRACE INTERVAL: 1.00 UNIT
SAMPLE RATE: 4.000 MS
DB LEVEL: .3000E+01
-0.35
0.00
0.35
FREQUENCY (HZ)
18.00
16.00
14.00
12.00
10.00
8.00
6.00
4.00
2.00
0.00
WAVE NUMBER (1/UNIT)
-3.0
-6.0
-9.0
-12.0
-15.0
-18.0
-21.0
-24.0
-27.0
(DB)

Wave number in the FKANLYZ plot is expressed in 1/UNIT values, where UNIT is trace increment in metres. Trace increment in our specific survey equals to the shot increment, 100 m. So to get the correct estimate of the apparent velocity of any slope in Figure 10 we have to divide a value taken from the horizontal axis by 100 m. For example, wave number value of 0.3 in Figure 11 translates into 0.003 m^{-1} (=0.3/100) and after dividing a frequency of 18 Hz by a wave number of 0.003 m^{-1} we arrive at the correct value of apparent velocity of 6000 m/s represented by the bold line in Figure 11.

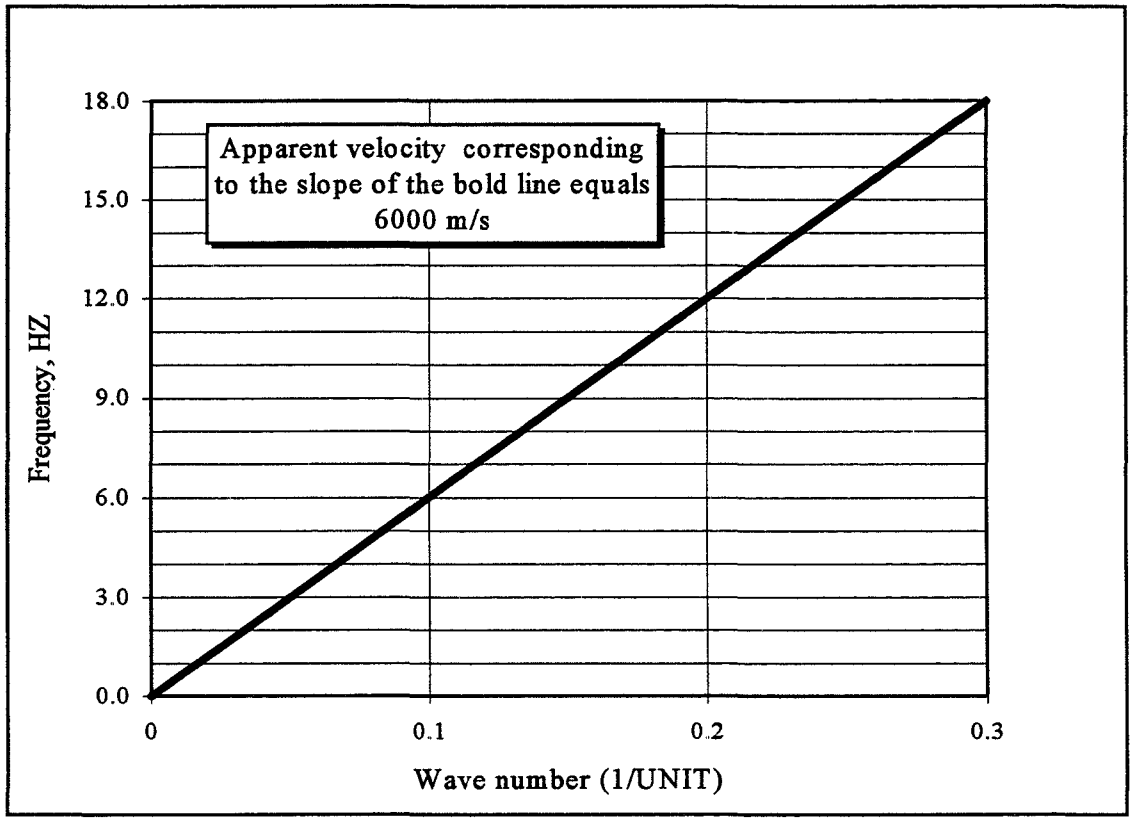

Figure 11 - Apparent velocity

So the slope of any line in the FK plot corresponds to the apparent velocity of corresponding seismic energy; low slopes (close to the horizontal axis) correspond to low apparent velocities, steep slopes (close to the vertical axis) correspond to high apparent velocities; the vertical axis itself represents infinite apparent velocity. FK analysis is a powerful tool to distinguish between useful seismic energy and noise or between different types of seismic energy because any two types of seismic energy which have similar frequency composition may have different velocity composition which gives an additional parameter to distinguish them.

In the case of OBS data the frequency spectrum of the noise often coincides with that of the seismic signal but the noise is not coherent. This enables easy detection of the signal on the basis of its velocity characteristics.

The results of the FK analysis of noisy bands where seismic signal may be completely obscured can be summarised as follows:

- Alternating bands of spatially narrow low frequency (2 Hz) noise and spatially wide wide-spectrum (5-18 Hz) noise have been observed for all OBSs.

- Spatial boundaries of noise bands of different spectra correspond to certain shot numbers for most OBSs.

Spectral characteristics of noisy bands on Petrel line record sections are summarised in Table 13.

Table 13 - Spectral characteristics of noisy bands on Petrel line record sections

Shot numbers	Length of intervals, km	Predominant frequencies, Hz	On which OBSs observed
100-200	10	5-18	76-83
200-400	20	2	69, 76-83
400-1000(1100)*	60	5-18	78-83
1000(1100)-1200(1300)	20-30	2	74-83
1200(1300)-1800(1900)	60	5-18	74-80
1800(1900)-2100(2200)	20-30	2	68-83
2100(2200)-2500(2600)	40-50	5-18	69-79
2500(2600)-2700(2800)	20-30	2	69-80
2700(2800)-3200	40-50	5-18	69-79
3200-3580	38	2	71-79, 82-83
*Numbers in brackets indicate variation in spatial boundaries			

Two types of spatially alternating noisy bands of different spectra have been identified which essentially differ in the sharpness of their spatial boundaries (Figure 12). Several types of noise were identified and systematised according to their spectra (Figure 13). High frequency noise (shown in italics in Figure 13) does not dominate over signal which has lower frequencies (6-10 Hz).

The existence of noise bands of different spectra in an alternating pattern (ABABA...) is typical for most OBSs and it is correlated to certain shot numbers (Table 13). Shots were fired during the survey in sequential order and each shot corresponds to a certain moment in real time.

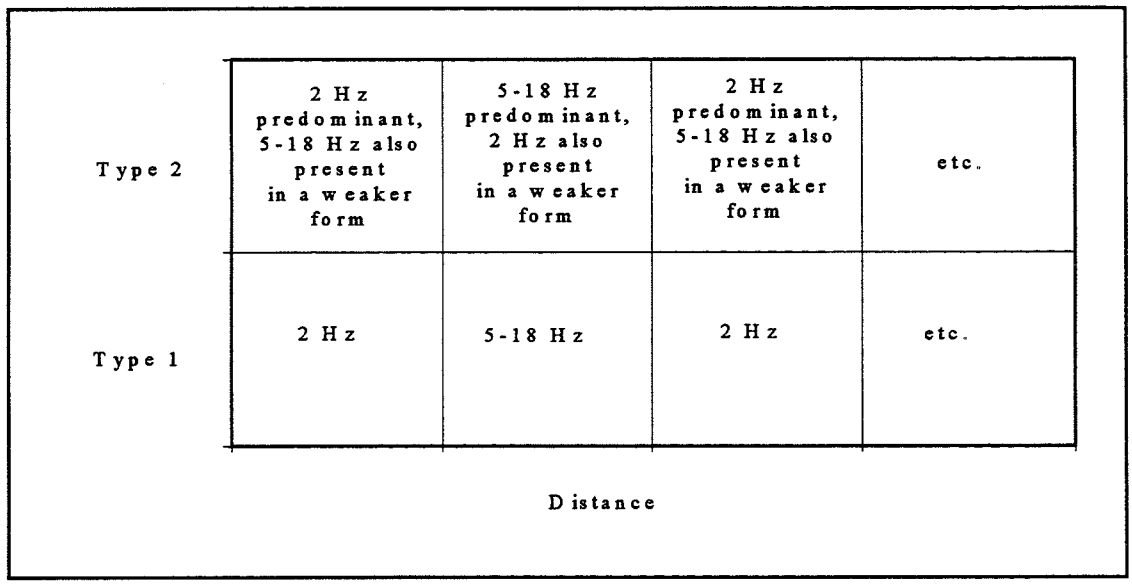

Figure 12 - Types of spatial alteration of noisy bands

This suggests that various types of noise correspond to temporary processes which vary with time such as ship traffic and weather conditions.

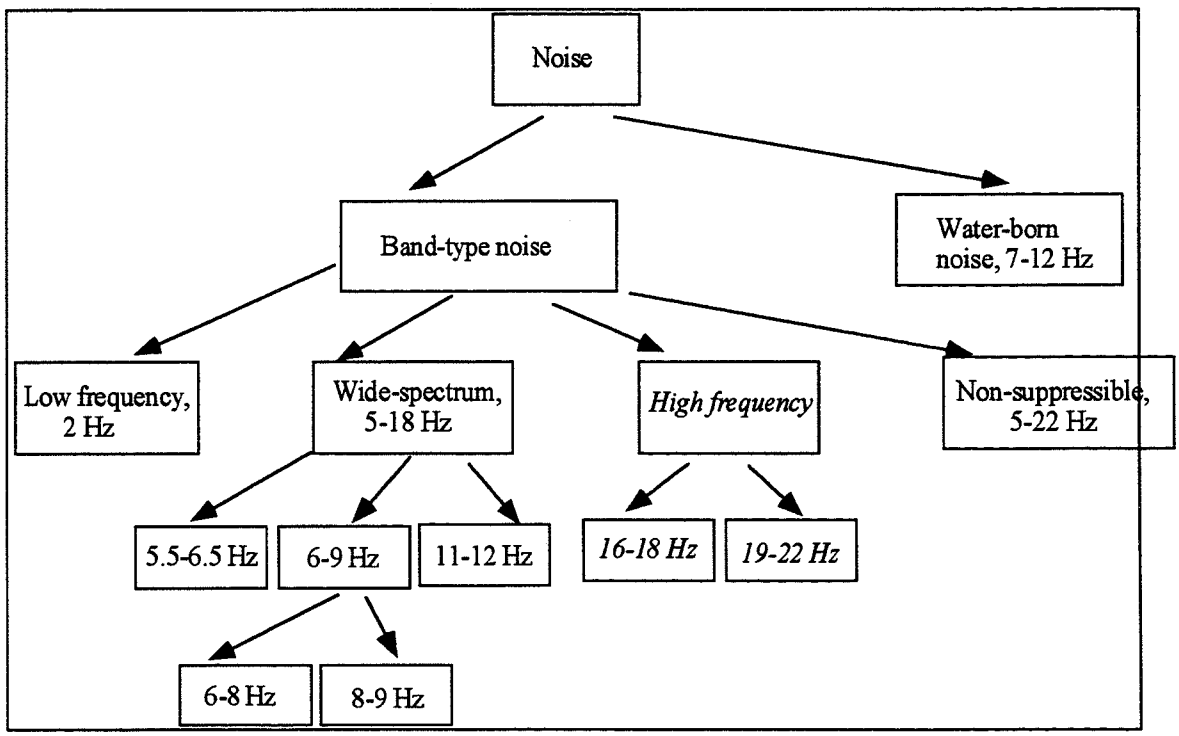

Figure 13 - Types of noise

Low frequency (2 Hz) noise and one of the sub-types of wide-spectrum noise (11-12 Hz, Figure 13) which appear to be most stable may originate from some instrumental problems in the recorders.

Studying the nature of various types of noise in the OBS experiments may be a theme of separate research. For our purposes we were mostly interested in improving signal/noise ratio regardless of the type of noise.

FK-filters were designed on the basis of FK-analysis.

Original SEG-Y files produced by OBSTOOL contained data in a time scale reduced by a velocity value of 8 km/s:

$$\text{Reduced time} = \text{Time} - \text{Distance}/8.0$$

Because of this reduction, velocity values estimated from the FK-analysis were distorted. It is important to understand the nature of this distortion. Firstly, mantle refractions recorded at offsets of more than 100 km, and characterised by apparent velocities of 8 km/s, will be translated into velocities with infinite apparent velocities. Consequently this type of seismic energy will be concentrated close to the frequency axis in the FK-plots. This is where reflected energy normally concentrates when FK analysis is applied to conventional reflection data recorded at relatively small offsets. Secondly, near-vertical reflections which are recorded in the OBS survey look like waves with negative apparent velocities in a certain range of offsets. Consequently there is the likelihood that they will be indistinguishable from other types of seismic energy characterised by negative slopes if FK-analysed after time reduction (e.g. PMP near- but pre-critical reflections recorded at larger offsets, and Pn mantle refractions recorded up the dip of the Moho).

To avoid artifacts which may appear in the FK-plots as a result of the time reduction, the OBS data were "de-reduced" (ie, true time restored) prior to the FK-analysis.

This was achieved by writing values of "negative reduced time" (Distance/8.0 - time) into the SHT-STAT field of the trace headers with the help of HDRMATH module. The "negative reduced time" so defined was treated as a distance dependant static correction and the STATIC module was used to apply these corrections to traces.

A side-effect of these modifications was that the trace length of 20 s prior to the dereduction was increased to 45 s, and the de-reduced data had to be re-read prior to writing to the disk. The new trace length of 45 s was indicated as a parameter for GIN module which was used to reload the data into the system after the de-reduction.

A shortcoming of the FKBUILD module is that the FK-filter can not be applied to a specified time window and the total length of the trace has to be filtered which increases time consumption for the processing. For trace lengths of more than 32 s FK filtering can not be performed because of lack of computer memory and we had to limit de-reduced trace lengths to 0-32 s window only. This was enough for practical purposes.

The FKBUILD module was used to create FK-filters. These filters can be designed to pass or reject seismic energy of specified frequencies and apparent velocities. FK analysis of a time-distance interval neighbouring a noise band (Figure 14) was performed as well as the FK-analysis of the noise band itself (Figure 15). On the basis

of these analyses, an FK-filter was created which rejected everything except the frequency/velocity domain corresponding to the useful seismic signal. This frequency/velocity domain estimated from the pre-noise-obscured time/distance interval was assumed to remain unchanged within the noise-obscured interval of the data. The useful seismic signal generally has a stable frequency spectrum of 6-10 Hz and so the FK-filter passband was set to 6-9 Hz. In specific cases individual FK-filters were designed to suppress noise with significant overlap over the signal spectrum.

OBSTOOL was used to digitise the travel times after FK-filtering. These picks supplement those taken from the original band-pass filtered data. The level of the data improvement after the FK-filtering, compared to the band-pass filtering only, is illustrated by Appendix 11 where the supplementary and pre-existing picks are shown.

Results of the FK-filtering applied to improve the OBS data recorded on the Petrel line can be summarised as follows:

- Generally FK-filtering was an effective tool for improving signal/noise ratio.

- If the signal can be detected as a result of the FK-analysis it will become clearer after FK-filtering even in case when time frequencies of signal and noise overlap and signal is not visible in the original record sections (Figure 16 - prior to the FK-filtering, Figure 17 - after it).

- If the FK-analysis does not detect the signal within the noise band, then it will not become visible after FK-filtering. Remarkably it appeared to be so even in cases when the prevailing noise frequencies did not overlap those expected for the signal, ie 6-10 Hz. Obviously this can be explained by a very poor signal/noise ratio typical for the original data in such cases.

- In some cases noise of certain spectra and amplitude masks the signal completely, in other cases similar or identical noise does not do this which may be due to the variation of the amplitude level of the signal itself. This level certainly varies depending on specific seismo-geological conditions and distance from the source.

- Complete masking of the signal by noise bands was never observed at small offsets where the signal amplitude is high.

- In some cases we were forced to apply very narrow band-pass filters to delineate the signal which resulted in creation of false coherency. In such cases a subjective factor in identifying arrivals may not be excluded and the interpreter has to be very careful. Interpolation of arrivals from both sides of noise bands may be helpful in distinguishing false and true coherency in such circumstances.

Figure 14

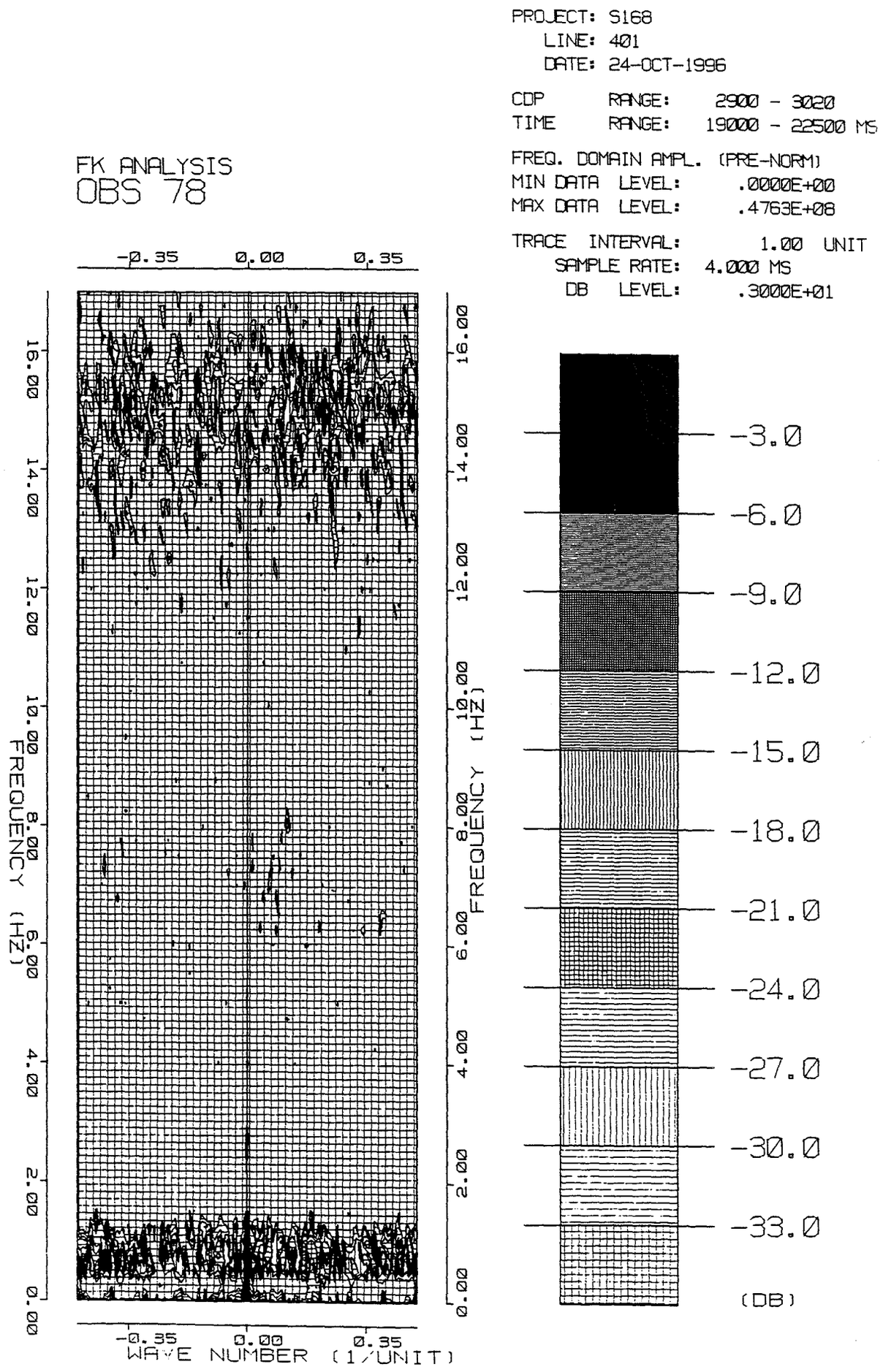
PROJECT: S168
LINE: 401
DATE: 24-OCT-1996
CDP RANGE: 2900 - 3020
TIME RANGE: 19000 - 22500 MS
FREQ. DOMAIN AMPL. (PRE-NORM)
MIN DATA LEVEL: .0000E+00
MAX DATA LEVEL: .4763E+08
TRACE INTERVAL: 1.00 UNIT
SAMPLE RATE: 4.000 MS
DB LEVEL: .3000E+01
FK ANALYSIS
OBS 78
-0.35
0.00
0.35
16.00
14.00
12.00
10.00
8.00
6.00
4.00
2.00
0.00
FREQUENCY (HZ)
-3.0
-6.0
-9.0
-12.0
-15.0
-18.0
-21.0
-24.0
-27.0
-30.0
-33.0
(DB)
WAVE NUMBER (1/UNIT)

Figure 15

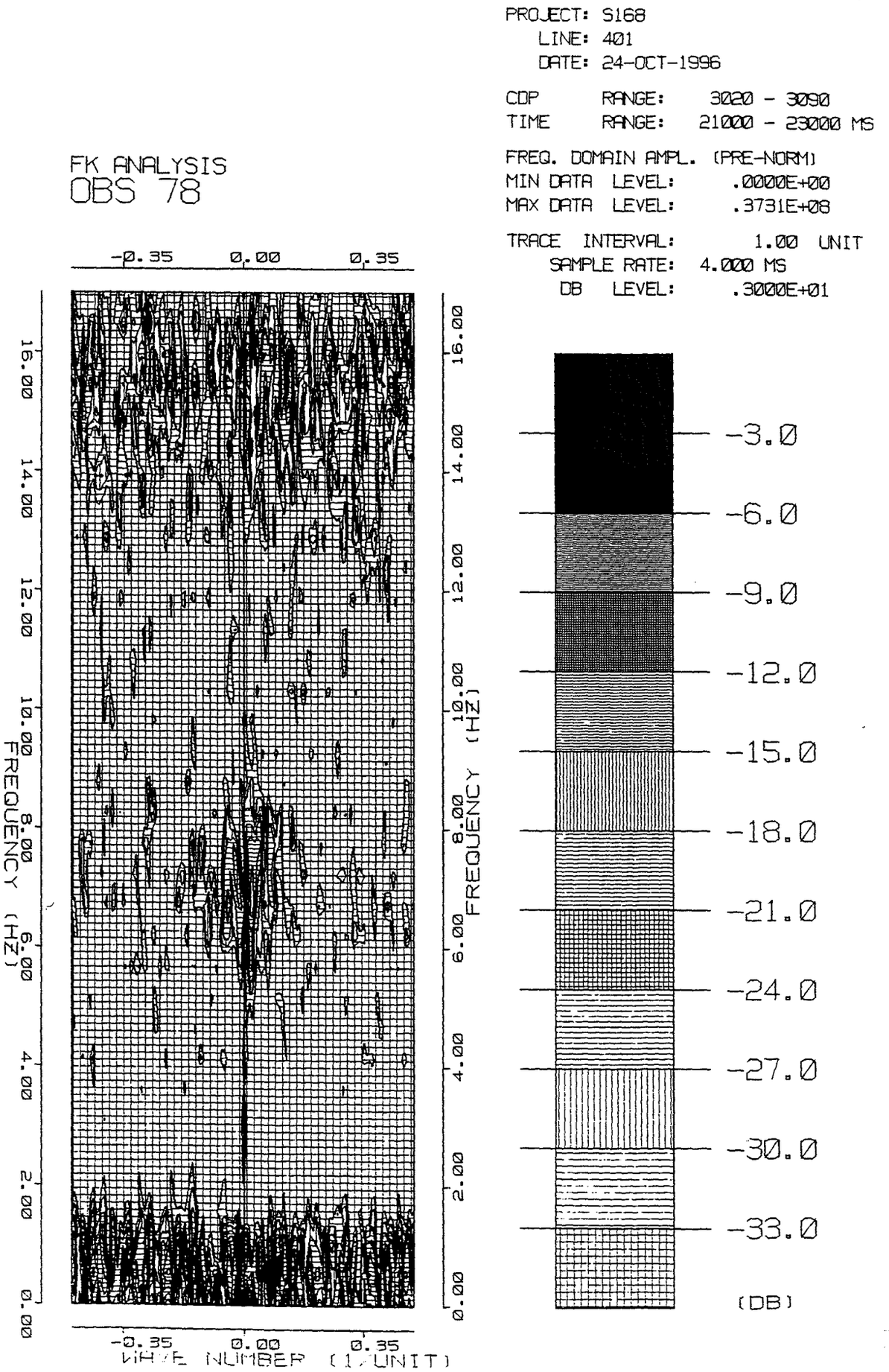
PROJECT: S168
LINE: 401
DATE: 24-OCT-1996
CDP RANGE: 3020 - 3090
TIME RANGE: 21000 - 23000 MS
FREQ. DOMAIN AMPL. (PRE-NORM)
MIN DATA LEVEL: .0000E+00
MAX DATA LEVEL: .3731E+08
TRACE INTERVAL: 1.00 UNIT
SAMPLE RATE: 4.000 MS
DB LEVEL: .3000E+01
FK ANALYSIS
OBS 78
-0.35
0.00
0.35
16.00
14.00
12.00
10.00
8.00
6.00
4.00
2.00
0.00
FREQUENCY (HZ)
-3.0
-6.0
-9.0
-12.0
-15.0
-18.0
-21.0
-24.0
-27.0
-30.0
-33.0
(DB)
WAVE NUMBER (1/UNIT)

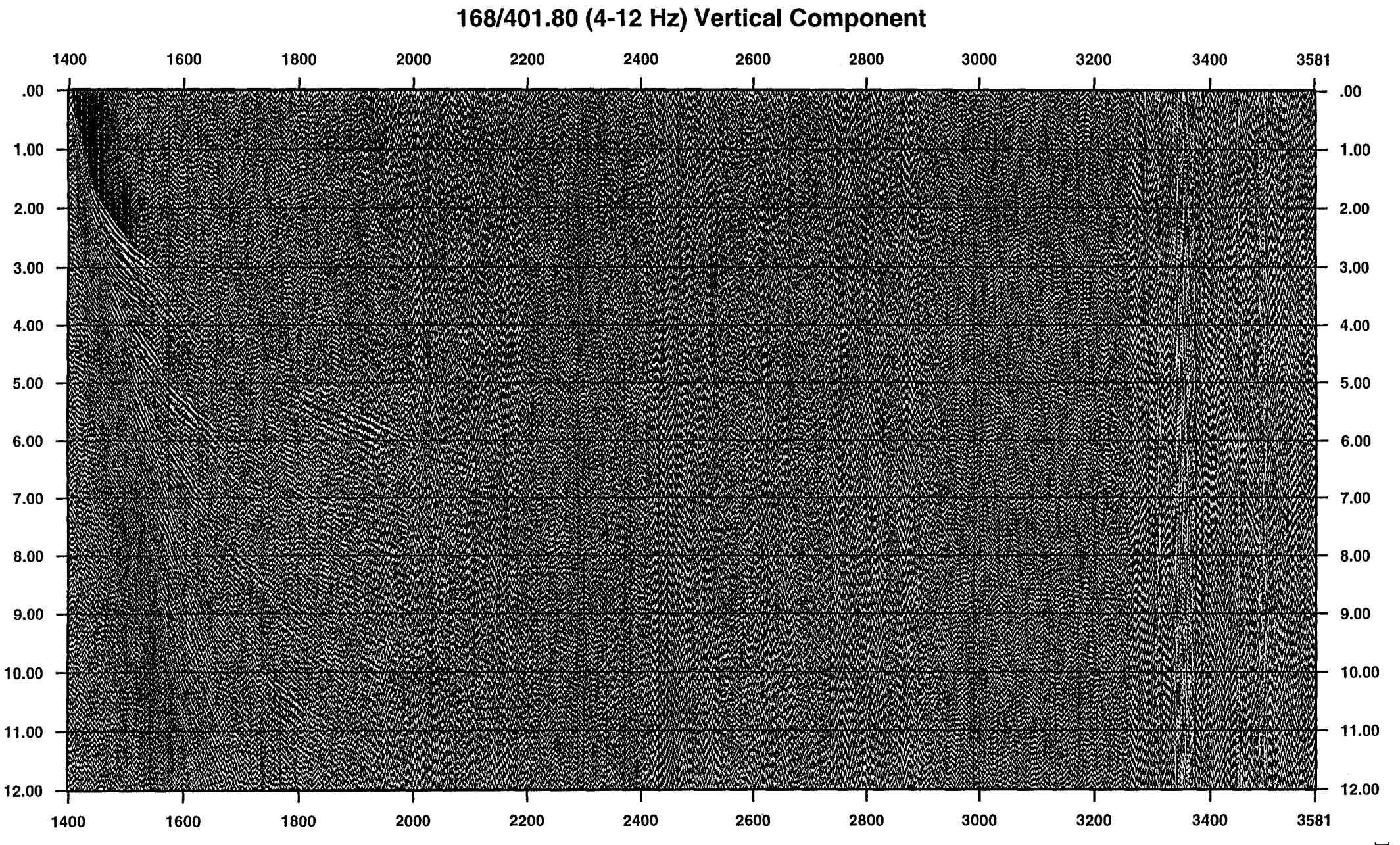
168/401.80 (4-12 Hz) Vertical Component
1400
1600
1800
2000
2200
2400
2600
2800
3000
3200
3400
3581
.00
1.00
2.00
3.00
4.00
5.00
6.00
7.00
8.00
9.00
10.00
11.00
12.00

Figure 16

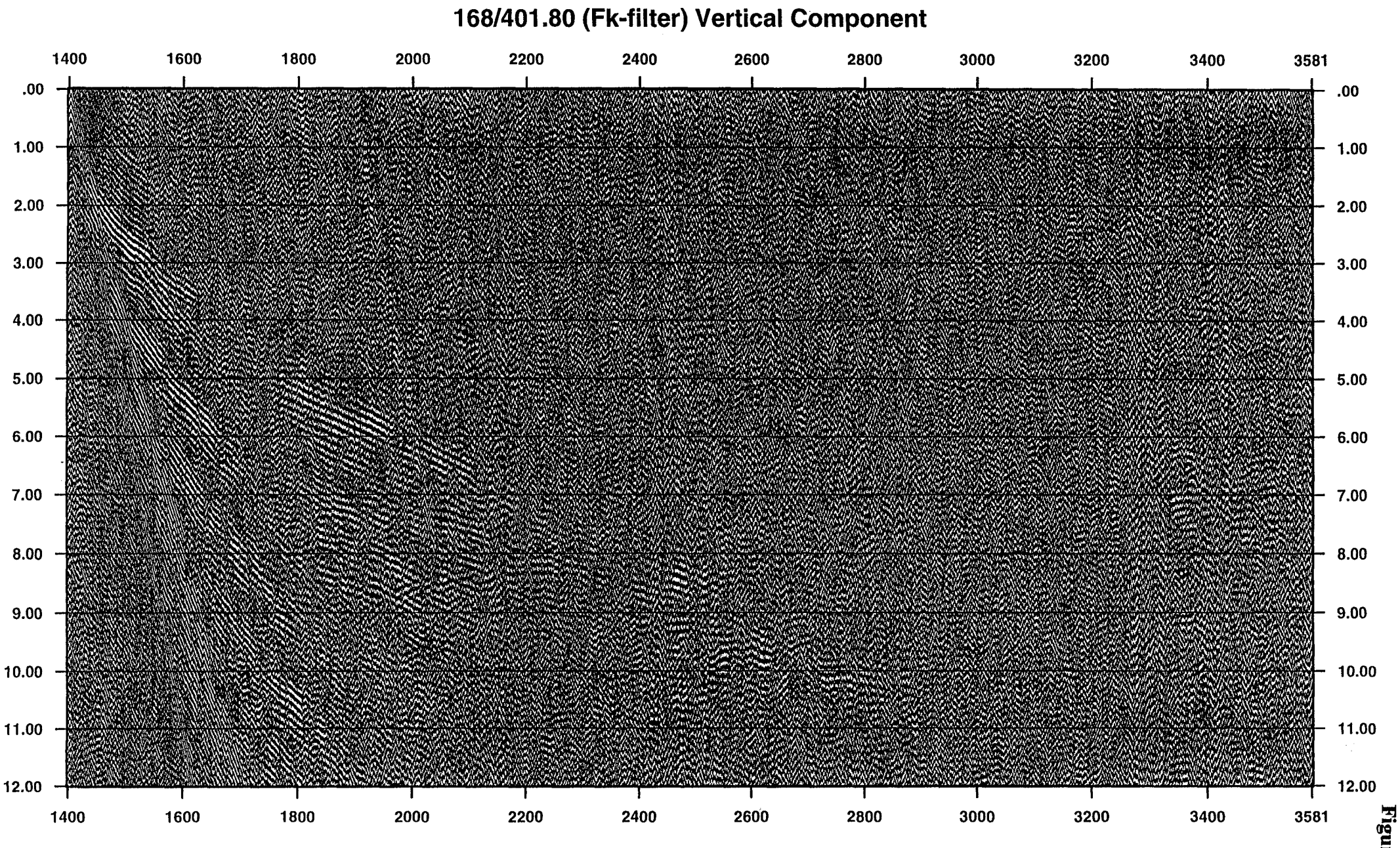
168/401.80 (Fk-filter) Vertical Component
1400
1600
1800
2000
2200
2400
2600
2800
3000
3200
3400
3581
.00
1.00
2.00
3.00
4.00
5.00
6.00
7.00
8.00
9.00
10.00
11.00
12.00

Figure 17

Suppression of low velocity noise at small offsets

The task of suppressing low velocity and water wave energy recorded at small offsets where it can mask near-vertical reflections, seemed to be simple and obvious. In reality this turned out to be not so.

Suppression of the water-borne and other low velocity energy was supposed to reveal reflections from deep boundaries in the crust. The same FK-filtering methodology was applied to do this job as the one used to improve signal/noise ratio in the band-type noise environment. In this case FK-filtering was aimed at the separation of energy with contrasting apparent velocities: less than 2 km/s for the noise to be suppressed, and 5 km/s and higher (up to infinite apparent velocities) for the expected deep near-vertical reflections. Unfortunately low velocity energy appeared to be too strong compared to weaker near-vertical reflections and none of the FK-filters applied suppressed this energy sufficiently (Figure 18).

This can be illustrated by the results presented in Figure 19 and Figure 20. They both show results of the FK-analysis performed for the same time-spatial window which was 80 km wide and centred around the OBS 78. Time length of the window was from 7 to17 s. The only difference between the FK-plots presented in Figure 19 and Figure 20 is that the first one has a dynamic range of 30 dB while the second one corresponds to 36 dB dynamic range. In the first case (Figure 19) the area near the vertical axis where reflected energy normally concentrates appears to be blank, while in the second case some energy is visible there (Figure 19). This confirms that difference in amplitudes of near-vertical reflections and low velocity noise is more than 31.6 times (equivalent to 30 dB) and it may reach 63 times (equivalent to 36 dB). Obviously this is too much for effective suppression of the low-velocity noise by the FK-filtering.

Remnants of the low velocity energy after FK-filtering are still strong enough to hide possible continuations of near vertical reflections to larger offsets where they come closer to the first arrivals .

The same refers to the near-critical reflections from the Moho (marked as PMP in Figure 21): in most cases they are quite distinctive at ~40 km offset but it is impossible to trace them through the under-suppressed low velocity energy back to the source and to relate them directly to any of the distinctive near-vertical reflections. These latter ones remain no more than good candidates to be near-vertical reflections from the Moho. But they can also be multiples from some of the shallower boundaries. The travel times of these waves are plotted in Figure 22. Further modelling of the travel times and amplitudes of these arrivals may help to constrain their origin more accurately.

FK-filtering applied to the OBS data from the Petrel line improved the data in several important ways. Additional travel times have become available for picking and using these will improve the velocity model of the region.

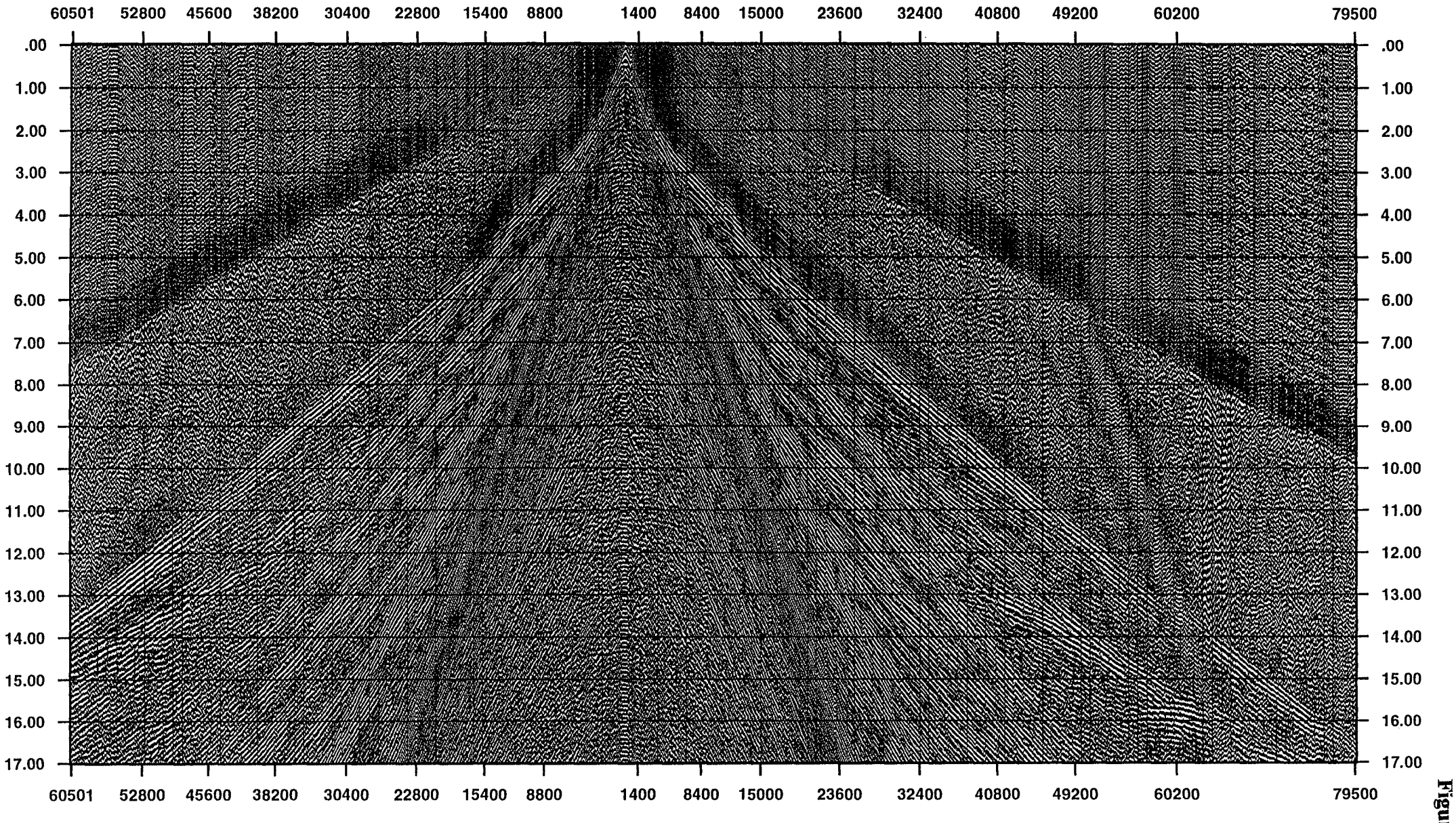
168/401.78 FK filter Vertical Component
60501 52800 45600 38200 30400 22800 15400 8800 1400 8400 15000 23600 32400 40800 49200 60200 79500
.00 1.00 2.00 3.00 4.00 5.00 6.00 7.00 8.00 9.00 10.00 11.00 12.00 13.00 14.00 15.00 16.00 17.00
60501 52800 45600 38200 30400 22800 15400 8800 1400 8400 15000 23600 32400 40800 49200 60200 79500

Figure 18

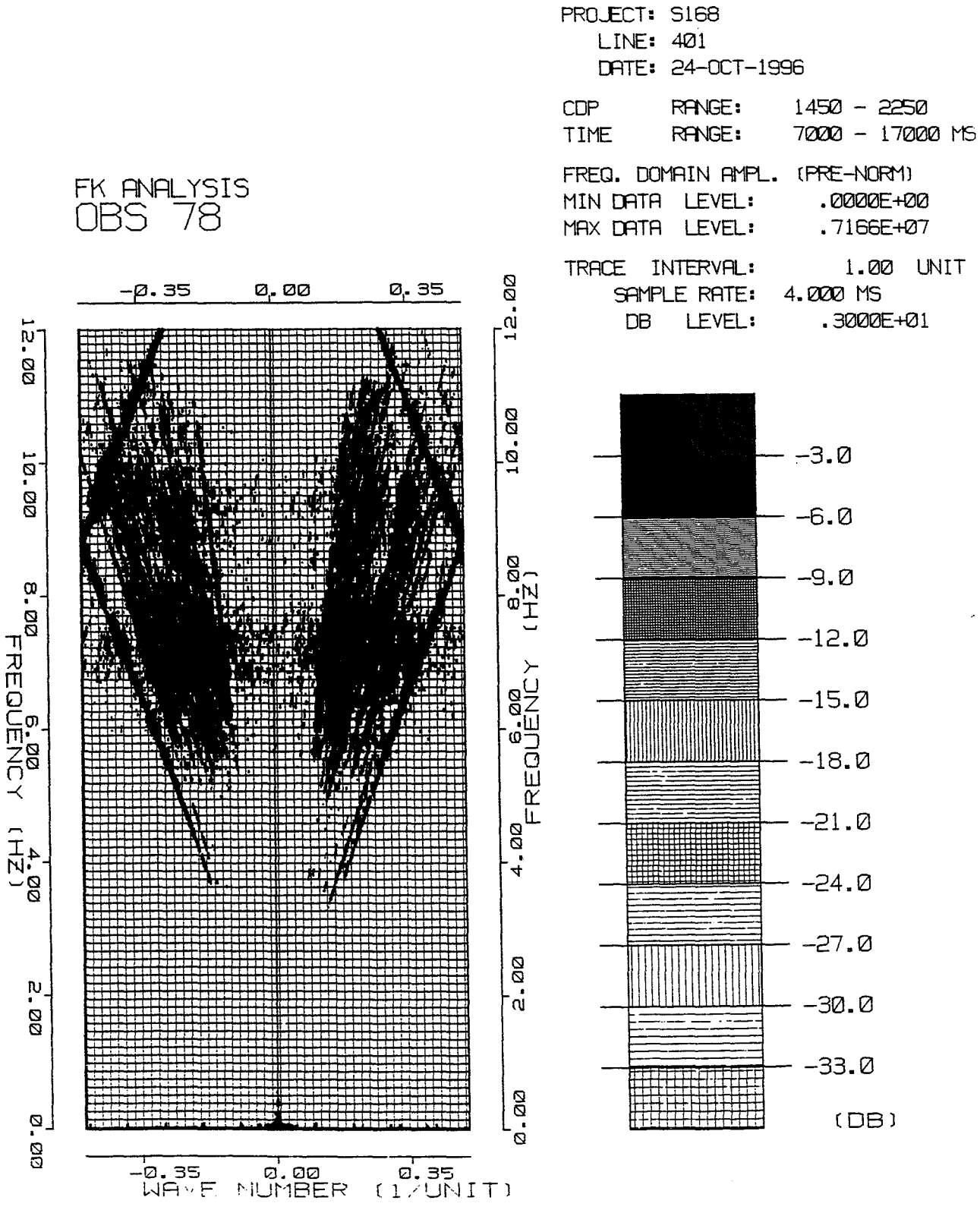
PROJECT: S168
LINE: 401
DATE: 24-OCT-1996
CDP RANGE: 1450 - 2250
TIME RANGE: 7000 - 17000 MS
FREQ. DOMAIN AMPL. (PRE-NORM)
MIN DATA LEVEL: .0000E+00
MAX DATA LEVEL: .7166E+07
TRACE INTERVAL: 1.00 UNIT
SAMPLE RATE: 4.000 MS
DB LEVEL: .3000E+01
FK ANALYSIS
OBS 78
-0.35
0.00
0.35
12.00
10.00
8.00
6.00
4.00
2.00
0.00
FREQUENCY (HZ)
WAVE NUMBER (1/UNIT)
-3.0
-6.0
-9.0
-12.0
-15.0
-18.0
-21.0
-24.0
-27.0
-30.0
-33.0
(DB)

Figure 20

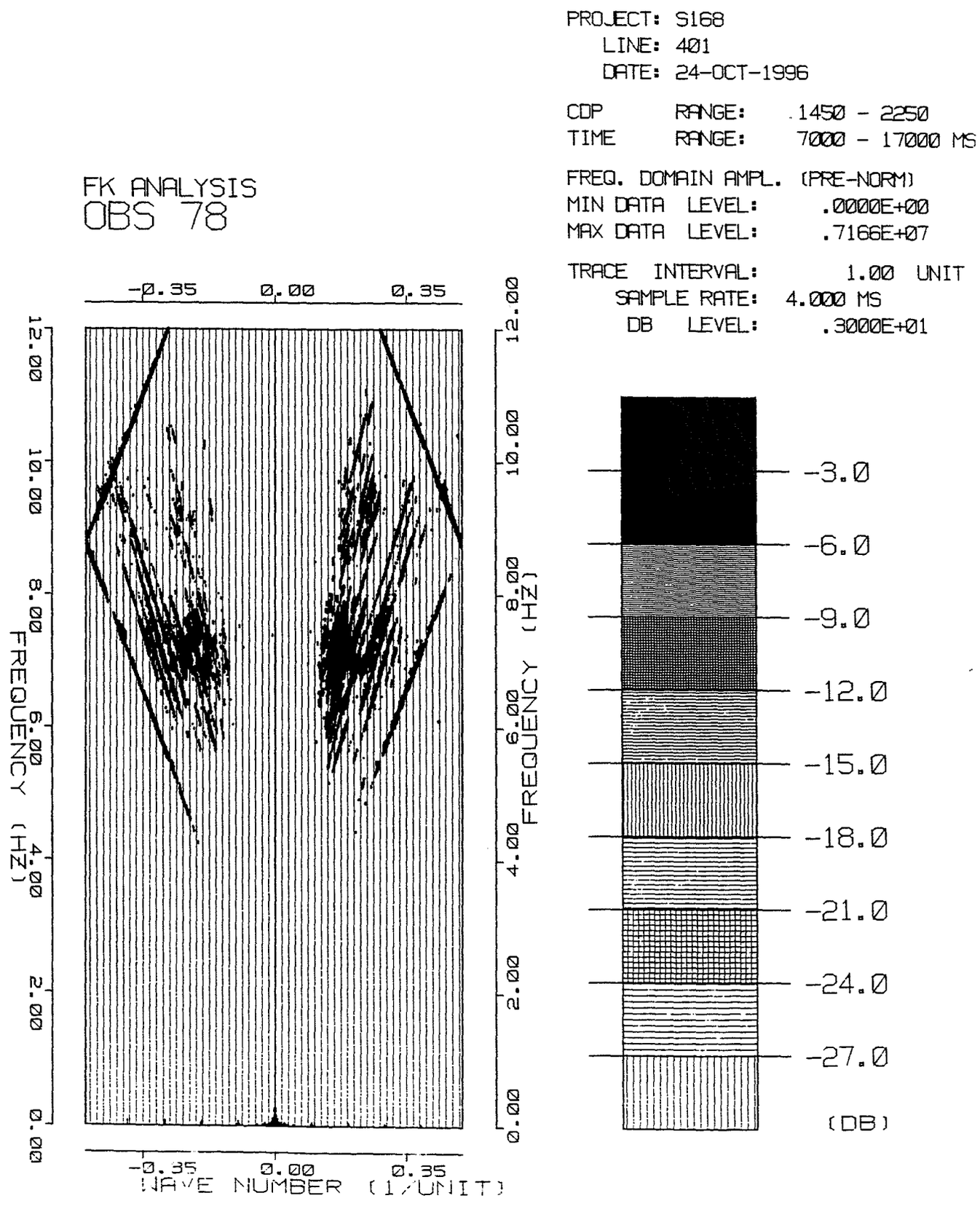
PROJECT: S168
LINE: 401
DATE: 24-OCT-1996
CDP RANGE: 1450 - 2250
TIME RANGE: 7000 - 17000 MS
FREQ. DOMAIN AMPL. (PRE-NORM)
MIN DATA LEVEL: .0000E+00
MAX DATA LEVEL: .7166E+07
TRACE INTERVAL: 1.00 UNIT
SAMPLE RATE: 4.000 MS
DB LEVEL: .3000E+01
FK ANALYSIS
OBS 78
-0.35
0.00
0.35
12.00
10.00
8.00
6.00
4.00
2.00
0.00
FREQUENCY (HZ)
WAVE NUMBER (1/UNIT)
-3.0
-6.0
-9.0
-12.0
-15.0
-18.0
-21.0
-24.0
-27.0
(DB)

Figure 21

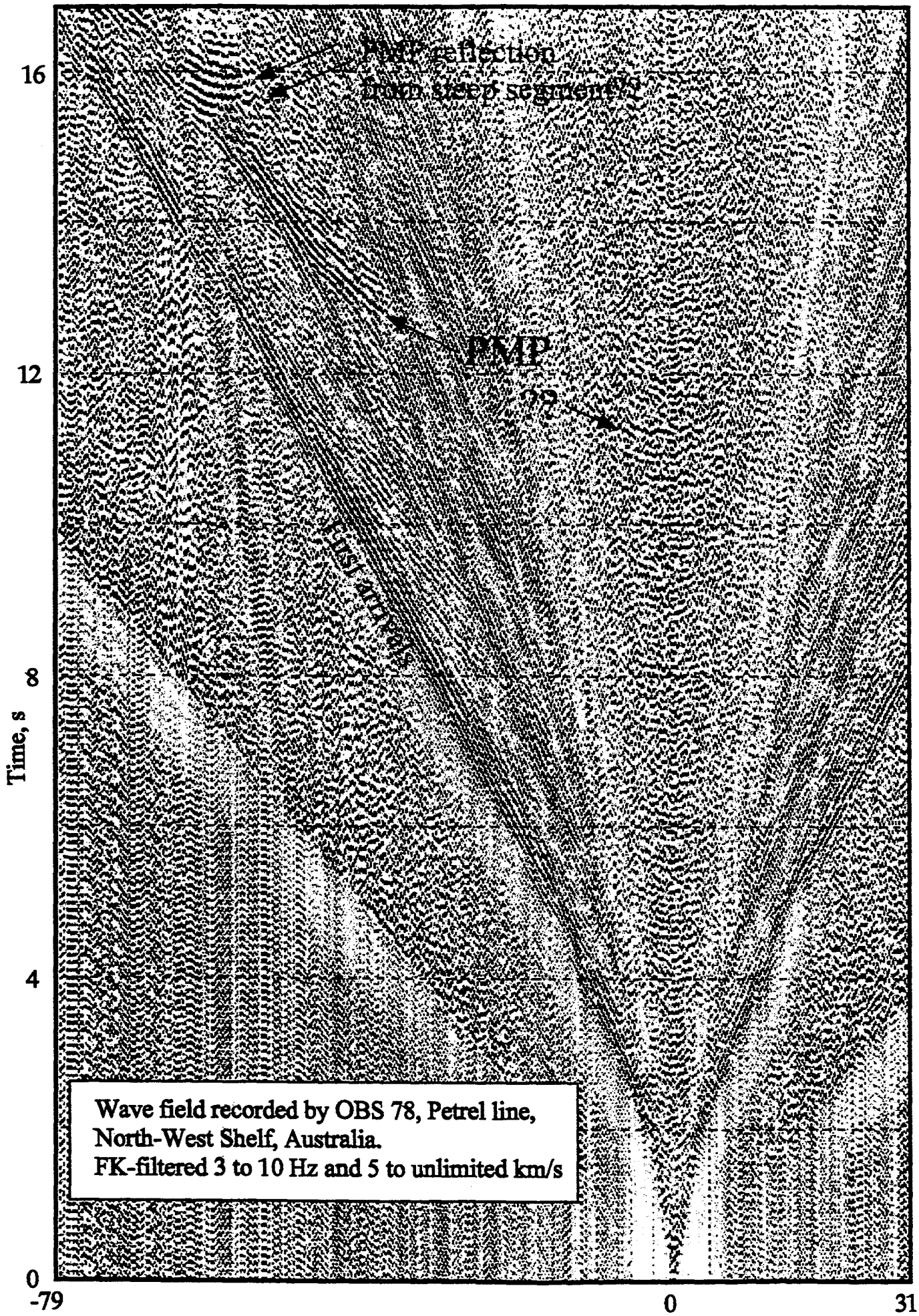
16
12
8
4
0
Time, s
-79
0
31
Distance, km
PMP
??
First arrivals
Wave field recorded by OBS 78, Petrel line,
North-West Shelf, Australia.
FK-filtered 3 to 10 Hz and 5 to unlimited km/s

Travel times of near vertical and near critical reflection from Moho
OBS 78

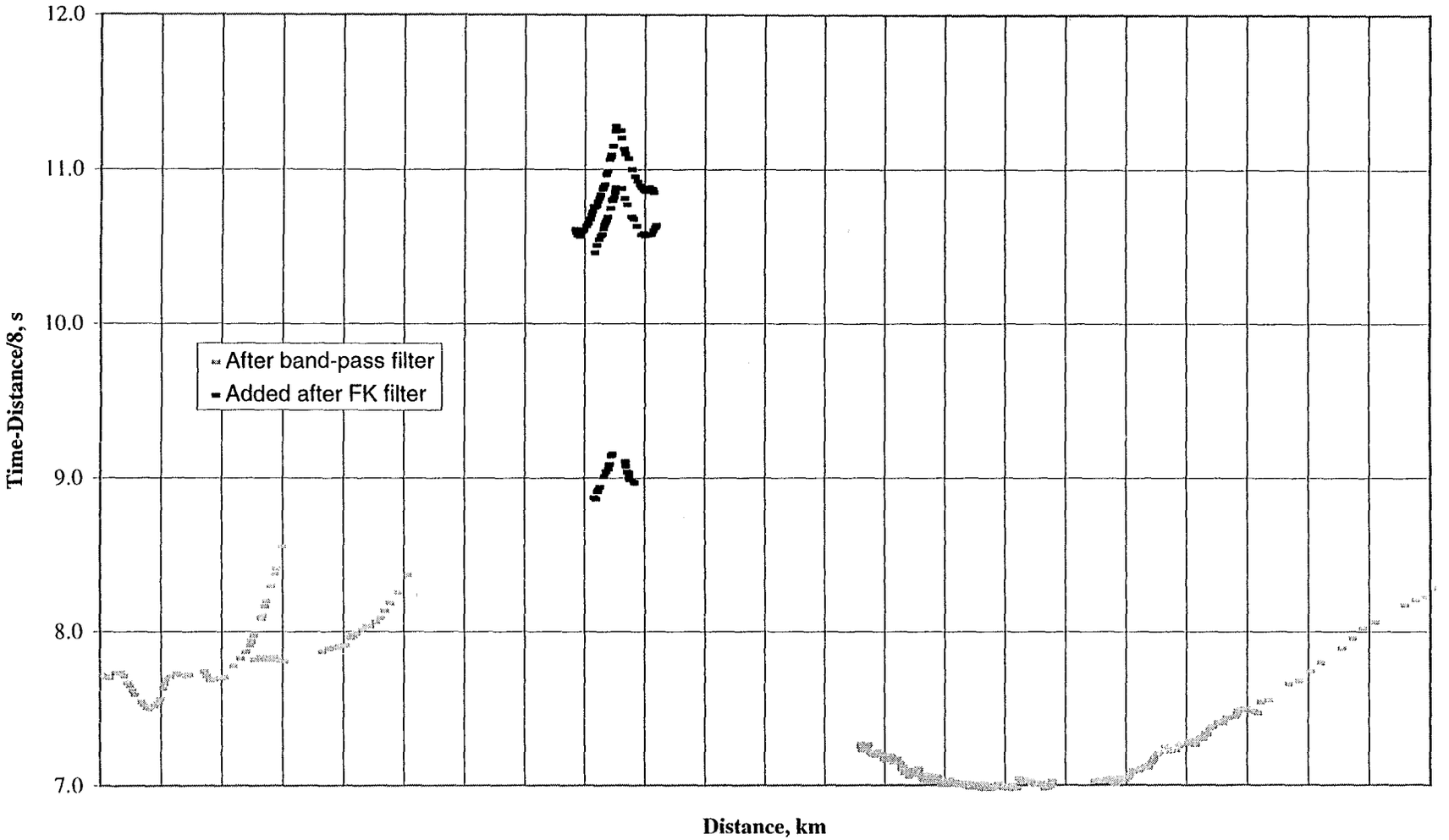

Figure 22

Polarisation processing

OBS data were recorded by three-component equipment. Conventional registration of the vertical component of the wave field was supplemented by recording two orthogonal horizontal components H1 and H2 (channel 2 and 3 following the OBSTOOL terminology).

One of the reasons for processing the horizontal components was the possibility that the noise discussed above would behave differently when recorded by horizontal geophones. This expectation proved to be wrong: noise bands observed in the record sections of horizontal components in general spatially coincide with those in the vertical component record sections. Frequency spectra of the noise recorded by vertical and horizontal channels also coincide. Nevertheless polarisation processing was useful, so the processing sequence and its preliminary results will be discussed below.

The FOCUS/DISCO seismic processing package does not handle 3-component data, and so processing was done using OBSTOOL. The data for trial processing were sourced from the original file of the OBS 78 which contained 4 - component (1 vertical and 2 horizontal geophones plus hydrophone) data in the OBS internal format. A SEG-Y file containing all 4 components was then created in OBSTOOL and it was later split into 4 separate files corresponding to each of the recorded components. Only 2 of these files corresponding to the horizontal channels were used in further processing.

Polarisation processing enables such analysis of the wave field when the selection of waves on the basis of frequency and apparent velocity is supplemented by that based on differences in polarisation and angles of emergence.

OBSTOOL performs orientation of the horizontal components in the same module which defines location of the OBS unit on the sea floor. The direct water wave which is assumed to be linearly polarised and which is recorded as first arrivals when shooting on top of the OBS is used to perform this orientation. If 3 components of the direct water wave amplitude are known, and the shot-receiver direction is also known, the orientation of horizontal channels can be performed. Orientation of the horizontal geophones on the sea floor is imporant because it enables 'rotation' of the horizontal components. This is a computational process when the full horizontal component of the seismic displacement vector is projected to the radial (shot-receiver) and transverse (orthogonal to shot-receiver) directions.

The OBSTOOL terminology is ambiguous in that H1/ H2 names (and CHANNEL 2 / CHANNEL 3 names) are used to call both original non-oriented horizontal components, and those obtained after orientation and rotation when they are supposed to become radial and transverse components rather than just 2 orthogonal horizontal ones. This ambiguity produced some confusion at the initial stages of this work.

The problem with orientation/rotation of horizontal components is that the location of the OBS on the sea floor which defines the shot-receiver direction must be defined from the same data set as the orientation of horizontal channels. Potentially this

problem depends on the solution of the over-defined system of linear equations (number of equations is greater than the number of unknowns). But all values in the equations are experimentally measured, hence contain errors. Uncertainty of the solution follows from this. The smaller the number of equations is, the greater the uncertainty of the solution becomes.

Water depth on the Petrel line was small (less than 100m). Consequently the number of shots for which the direct water wave was recorded as first arrivals was also small. This resulted in large errors in the orientation of horizontal components. So the orientation formally performed for all OBSs on the Petrel line was recognised to be unsuitable for further polarisation processing. So we had to search for another way of orientation of horizontal components.

"Forced" orientation was suggested as a substitute. During this "forced" orientation OBSTOOL was prompted to assume that azimuth of the H1 channel was 10^0 and orientation was worked out from this, then 30^0 and the exercise was repeated and so forth with a step of 20^0 up to 170^0. Keeping in mind that the angle between H1 and H2 directions is 90^0 and that rotation of the H1 (or H2) components can not be performed separately from the other one, we ended up with "forced" oriented/rotated horizontal components corresponding to azimuths:

H1:	10	30	50	70	90	110	130	150	170^0
H2:	100	120	140	160	180	200	220	240	260^0

Each of the newly created formal radial and formal transverse component record sections was plotted and assessed to define which of them was close to true radial and transverse components.

True radial component was defined as one which contained most clear and earliest arrivals of the first P-wave at small offsets (i.e. immediately after the direct water wave is replaced by it in the first arrivals). As the analysis of wave field and seismic modelling show this first P-wave is a refracted wave from the boundary with relatively small velocity contrast (~1.5/2.0 km/s), consequently it arrives at the OBS with emergent angle of $\sim 40^0$ and its amplitude should be equally represented on vertical and horizontal components given that it is linearly polarised in the direction of propagation. P-refractions recorded at larger offsets should generally arrive with steeper angles and should be less favourably recorded by horizontal geophones.

The following preliminary conclusions were derived from the analysis of the data recorded by horizontal channels:

- Direct S-wave was not identified in the record sections of the horizontal components.

- True radial component for the OBS 78 corresponds to the horizontal component which was "force" oriented to 70^0 azimuth while the water wave based orientation gave the azimuth of 150^0.

- First arrivals taken from vertical and true radial component record sections practically coincide up to 20-40 km offset (Figure 23). At large offsets (100-180 km) the earliest arrivals taken from the horizontal component are delayed up to 1.2 s compared to the earliest arrivals in the vertical component record section (Figure 24). Remarkably there are no traces of this delayed energy in second arrivals recorded by the vertical geophone. At the same time apparent velocities of the arrivals on both components are close to 8 km/s. We suggest that the arrivals recorded on the true radial component close to 8 s reduced time (Figure 25) and characterised by apparent velocity of ~8 km/s correspond to PS-converted refractions from the Moho. Propagation in P-segments of their rays will explain high apparent velocity while propagation in S-segment(s) will provide the time delay and high amplitude of the horizontal component. These considerations can be further tested by seismic modelling.

- Some reflections seen in the radial component record section between 40 and 80 km from the OBS 78 at the times of ~9.2 and ~13 s (Figure 26) are not observed in the vertical component record section, which indicates the S-nature of these arrivals in at least some of their ray segments. The wave at 13 s seems to meet kinematic criteria for a mode-converted reflection from the Moho (PMS).

- Indirect indication of the PS nature of the arrivals discussed above can be found in the results of their spectral analysis. The frequencies of PS mode converted reflections are known (Berzon, 1976) to be lower than that of the direct P waves and PP reflections. This can be explained by differencies in absorbtion of P and S-energy in the covering medium, lowering the frequencies of PS waves occurs near the converting boundary. Spectral analysis performed for the OBS 78 radial component showed that signal of 4-5 Hz is present there (Figure 27). Frequencies estimated for the similar window containing signal recorded by the vertical geophone are higher: 6-8 Hz, and lower frequencies were not detected there.

Finally we conclude that processing and analysis of horizontal component data performed for one OBS provided extra information which is valuable for general understanding of the wave field. Some information about S-waves was also obtained. From this experience we recommend that similar processing and analysis should be performed for other OBSs. This will improve the model of the crust derived from the processing and interpretation of P-waves.

Comparison of arrivals picked from vertical and horizontal components
OBS 78

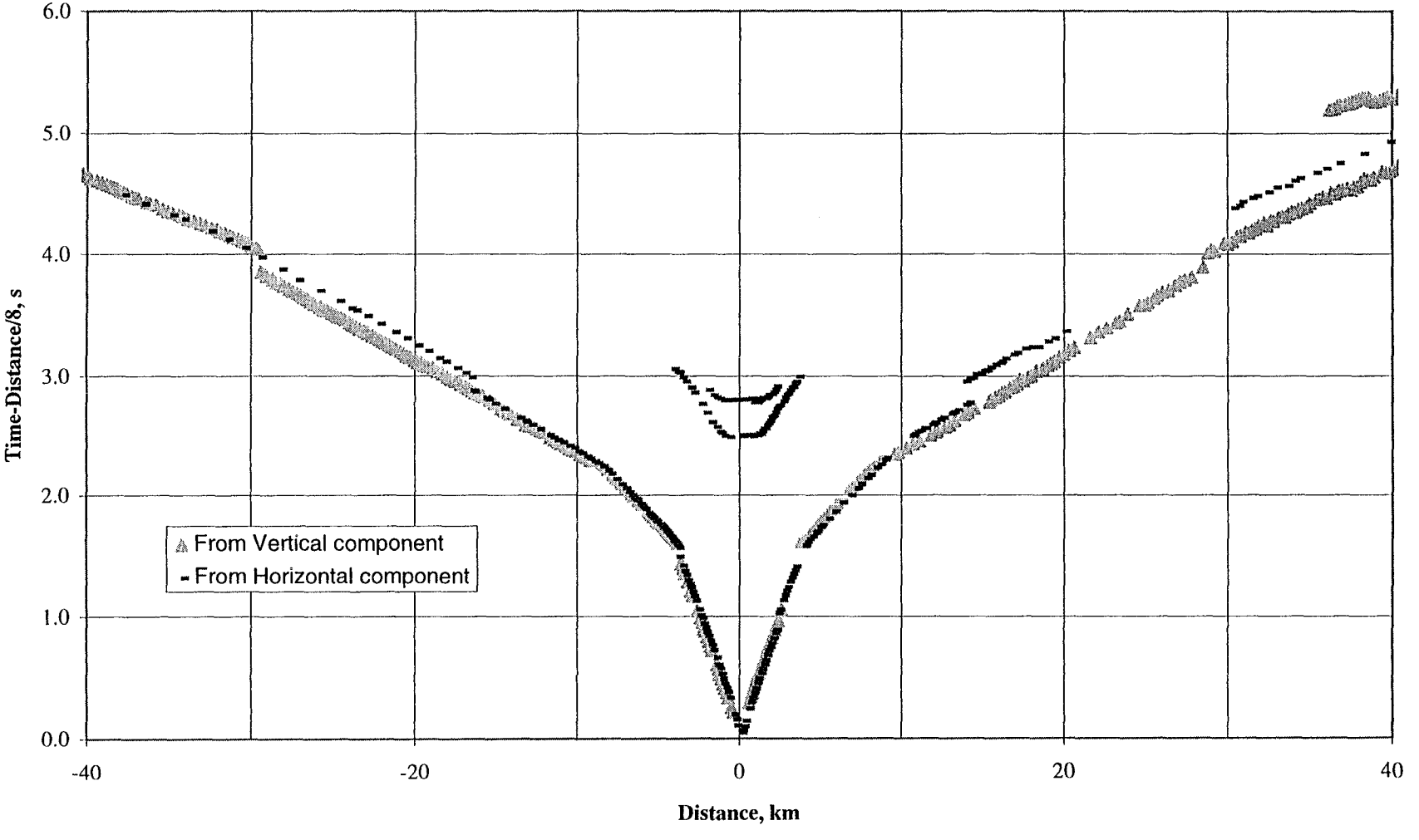

Figure 23

Comparison of arrivals picked on vertical and horizontal components
OBS 78

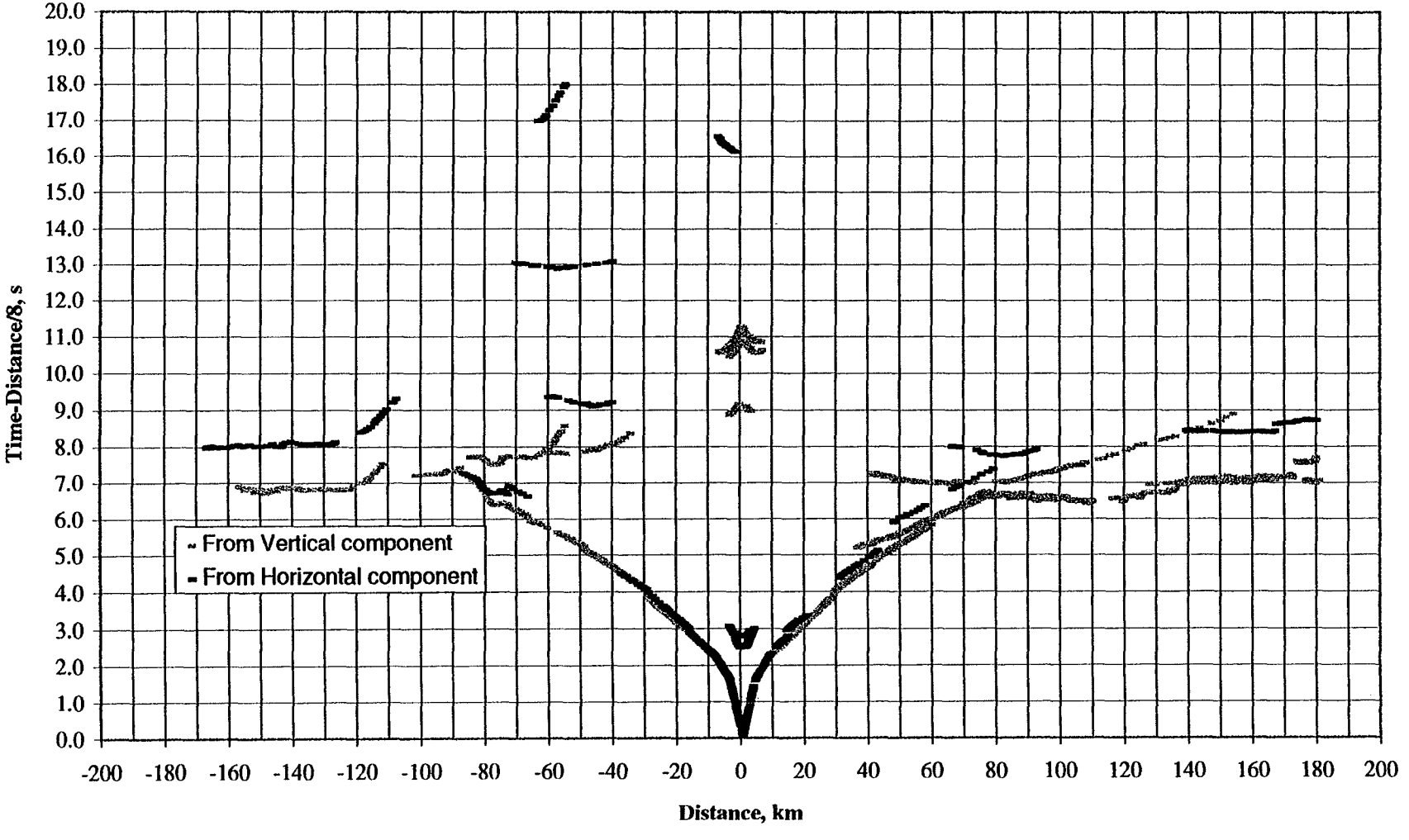

Figure 24

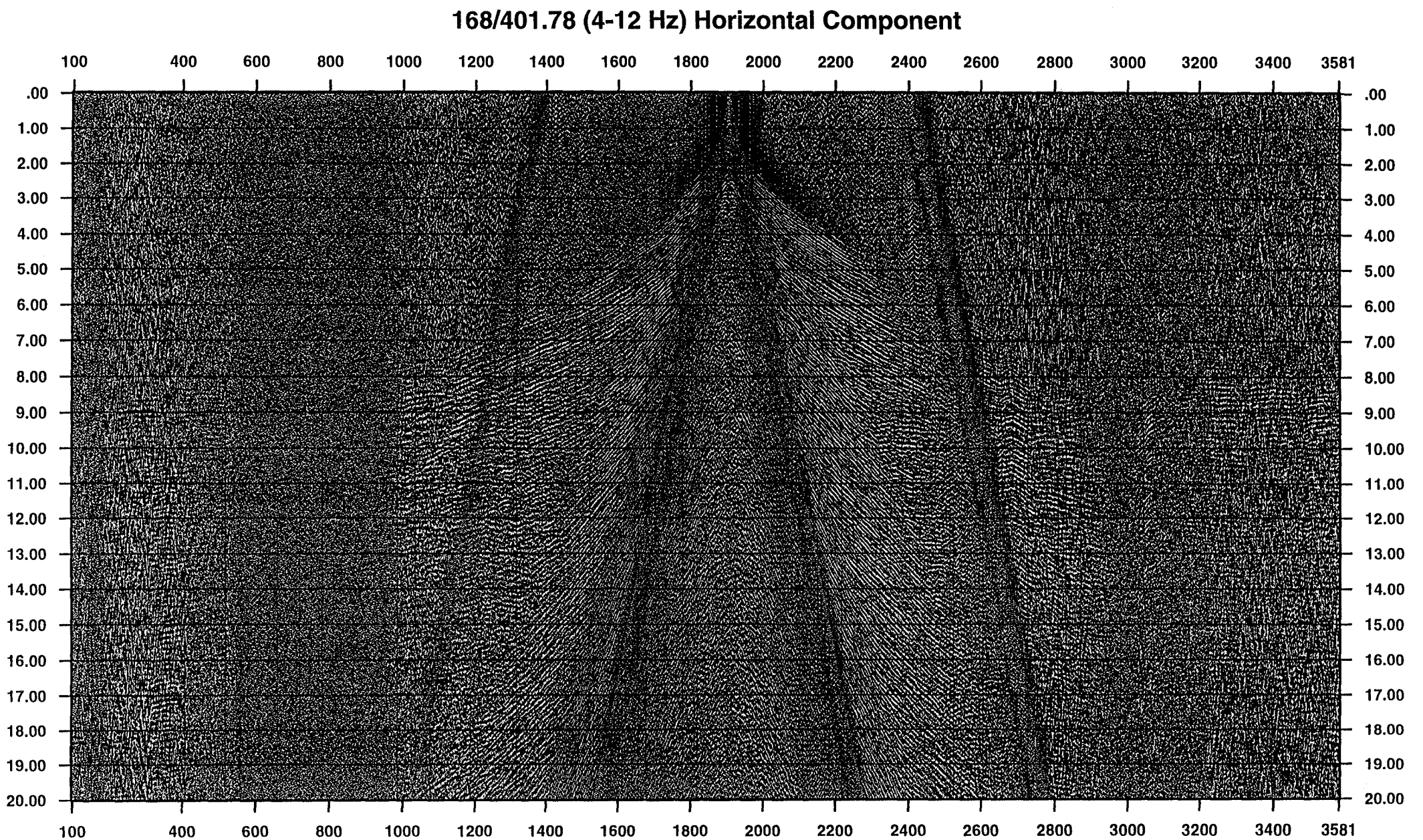
168/401.78 (4-12 Hz) Horizontal Component
100
400
600
800
1000
1200
1400
1600
1800
2000
2200
2400
2600
2800
3000
3200
3400
3581
.00
1.00
2.00
3.00
4.00
5.00
6.00
7.00
8.00
9.00
10.00
11.00
12.00
13.00
14.00
15.00
16.00
17.00
18.00
19.00
20.00

Figure 25

Figure 26

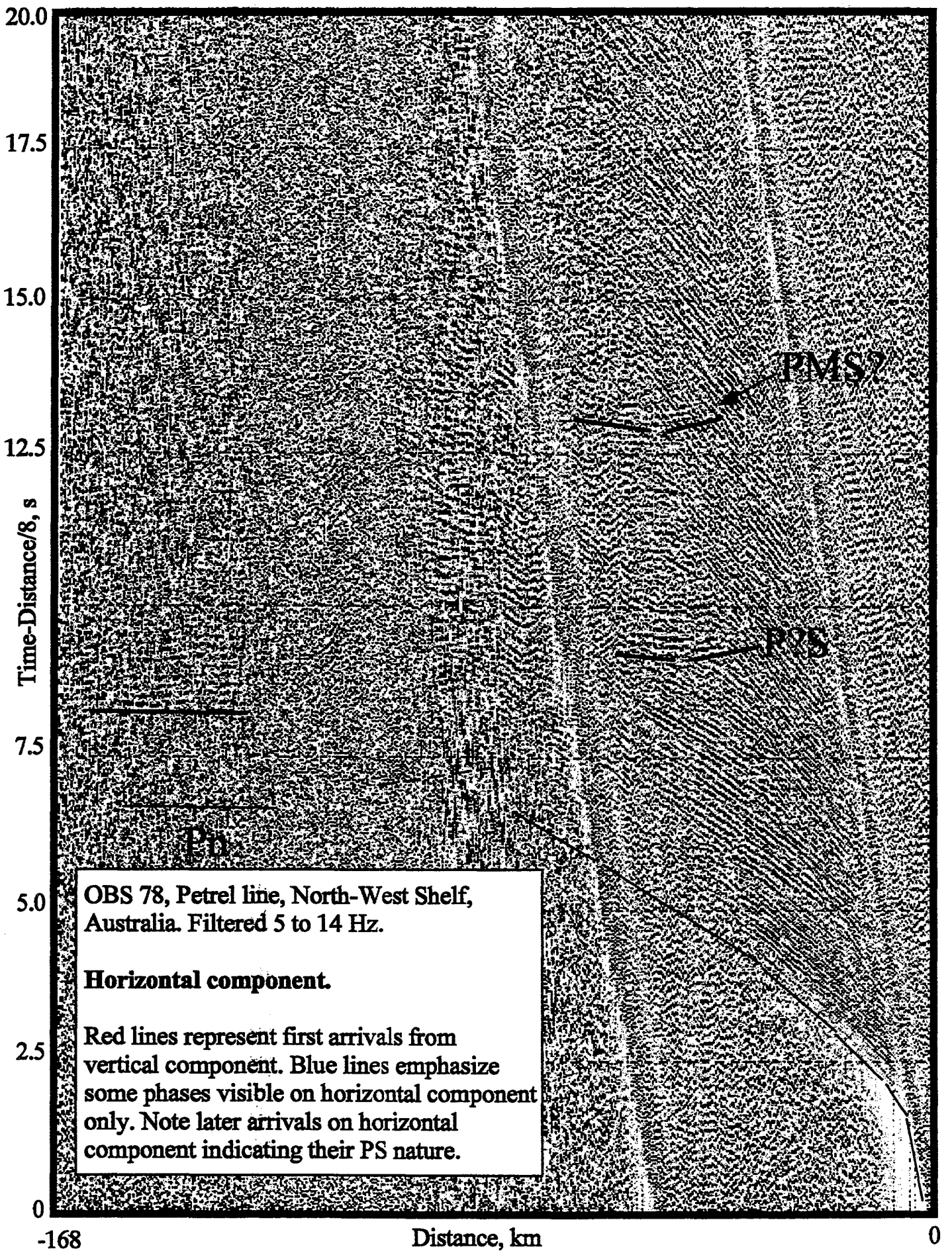
20.0
17.5
15.0
12.5
7.5
5.0
2.5
0
Time-Distance/8, s
PMS?
P?S
Pn
OBS 78, Petrel line, North-West Shelf, Australia. Filtered 5 to 14 Hz.
Horizontal component.
Red lines represent first arrivals from vertical component. Blue lines emphasize some phases visible on horizontal component only. Note later arrivals on horizontal component indicating their PS nature.
-168
Distance, km
0

Figure 27

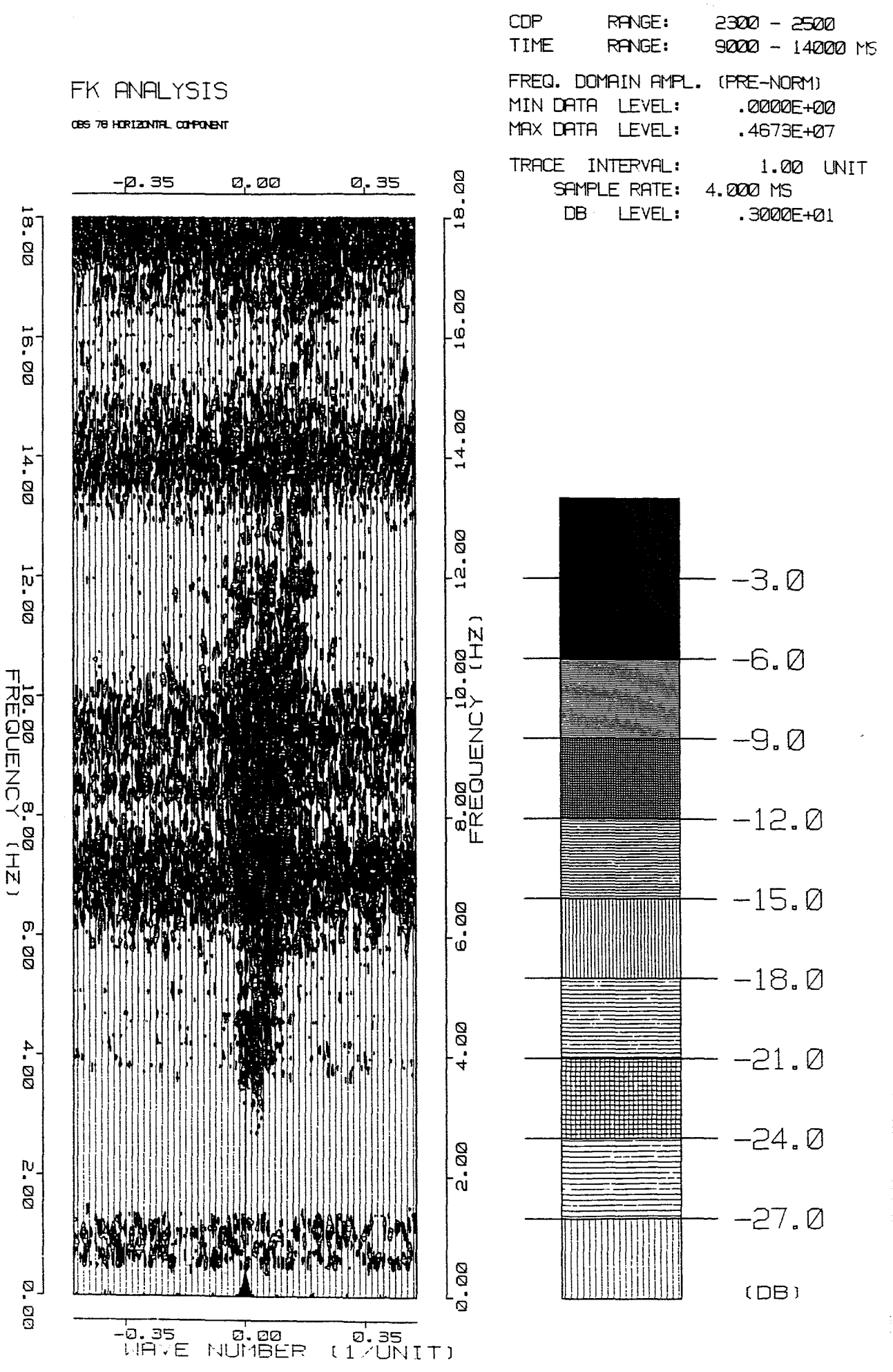
CDP RANGE: 2300 - 2500
TIME RANGE: 9000 - 14000 MS
FREQ. DOMAIN AMPL. (PRE-NORM)
MIN DATA LEVEL: .0000E+00
MAX DATA LEVEL: .4673E+07
TRACE INTERVAL: 1.00 UNIT
SAMPLE RATE: 4.000 MS
DB LEVEL: .3000E+01
FK ANALYSIS
OBS 78 HORIZONTAL COMPONENT
-0.35
0.00
0.35
18.00
16.00
14.00
12.00
10.00
8.00
6.00
4.00
2.00
0.00
FREQUENCY (HZ)
WAVE NUMBER (1/UNIT)
-3.0
-6.0
-9.0
-12.0
-15.0
-18.0
-21.0
-24.0
-27.0
(DB)

Data Output

Display

The data were plotted using SECPLOT, as in the typical DISCO job segment given below:

```
*CALL   SECPLOT RL      VA      40      1.181   1       0
SETAMP  CONSTANT1.33e8                  1
XPLOT   offset  5000    0.01    100
PLOTOPT /name=sec0
LABEL   offset  5       1       shot    20
LABELSZ 0.09    0.075
TITLE   168/401.77 (5-10 Hz) Vertical Component
TRANGE  0       12000
TITLE2      Runmix 3 traces (1,2,1)
*CALL   SIDELBL 0.5
HISTORY ALLCALL 2       8
PLOTOPT /segment=every/pos=(after,sec0)
```

An output file was written in SEG-Y format for digitisation using OBSTOOL as in the DISCO job segment given below:

```
*CALL   GOUT
DENSITY 6250
REEL    SGYDISK
TAPEOPT /tapefile="/export/mpsr/obs2/401/obs77.sgy"
```

A4 size plots (Appendix 10) were produced using a DISCO job similar to the one shown below:

```
*CALL   PSPLOT  RL      VDEN    9.8     5.5
VDENPRM CURVE
FILE    psplot.eps
TITLE   14      HELV    BOLD    CENTER
168/401.77 (5-10 Hz) Vertical Component
MAXTR   3482
PGPARM  1       1       LAND    8.3
TRLABEL shot    200
TLABEL
TLGRID
SETAMP
```

Variable density was used instead of variable area, to reduce the size of postscript plot files. The VDENPRM parameter required experimentation for optimum display.

Digitisation

Digitisation of the events picked on each section was initially done on the digitising table using the VMS program DIGREF. An example of DIGREF output is:

```
*EVENT: 168/401.77.d2
 -53452.13   5374.94
 -49298.35   5139.62
 -44334.25   4870.16
 -38530.41   4552.93
 -33051.92   4244.62
 -27273.37   3922.35
```

```
*EVENT: 168/401.77.c2
 -25827.51    3652.24
 -22975.57    3439.47
 -19702.03    3206.57
 -16152.58    2958.02
 -12954.55    2724.39
 -10047.06    2515.77
```

where the first column is the offset in metres, and the second column is the reduced time in msec. These files were then input to REFVEL, which computed velocity and intercept time written to the log file, and produced an output file in the format:

```
*EVENT: 168/401.77.d2
 -53.45213    12.0565
 -49.29835    11.3019
 -44.33425    10.4119
 -38.53041     9.3692
 -33.05192     8.3761
 -27.27337     7.3315
*EVENT: 168/401.77.c2
 -25.82751     6.8807
 -22.97557     6.3114
 -19.70203     5.6693
 -16.15258     4.9771
 -12.95455     4.3437
 -10.04706     3.7717
```

where the first column is the offset in km, and the second column is the time in seconds. This file was input to program REFOBS2 for conversion to SIGMA format.

The velocity and intercept times are logged by REFVEL as presented in the example below:

```
 168/401.77.d2            5545 m/s, y0=  2.41 s, sd= 0.003 s
 168/401.77.c2            5082 m/s, y0=  1.80 s, sd= 0.003 s
```

These data were then entered for pairs of stations for computation of depths. The REFRAN output for the pair 74 to 77 is as follows:

```
168/401 74-77
 1584.000  0.100 1522.000  0.140
 1977.000  0.200 2042.000  0.260
 3389.000  0.960 3723.000  1.180
 4583.000  1.400 5082.000  1.860
 5538.000  2.440 5545.000  2.470
    0.000  0.060    0.000  0.060
```

where 1st column is velocity and 2nd column is intercept time for OBS 74, and 3rd column is velocity and 4th column is intercept time for OBS 77.

Digitisation of the final data was done using the graphical interface of OBSTOOL. The format of the output file is given in the following example:

```
-3484      1.8351  772025      1
-3583      1.8948  772026      1
-3884      2.1027  772029      2
-3984      2.1434  772030      2
-4583      2.3052  772036      2
```

where the columns are offset from OBS (m), time (s), station number, shot number, and event number.

This file was then input to DTOBS which shifted times for events picked on subsequent cycles. REFOBS3 reformatted the output from DTOBS to SIGMA format, decimating the data as required. The format of the REFOBS3 output file is given in the following example:

```
132.716         1.835         0.010           1
132.617         1.895         0.010           1
132.316         2.103         0.010           2
132.216         2.143         0.010           2
131.617         2.305         0.010           2
```

where the columns are offset from model origin (km), time (s), uncertainty (s), and event number.

The individual files were concatenated, and finally selective decimation was done by DECIMATE to further reduce the size of the picks file for SIGMA.

Archiving of Processing Files

There are 4 sets of archive tapes, created on a Unix system with the 'tar' command:

- raw OBS file
- raw SEG-Y file
- final SEG-Y file
- all files, including OBSTOOL log files

The first two are considered field data, and are stored in the MPSR Physical Databases. Table 14 contains a listing of these data.

Table 14 - Archive of Field Data

Sequence number	2nd Reference	Time (start)	Time (stop)
168/7001	168/0001	357:2335	359:1958
168/7002	168/0002		
168/7003	168/0003		
168/7004	168/0004	358:2014	359:0857
168/7005	168/0005	358:2014	359:2221
168/7006	168/0006		
168/7007	168/0007	361:1515	362:1949
168/7008	168/0008	361:1556	363:0009
168/7009	168/0009		
168/7010	168/0010	365:1745	001:0503
168/7011	168/0011	365:1745	001:0503
168/7012	168/0012		
168/7013	168/0013	001:0700	002:1117
168/7014	168/0014	001:0700	002:1300
168/7015	168/0015		
168/7016	168/0016	004:0444	004:1425
168/7017	168/0017	004:0444	004:2041
168/7018	168/0018		
168/7019	168/0019		
168/7020	168/0020	004:1630	005:0131
168/7021	168/0021		
168/7022	168/0022	008:0140	009:1939
168/7023	168/0023	008:0140	008:1939
168/7024	168/0024		
168/7025	168/0025	011:0635	011:1724
168/7026	168/0026	011:0635	011:2311
168/7027	168/0027		
168/7028	168/0028	011:2137	012:1049
168/7029	168/0029	011:2137	012:1623
168/7030	168/0030		
168/7031	168/0031	016:0358	016:1540
168/7032	168/0032	016:0358	016:1540
168/7033	168/0033		
168/7034	168/0034	016:1619	017:1013
168/7035	168/0035	016:1619	017:1013
168/7036	168/0036		
168/7037	168/0037	020:0817	020:2321
168/7038	168/0038	020:0817	020:2321
168/7039	168/0039		
168/7040	168/0040	020:2308	021:0541
168/7041	168/0041	020:2308	021:0541
168/7042	168/0042		

The final SEG-Y file tape is stored in the Seismic Catalogue in the '40000' series, physically located in the computer room. Table 15, generated by the Tape Management System (TMS) contains a listing of these data.

Table 15 - Archive of Processed Data

LIST OF TAPE LIBRARY AT 3-OCT-96 10:30:57 Page 1

NUMBER	ST	PROJECT	SETNAME	USER	DATE ASSIGNED	MEDIUM
40023	1	S168	401.69.SEGY	PETKOVIC	30-SEP-1996	EXAB
40024	1	S168	401.70.SEGY	PETKOVIC	30-SEP-1996	EXAB
40025	1	S168	401.71.SEGY	PETKOVIC	30-SEP-1996	EXAB
40026	1	S168	401.72.SEGY	PETKOVIC	30-SEP-1996	EXAB
40027	1	S168	401.73.SEGY	PETKOVIC	30-SEP-1996	EXAB
40028	1	S168	401.74.SEGY	PETKOVIC	30-SEP-1996	EXAB
40029	1	S168	401.75.SEGY	PETKOVIC	30-SEP-1996	EXAB
40030	1	S168	401.76.SEGY	PETKOVIC	30-SEP-1996	EXAB
40031	1	S168	401.77.SEGY	PETKOVIC	30-SEP-1996	EXAB
40032	1	S168	401.78.SEGY	PETKOVIC	30-SEP-1996	EXAB
40033	1	S168	401.79.SEGY	PETKOVIC	30-SEP-1996	EXAB
40034	1	S168	401.80.SEGY	PETKOVIC	30-SEP-1996	EXAB
40035	1	S168	401.81.SEGY	PETKOVIC	30-SEP-1996	EXAB
40036	1	S168	401.82.SEGY	PETKOVIC	30-SEP-1996	EXAB
40037	1	S168	401.83.SEGY	PETKOVIC	30-SEP-1996	EXAB
40038	1	S168	401.69.STAGE-1	PETKOVIC	1-OCT-1996	EXAB
40039	1	S168	401.70.STAGE-1	PETKOVIC	1-OCT-1996	EXAB
40040	1	S168	401.71.STAGE-1	PETKOVIC	1-OCT-1996	EXAB
40041	1	S168	401.72.STAGE-1	PETKOVIC	1-OCT-1996	EXAB
40042	1	S168	401.73.STAGE-1	PETKOVIC	1-OCT-1996	EXAB
40043	1	S168	401.74.STAGE-1	PETKOVIC	1-OCT-1996	EXAB
40044	1	S168	401.75.STAGE-1	PETKOVIC	1-OCT-1996	EXAB
40045	1	S168	401.76.STAGE-1	PETKOVIC	1-OCT-1996	EXAB
40046	1	S168	401.77.STAGE-1	PETKOVIC	1-OCT-1996	EXAB
40047	1	S168	401.78.STAGE-1	PETKOVIC	1-OCT-1996	EXAB
40048	1	S168	401.79.STAGE-1	PETKOVIC	1-OCT-1996	EXAB
40049	1	S168	401.80.STAGE-1	PETKOVIC	1-OCT-1996	EXAB
40050	1	S168	401.81.STAGE-1	PETKOVIC	1-OCT-1996	EXAB
40051	1	S168	401.82.STAGE-1	PETKOVIC	1-OCT-1996	EXAB
40052	1	S168	401.83.STAGE-1	PETKOVIC	1-OCT-1996	EXAB

The 4th set of tapes, containing OBSTOOL log files and other files, was created with the 'tar' command and the -I switch, for example:

```
% tar -cvf /dev/rmt0 -I include_file
```

where `include_file` contained a list of pathnames to the files being archived. Table 15 contains a listing of these data. For example:

```
/d/mpsr/obs-11/cc168/cc.77                    <- clock calibration file
/d/mpsr/obs-11/logs/101.nav
/d/mpsr/obs-11/logs/102.nav
/d/mpsr/obs-11/logs/103.nav
/d/mpsr/obs-11/logs/202a.nav
/d/mpsr/obs-11/logs/202b.nav
/d/mpsr/obs-11/logs/202c.nav
/d/mpsr/obs-11/logs/301.nav
/d/mpsr/obs-11/logs/302.nav
/d/mpsr/obs-11/logs/401.nav                   <- navigation file
/d/mpsr/obs-11/logs/501.nav
/d/mpsr/obs-11/logs/401.nav.77.ww
/d/mpsr/obs-11/logs/cl_app.77.dat
/d/mpsr/obs-11/logs/hdrint.77
/d/mpsr/obs-11/logs/hdrlist.77
/d/mpsr/obs-11/logs/obsclock.77
```

```
/d/mpsr/obs-11/logs/obsdata.77.arr
/d/mpsr/obs-11/logs/obsdata.77.clock.dat
/d/mpsr/obs-11/logs/obsdata.77.corr
/d/mpsr/obs-11/logs/obsdata.77.log          <- OBSTOOL log file
/d/mpsr/obs-11/logs/obsloc.77.az
/d/mpsr/obs-11/logs/obsloc.77.llc
/d/mpsr/obs-11/logs/wwtta.77
/d/mpsr/obs-11/logs/wwtta_az.77
/d/mpsr/obs-11/logs/wwtta_orig.77
/d/agso/u/ppetkovi/401/obsdata.77.segy      <- raw SEG-Y file
/d/mpsr/obs-11/fsy/obsdata.77.segy.final    <- final SEG-Y file
/d/mpsr/obs-11/ps/77.az.ps                  <- plots for Appendix 6
/d/mpsr/obs-11/ps/77.cc.ps                  <- plots for Appendix 5
/d/mpsr/obs-11/ps/77.llc.ps                 <- plots for Appendix 7
/d/mpsr/obs-11/ps/77.pos.ps                 <- plots for Appendix 4
```

To extract data from the 4th set of tapes using the 'tar' command, the pathnames of the data in the archive must exist. If they don't, as will usually be the case, the following method should be used:

```
% dd if=/dev/rmt0 | tardy -Prefix "./" | tar -xvf /dev/rmt0
```

The effect of this is to place a prefix "./" before all directory names, and hence create the archived directories in the current directory. The files can then be moved to their required locations with the 'mv' command.

References

Berzon I.S., 1976. "Seismic prospecting of thin-layered media", Nauka Publishers, Moscow, 224 p. (in Russian)

Christeson, G., 1995, "Obstool: Software for Processing UTIG OBS Data", University of Texas Institute for Geophysics, Technical Report No. 134.

Collins, C.D.N., and Lee, C.S., "Survey 168 Post-Cruise Report", AGSO Record (in prep.)

Lukaszyk, I., and Soames, C., "North West Shelf AGSO Survey 168, Land Stations Data Processing Report ", AGSO Record (in prep.)

Appendices

Appendix 1 - Miscellaneous Computer Programs

To have access to these programs, ensure that the directory /usr/local/mpsr/progs is in your path.

CCSUMS - computes time differences between OBS clock and GPS clock in the OBS clock calibration file.

CLOSEST - works out the nearest shotpoint to a given location. For OBS processing also works out the current active in the area for an assumed OBS descent rate of 1 m/s.

DIGREF - digitisation program (VMS only).

MERT - merges times from a precise 'Nakamura' format shot times file with the position data from a given AGSO UKOOA format shotpoint location file. The output is an Obstool format shot file.

MODJOB - Modify Disco Job by commenting out all instances of a specified module.

MUTED - The OBS mutes traces during the time of writing to the disk, and the record of which traces are muted is written to the log file when Obstool creates the final SEG-Y file. As this log file is fixed format, it can be used as input to program MUTED to create a DISCO patch control file.

OBS2PSEIS - convert OBS deployment/retrieval file to 'Petroseis' format.

REF5A - reformat ASCII xyz file.

REFOBS1 - reformat obstool format navigation file to create a standard 'ship' format shot-time file

REFOBS3 - reformat OBSTOOL picks file to Sigma format. Several files may be converted using a batch file, and the individual outputs concatenated to form a single file for input to Sigma. If this is so, then supply 0 (no terminator) to REFOBS3, then, when the files are concatenated, add your own terminating record using an editor. The terminating record is 0.0 0.0 0.0 -1

REFOBS4 - reformat OBSTOOL picks file to MacRay format

REFOBS5 - Assign new event ids to Obstool format event pick file.

SPINFO - searches for a shotpoint in a UKOOA format shotpoint location file and reports its position, depth, gravity and mag value.

Appendix 2 - AGSO UKOOA Format

The following is an excerpt from the AGSO UKOOA format navigation file, containing the header records and the first seven data records.

```
#NAME: AGSO SURVEY 168, OBS - NORTHWEST SHELF
AREA: NORTH WEST AUSTRALIA
ACQUISITION DATE: 17 DECEMBER 1995 TO 23 JANUARY 1996
VERSION OF: 15-FEB-96
SOURCE FILE: S168FWD.DAT
CONTENTS: STATION POSITION, WATER DEPTH, SHOT TIME
NAVIGATION: DIFFERENTIAL GPS
POSITION DATUM: WGS84
GENERIC FORMAT: (A16,I7,2I2,F5.2,A1,I3,I2,F5.2,A1,I8,8X,I5,I3,3I2,I1,I5)
   LINE NAME                                                    COLS 1  - 16
   SHOT POINT NUMBER                                            COLS 17 - 23
   LATITUDE DEGREES                                             COLS 24 - 25
   LATITUDE MINUTES                                             COLS 26 - 27
   LATITUDE SECONDS                                             COLS 28 - 32
   N/S HEMISPHERE FLAG                                          COL  33
   LONGITUDE DEGREES                                            COLS 34 - 36
   LONGITUDE MINUTES                                            COLS 37 - 38
   LONGITUDE SECONDS                                            COLS 39 - 43
   E/W HEMISPHERE FLAG                                          COL  44
   GRAVITY FIELD IN MICROMETRES/SEC/SEC                         COLS 45 - 52
   NOT USED                                                     COLS 53 - 60
   WATER DEPTH IN METRES                                        COLS 61 - 65
   SHOT TIME: DAY                                               COLS 66 - 68
   SHOT TIME: HOUR                                              COLS 69 - 70
   SHOT TIME: MINUTE                                            COLS 71 - 72
   SHOT TIME: SECOND                                            COLS 73 - 74
   SHOT TIME: TENTH OF SECOND                                   COL  75
   TOTAL MAGNETIC FIELD IN NANO-TESLAS                          COLS 76 - 80
BLANKS: GIVEN AS 9'S TO FILL THE FIELD
STATION POSITION: THE STATION POSITION IS GIVEN AT THE SOURCE
WATER DEPTH DATA: DIGITAL VALUES DERIVED FROM RAYTHEON 12 KHZ AND 3.5 KHZ
 ECHO-SOUNDERS. BAD DIGITALLY RECORDED VALUES WERE RECOVERED USING VALUES
 DERIVED FROM ANALOGUE CHARTS. NO TIDAL OR MATTHEWS CORRECTIONS APPLIED.
 CORRECTION FOR TRANSDUCER DEPTH WAS APPLIED. SPEED OF SOUND 1500 M/S.
GRAVITY DATA: DATA AVAILABLE FROM BODENSEEWERK KSS-31 GRAVITY METER FOUR TIMES  PER SECOND.
 DATA RECORDED AT 10 SECOND INTERVALS WERE DE-SPIKED EDITED,
 SHIFTED BY -60 SECONDS TO ALLOW FOR FILTERS IN THE GRAVITY METER AND
 SMOOTHED USING A 15 MINUTE PERIOD SINC FUNCTION FILTER. THESE DATA WERE
 THEN INTERPOLATED TO THE CORRECTED SHOT TIMES.
ADDITIONAL NOTES: THE TIME IS THE TIME OF THE SHOT
#
168/101                          100181019.77S1134256.51E99999999          -1756354  4230399999
168/101                          101181018.01S1134253.70E99999999          -1757354  4303899999
168/101                          102181016.23S1134250.72E99999999          -1757354  4339099999
168/101                          103181014.70S1134247.80E99999999          -1757354  4411799999
168/101                          104181013.31S1134244.78E99999999          -1757354  4443499999
168/101                          105181011.71S1134241.85E99999999          -1759354  4515399999
168/101                          106181010.06S1134238.86E99999999          -1761354  4548199999
```

Appendix 3

Plots of Water Wave Arrivals

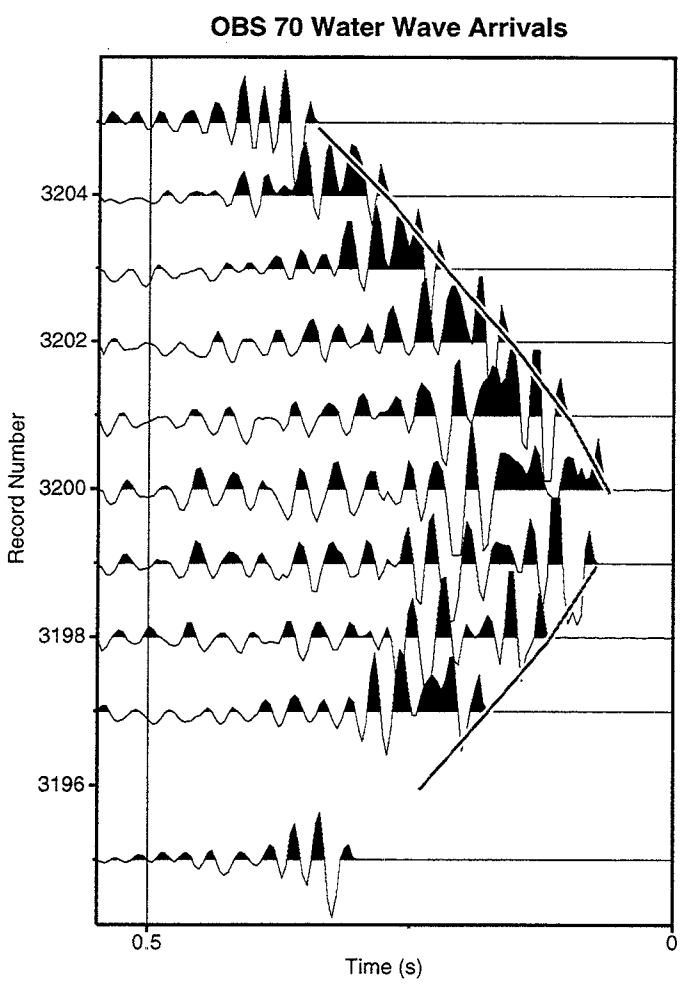
OBS 70 Water Wave Arrivals
Record Number
3204
3202
3200
3198
3196
0.5
0
Time (s)

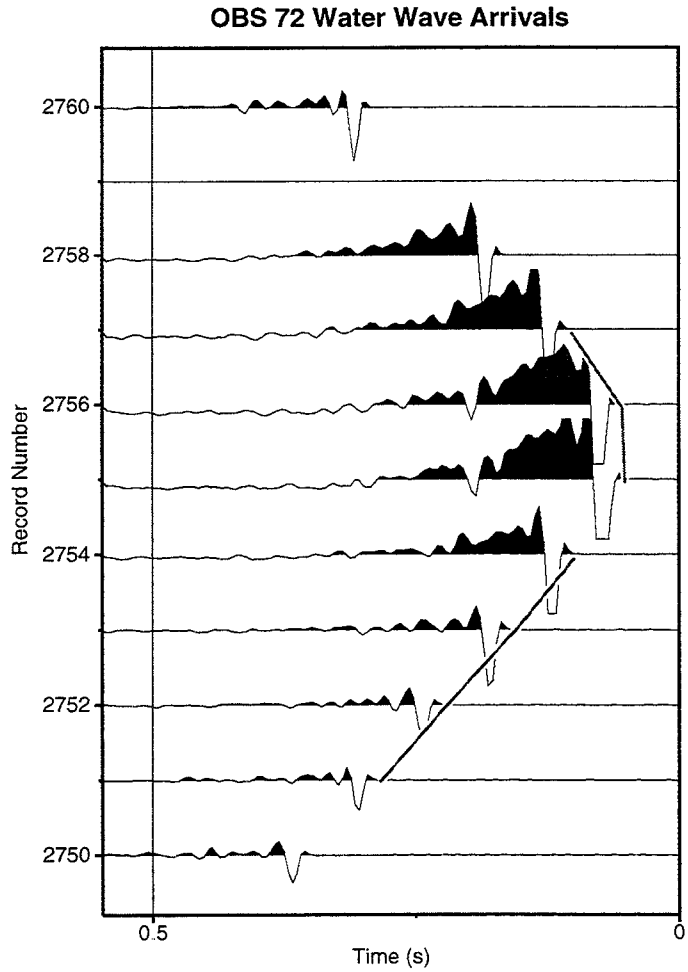
OBS 72 Water Wave Arrivals
Record Number
2760
2758
2756
2754
2752
2750
0.5
0
Time (s)

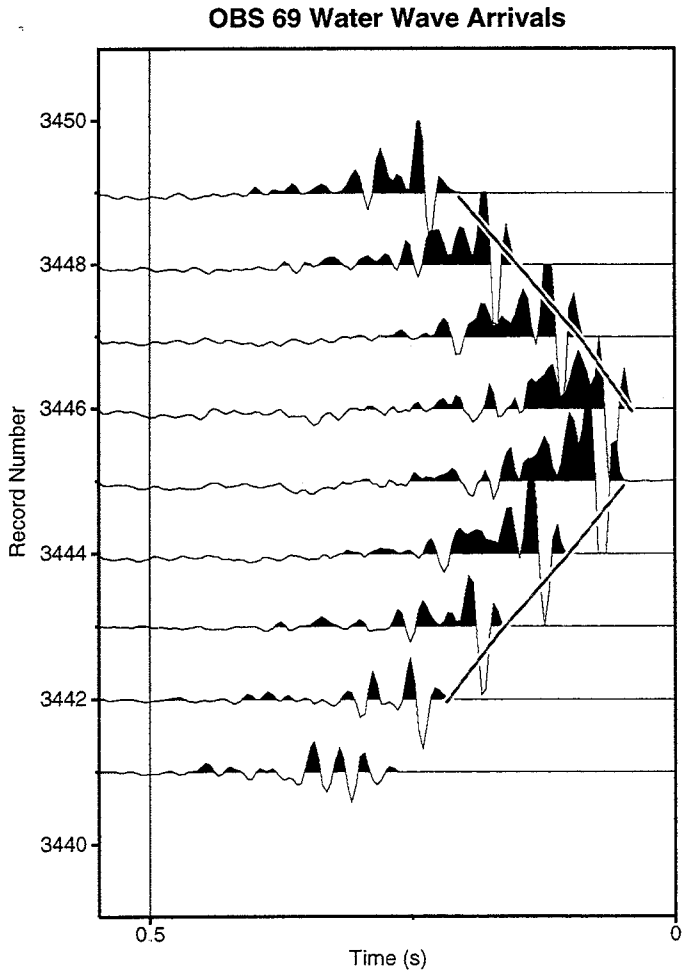
OBS 69 Water Wave Arrivals
Record Number
3450
3448
3446
3444
3442
3440
0.5
0
Time (s)

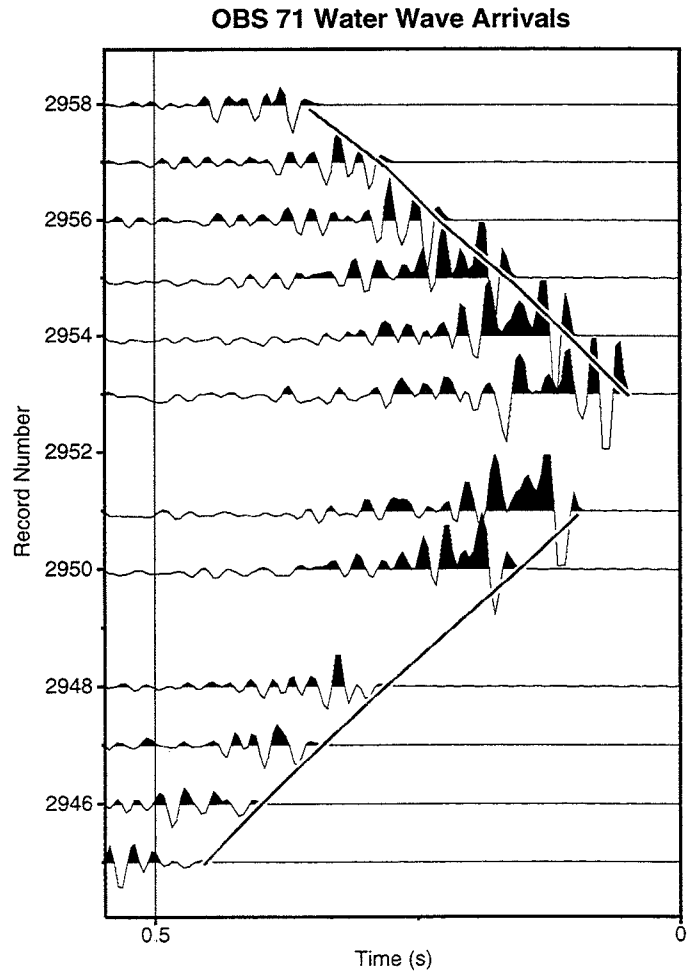
OBS 71 Water Wave Arrivals
Record Number
2958
2956
2954
2952
2950
2948
2946
0.5
0
Time (s)

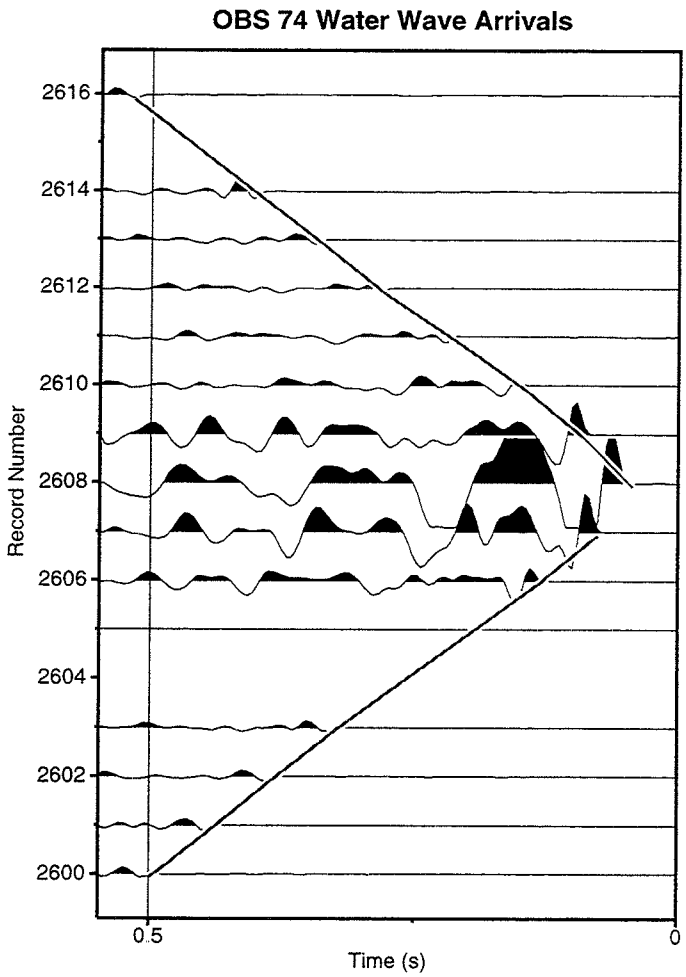
OBS 74 Water Wave Arrivals
Record Number
2616
2614
2612
2610
2608
2606
2604
2602
2600
0.5
0
Time (s)

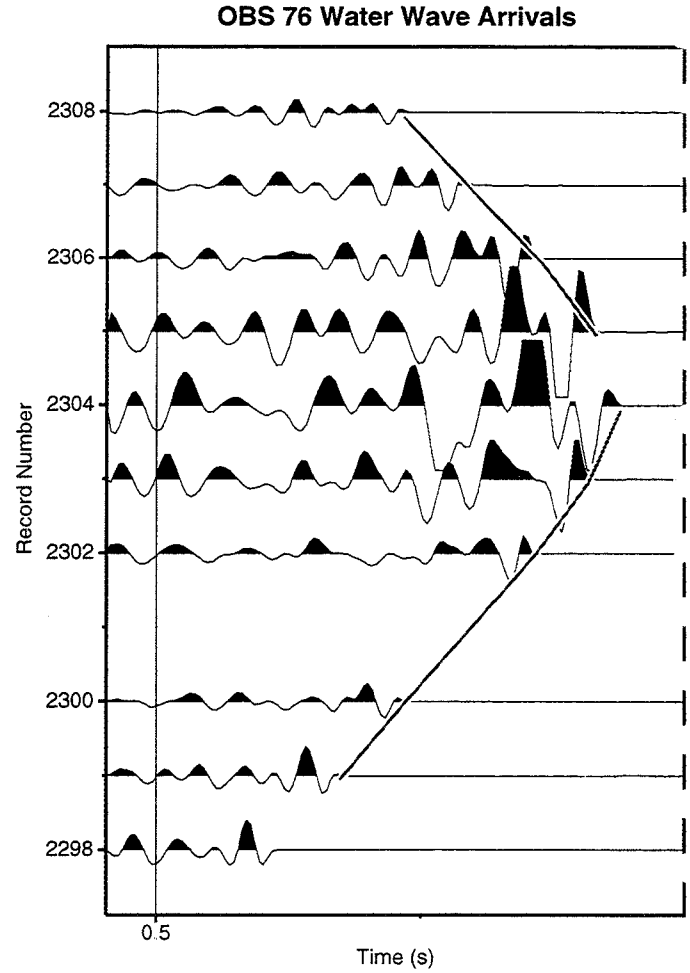
OBS 76 Water Wave Arrivals
Record Number
2308
2306
2304
2302
2300
2298
0.5
Time (s)

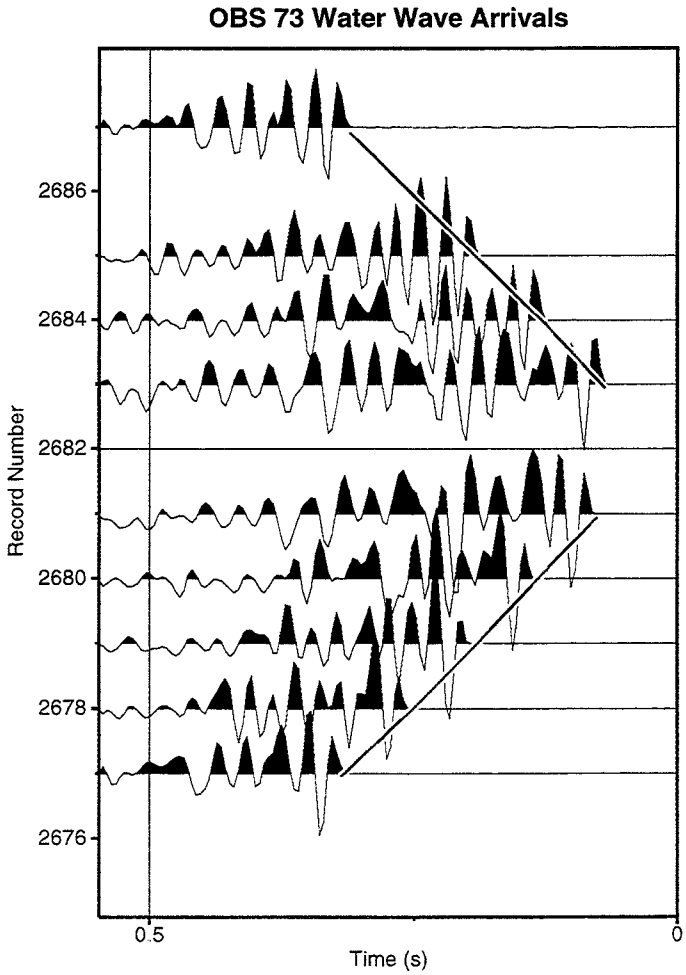
OBS 73 Water Wave Arrivals
Record Number
2686
2684
2682
2680
2678
2676
0.5
0
Time (s)

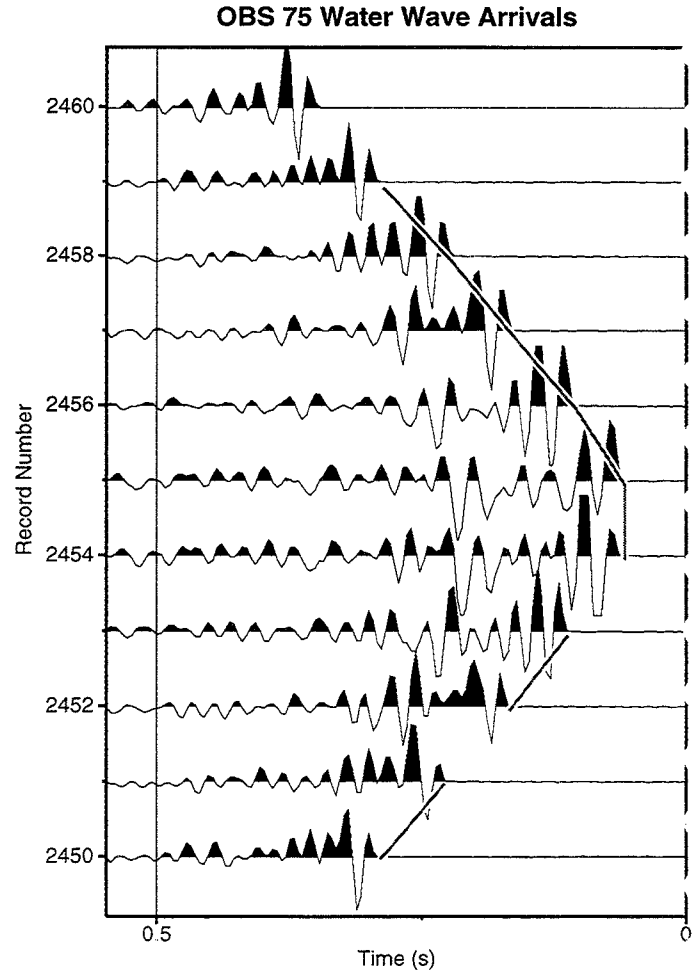
OBS 75 Water Wave Arrivals
Record Number
2460
2458
2456
2454
2452
2450
0.5
0
Time (s)

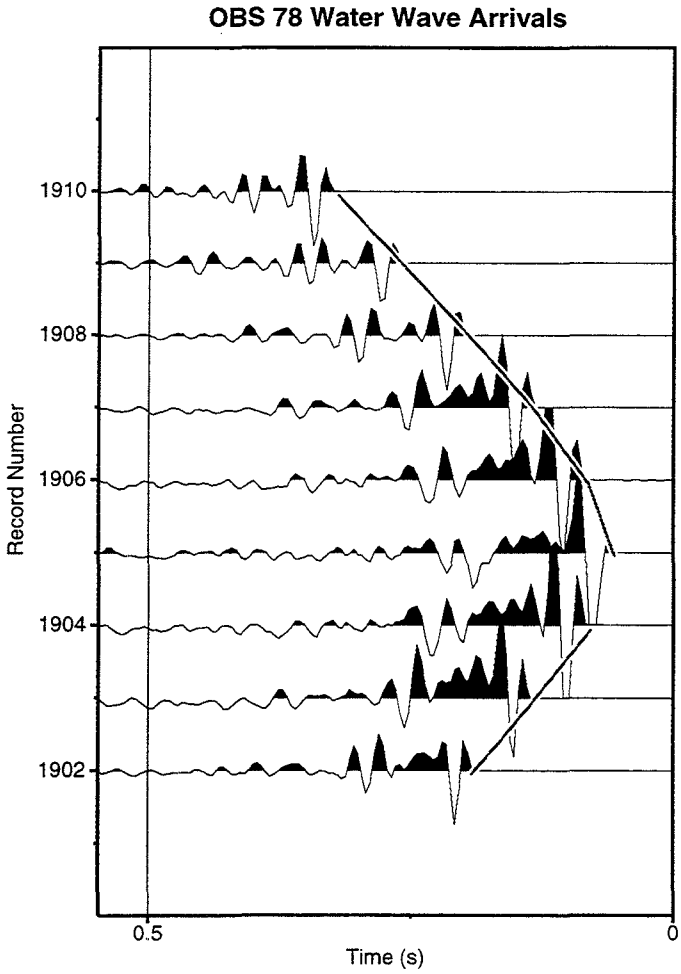
OBS 78 Water Wave Arrivals
Record Number
1910
1908
1906
1904
1902
0.5
0
Time (s)

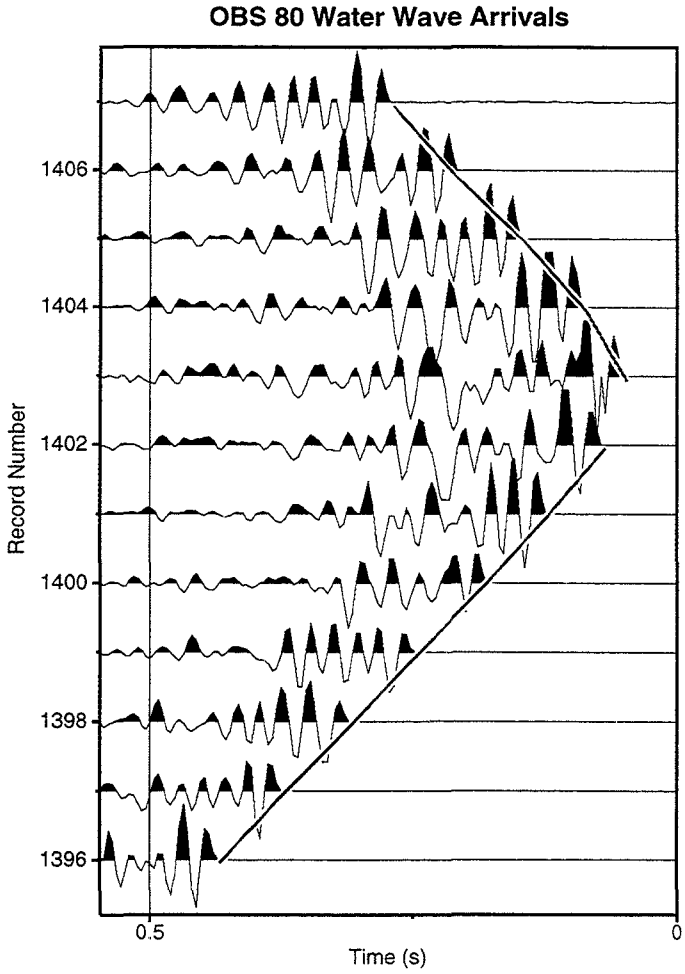
OBS 80 Water Wave Arrivals
Record Number
1406
1404
1402
1400
1398
1396
0.5
0
Time (s)

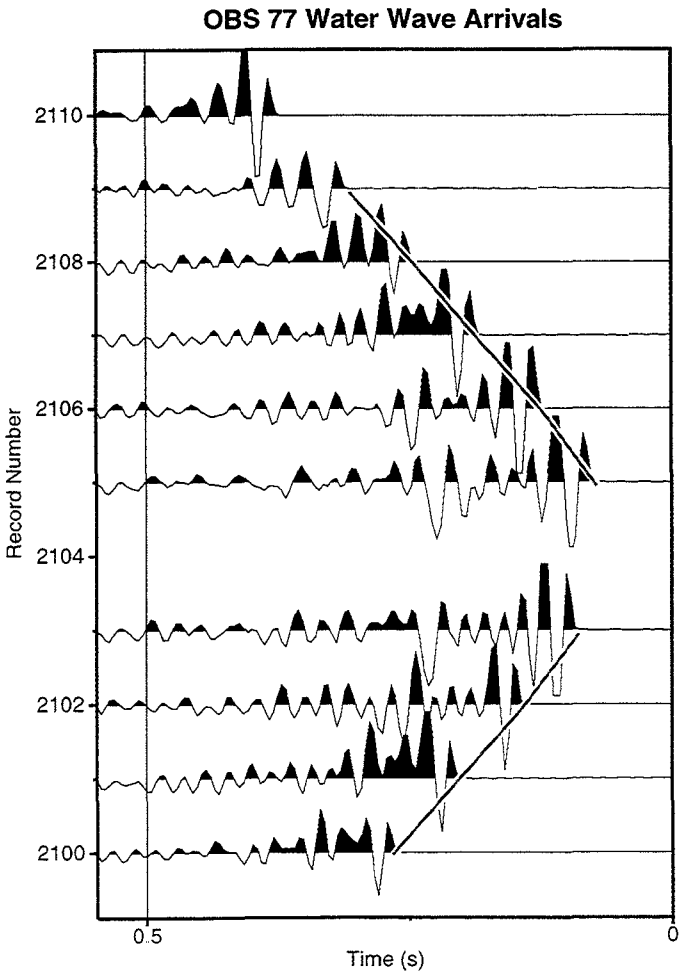
OBS 77 Water Wave Arrivals
Record Number
2110
2108
2106
2104
2102
2100
0.5
0
Time (s)

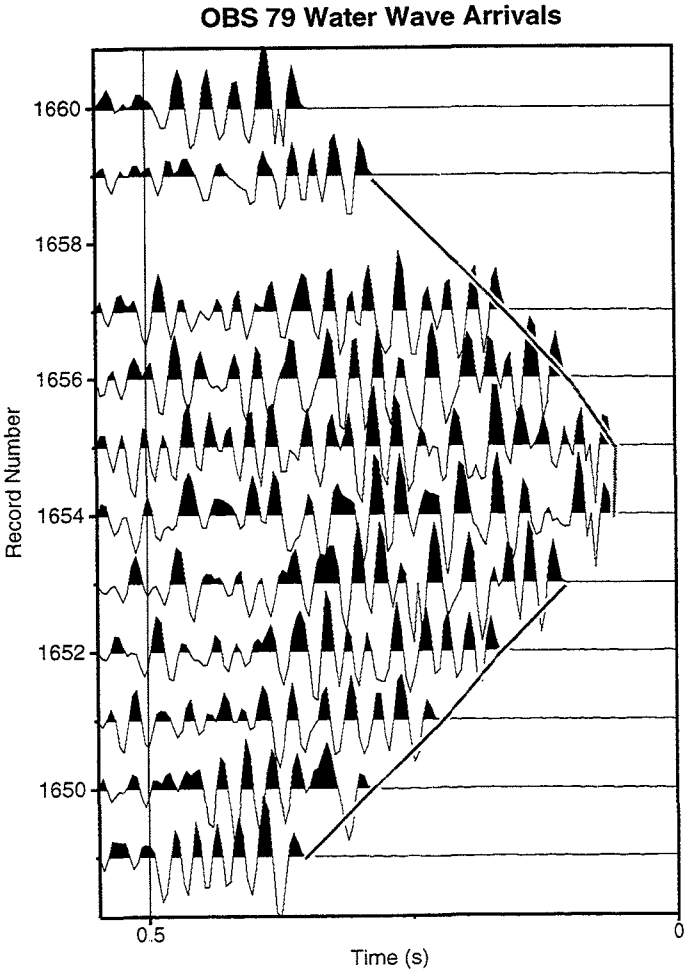
OBS 79 Water Wave Arrivals
Record Number
1660
1658
1656
1654
1652
1650
0.5
0
Time (s)

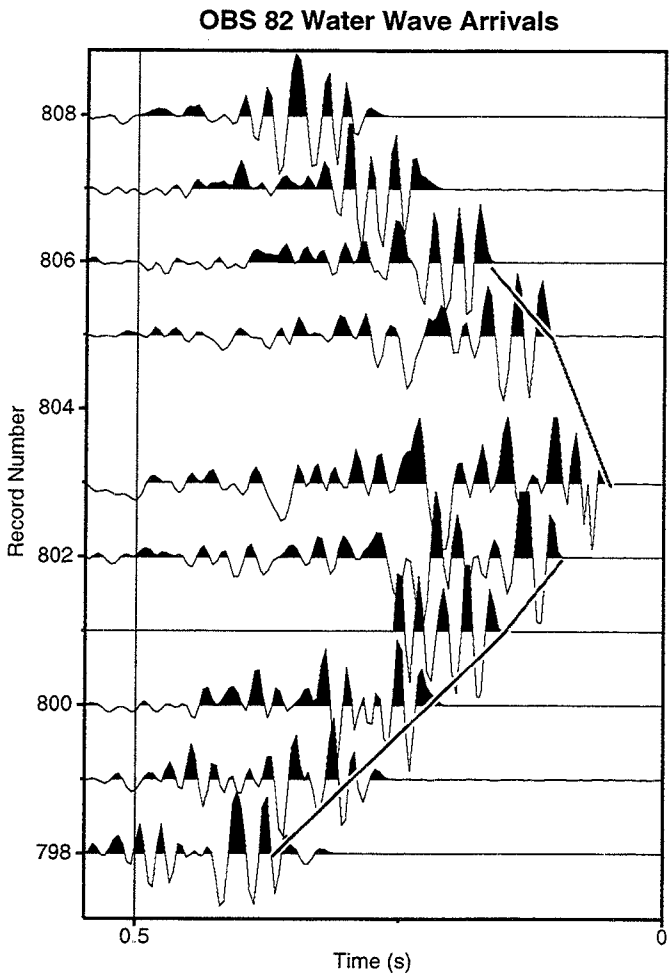
OBS 82 Water Wave Arrivals
808
806
804
802
800
798
Record Number
0.5
0
Time (s)

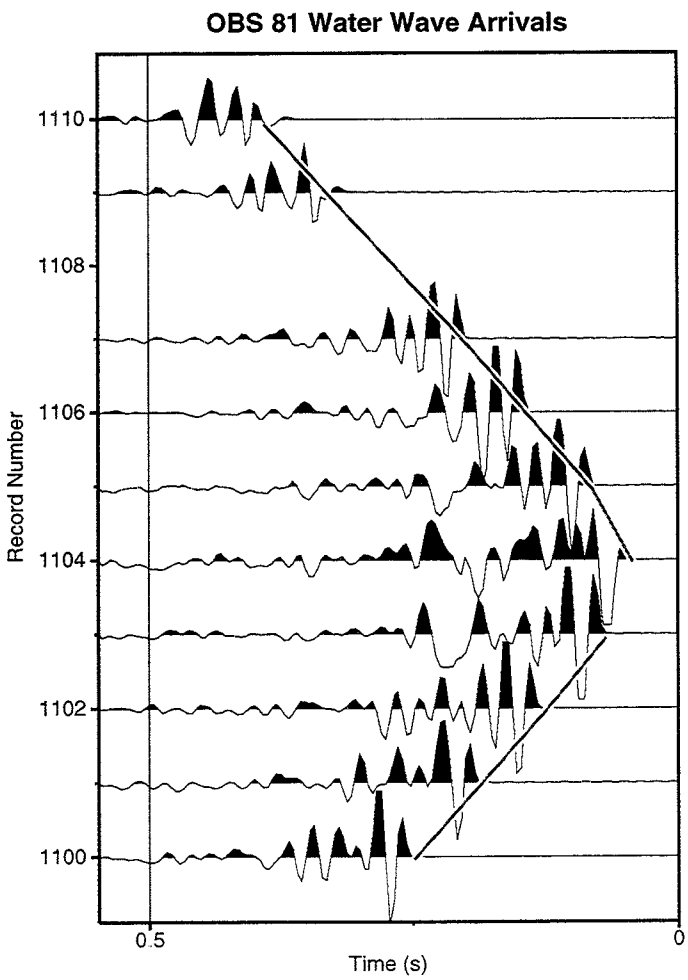
OBS 81 Water Wave Arrivals
1110
1108
1106
1104
1102
1100
Record Number
0.5
0
Time (s)

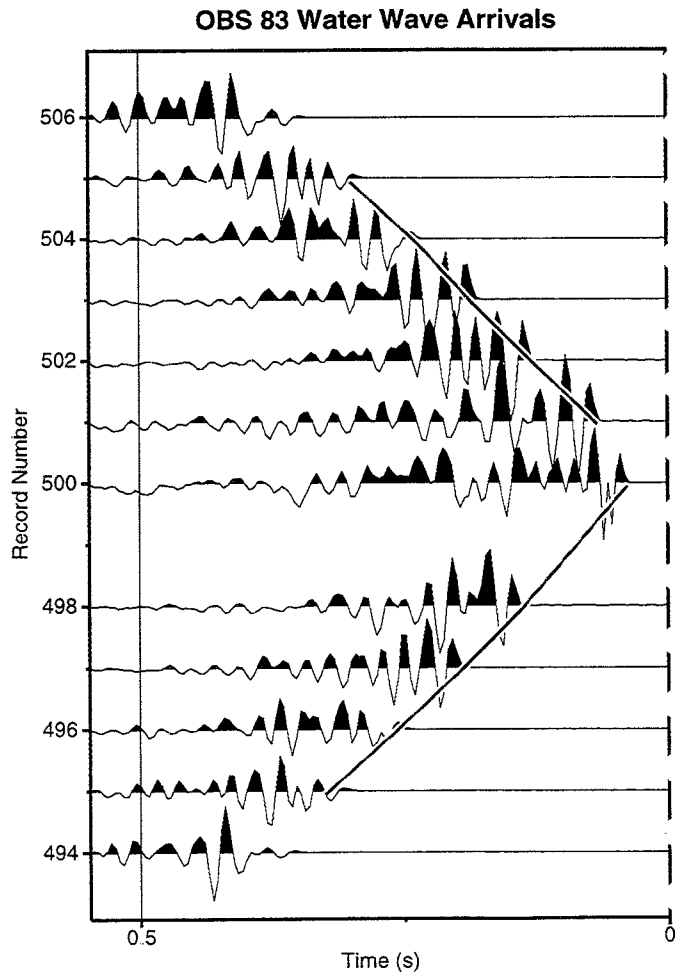
OBS 83 Water Wave Arrivals
506
504
502
500
498
496
494
Record Number
0.5
0
Time (s)

Appendix 4 - Plots of Inversion Results: OBS Position

The first set of plots indicate the position of the OBS computed via the inversion algorithm (Δ), the deployment (□) and retreival (■) positions. Table 16 gives these three positions in decimal degrees, and the closest shot reported by OBSLOC_LLC, which is not the correct closest shot as determined from the computed latitude and longitude.

The second set of diagrams show the OBS locations computed by OBSLOC_LLC plotted along an annotated line 168/401. The actual closest shots are given in the table below, together with the horizontal distance from OBS to these nearest shots.

Table 16 - OBS position

OBS	Deployment Latitude	Deployment Longitude	Retrieval Latitude	Retrieval Longitude	Computed Latitude	Computed Longitude	Closest Shot from obsloc_llc	Actual Closest Shot	Horizontal Distance to nearest shot (m)
69	-13.79872	127.46983	-13.79762	127.46743	-13.79899	127.46997	3442	3446	68
70	-13.64213	127.63142	-13.64295	127.63203	-13.64247	127.63149	3200	3200	51
71	-13.48423	127.79340	-13.48488	127.79378	-13.48511	127.79356	2953	2952	98
72	-13.35863	127.92257	-13.35995	127.92272	-13.35863	127.92257	2751	2755	29
73	-13.31188	127.97073	-13.31273	127.97072	-13.31154	127.96934	2681	2682	138
74	-13.26480	128.01937	-13.26498	128.01818	-13.26509	128.01874	2607	2608	31
75	-13.16688	128.11977	-13.16703	128.11805	-13.16725	128.11896	2455	2455	61
76	-13.07217	128.21890	-13.07148	128.21742	-13.07203	128.21811	2295	2304	78
77	-12.94568	128.35038	-12.94460	128.34960	-12.94568	128.34977	2103	2104	53
78	-12.81943	128.48077	-12.81917	128.48078	-12.81900	128.48014	1902	1905	84
79	-12.66075	128.64580	-12.66197	128.64678	-12.66098	128.64532	1649	1655	51
80	-12.50125	128.81085	-12.50193	128.81138	-12.50141	128.81048	1403	1403	31
81	-12.31198	129.00727	-12.31185	129.00648	-12.31212	129.00664	1104	1104	48
82	-12.12160	129.20423	-12.12145	129.20343	-12.12149	129.20333	803	803	94
83	-11.92942	129.40288	-11.92947	129.40245	-11.93019	129.40287	495	500	72

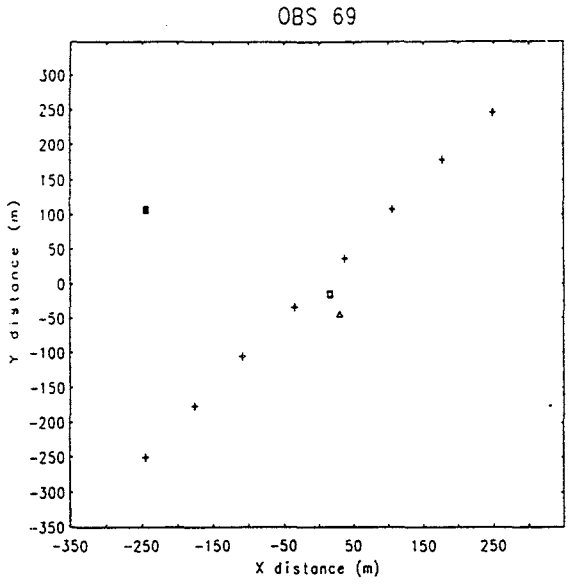
OBS 69
Y distance (m)
X distance (m)

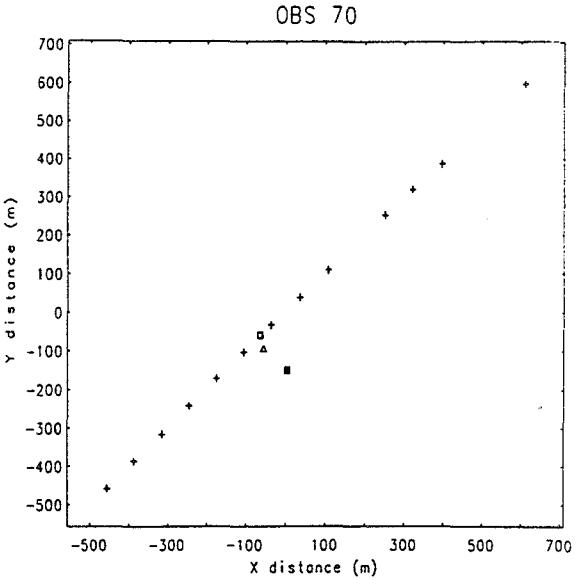
OBS 70
Y distance (m)
X distance (m)

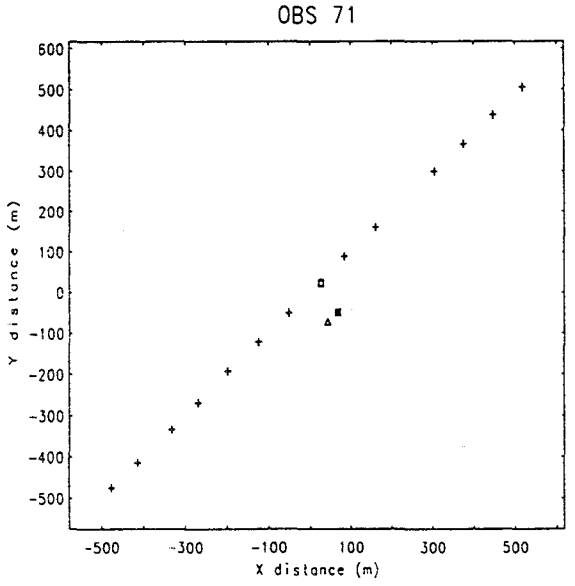
OBS 71
Y distance (m)
X distance (m)

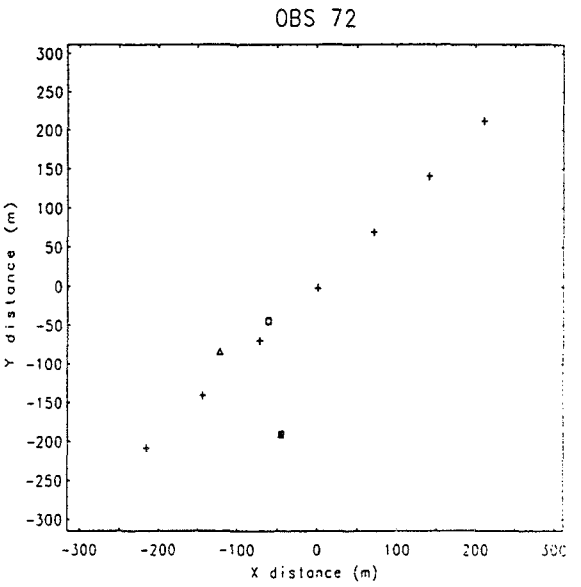
OBS 72
Y distance (m)
X distance (m)

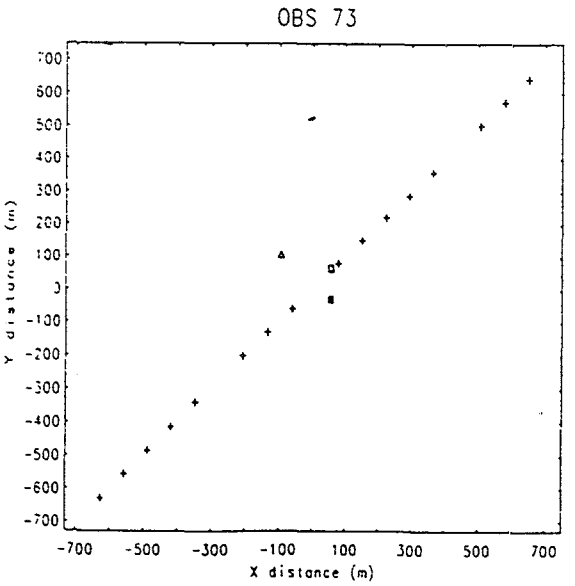
OBS 73
Y distance (m)
X distance (m)

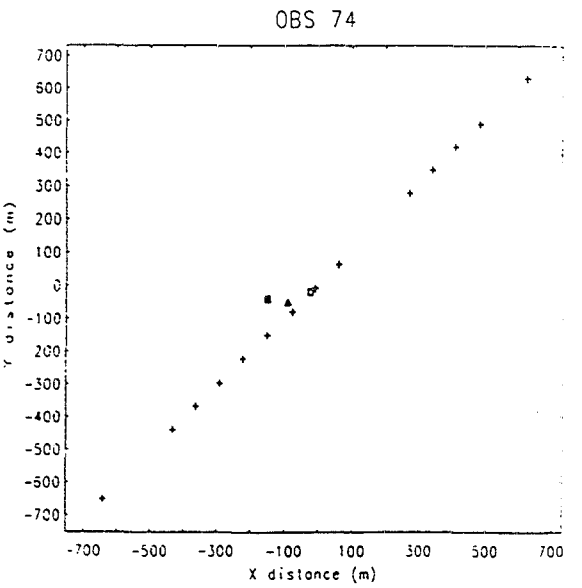
OBS 74
Y distance (m)
X distance (m)

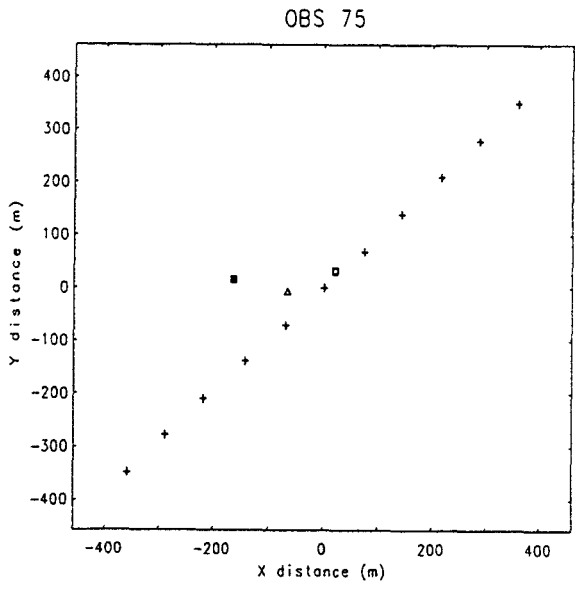
OBS 75
Y distance (m)
X distance (m)
400
300
200
100
0
-100
-200
-300
-400
-400
-200
0
200
400

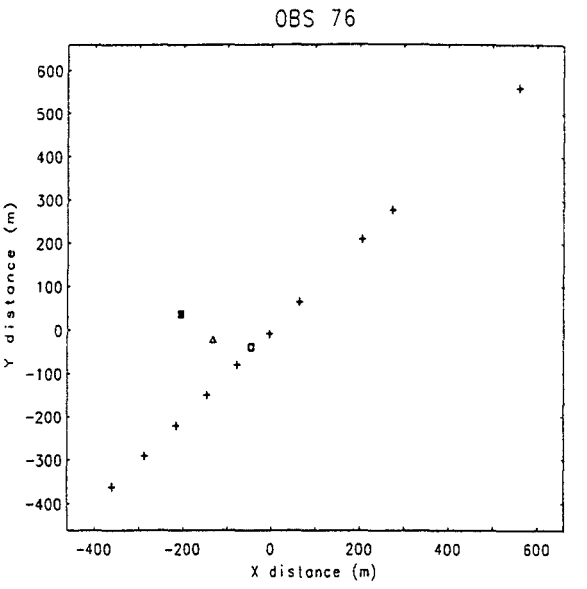
OBS 76
Y distance (m)
X distance (m)
600
500
400
300
200
100
0
-100
-200
-300
-400
-400
-200
0
200
400
600

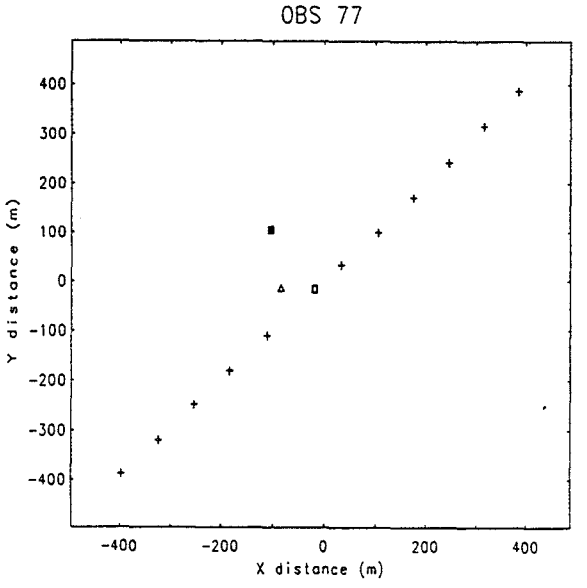
OBS 77
Y distance (m)
X distance (m)
400
300
200
100
0
-100
-200
-300
-400
-400
-200
0
200
400

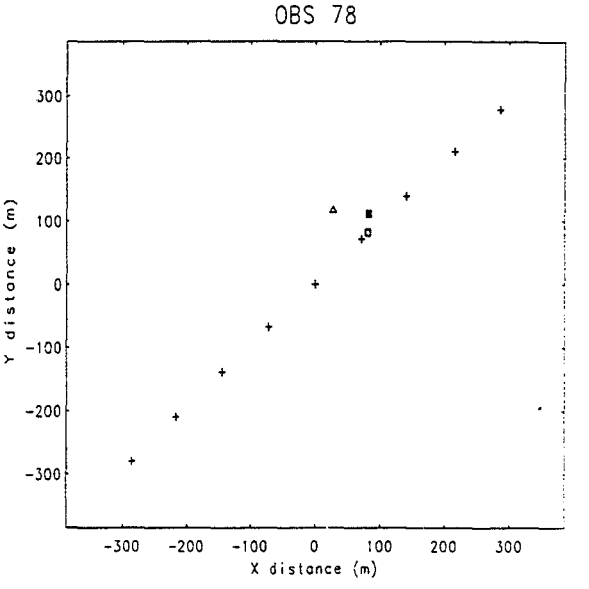
OBS 78
Y distance (m)
X distance (m)
300
200
100
0
-100
-200
-300
-300
-200
-100
0
100
200
300

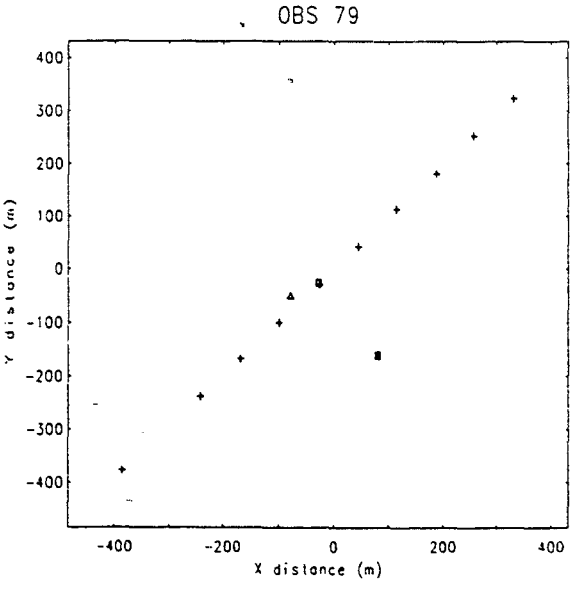
OBS 79
Y distance (m)
X distance (m)
400
300
200
100
0
-100
-200
-300
-400
-400
-200
0
200
400

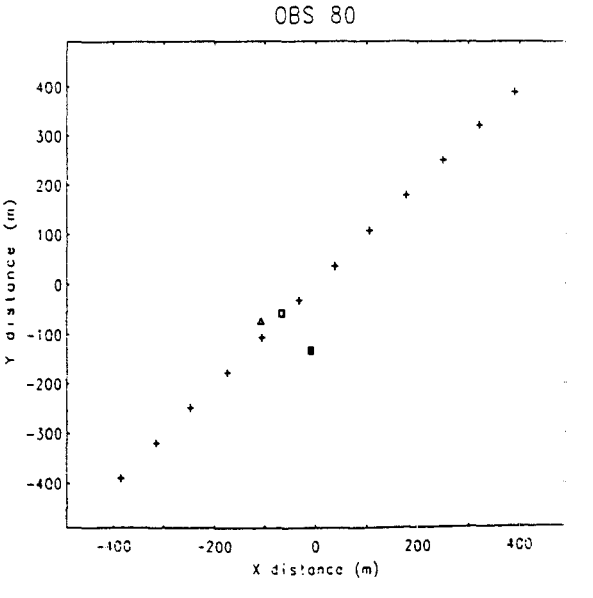
OBS 80
Y distance (m)
X distance (m)
400
300
200
100
0
-100
-200
-300
-400
-400
-200
0
200
400

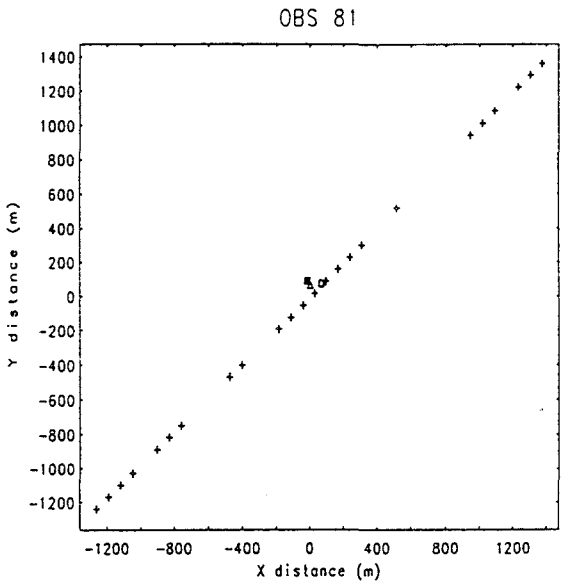
OBS 81
Y distance (m)
X distance (m)
1400
1200
1000
800
600
400
200
0
-200
-400
-600
-800
-1000
-1200
-1200
-800
-400
0
400
800
1200

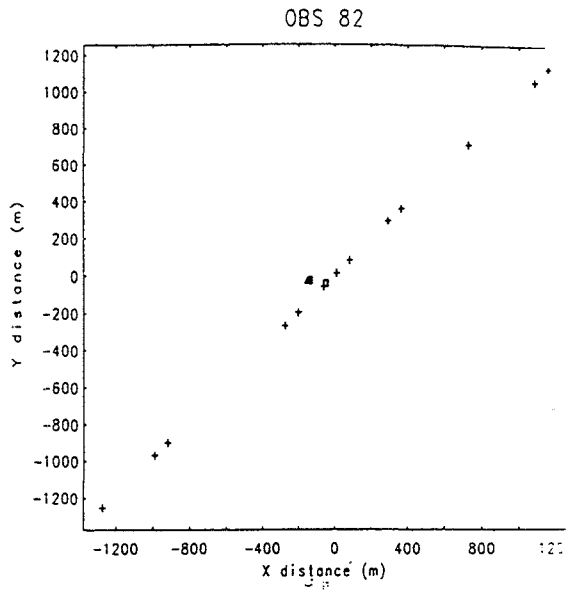
OBS 82
Y distance (m)
X distance (m)
1200
1000
800
600
400
200
0
-200
-400
-600
-800
-1000
-1200
-1200
-800
-400
0
400
800

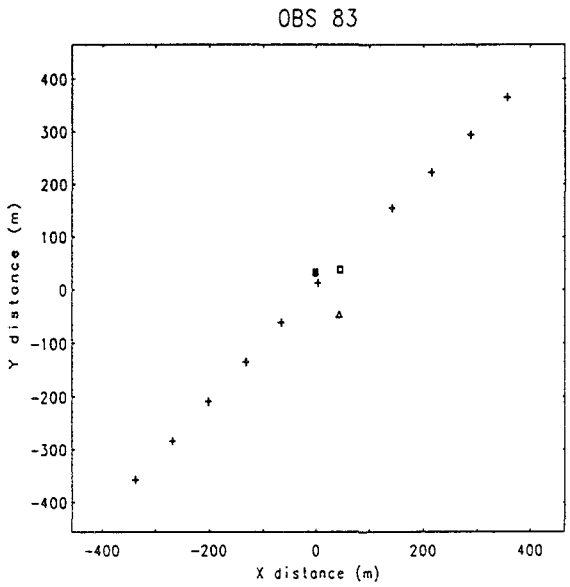
OBS 83
Y distance (m)
X distance (m)
400
300
200
100
0
-100
-200
-300
-400
-400
-200
0
200
400

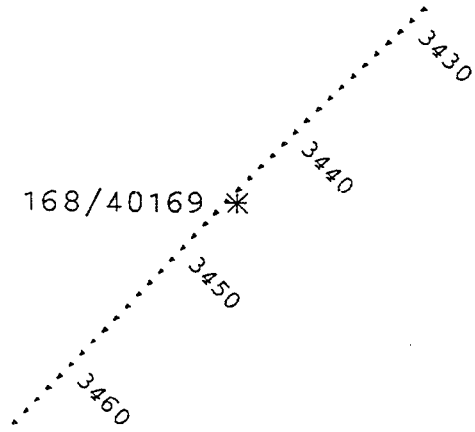
168/40169
3430
3440
3450
3460

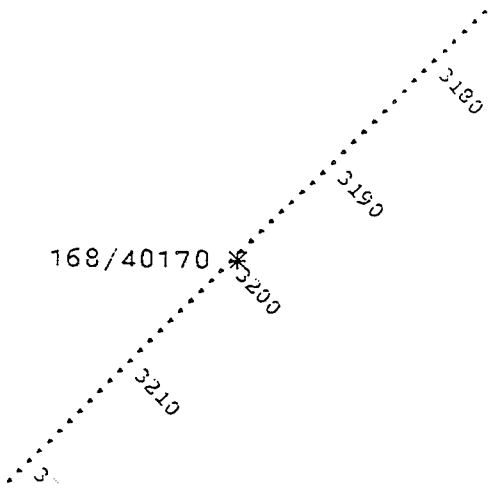
168/40170
3180
3190
3200
3210

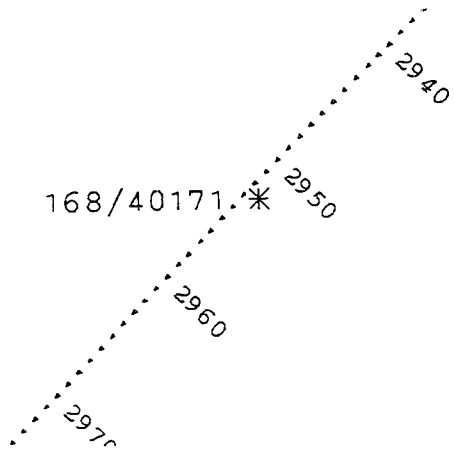
168/40171
2940
2950
2960

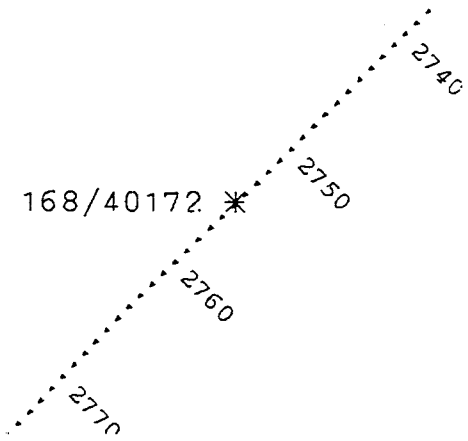
168/40172
2740
2750
2760
2770

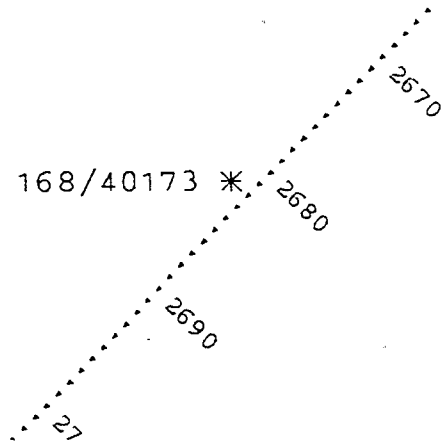
168/40173
2670
2680
2690
27

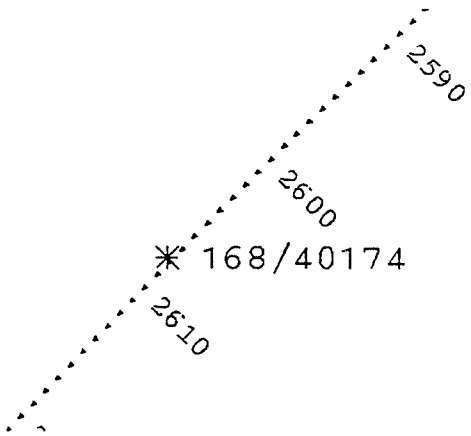
168/40174
2590
2600
2610

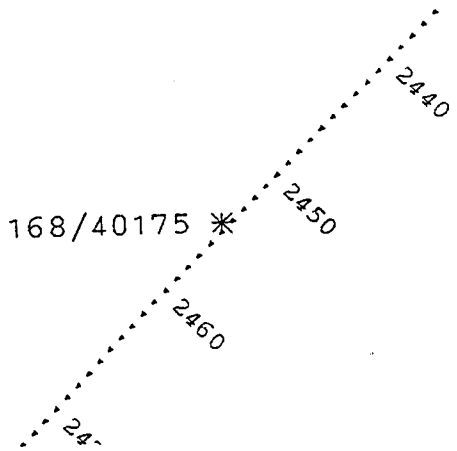
168/40175
2440
2450
2460
24

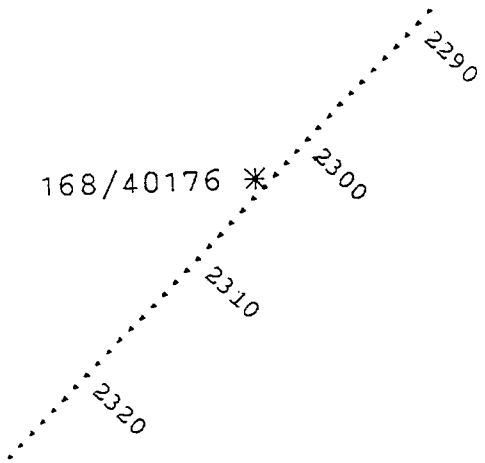
168/40176
2290
2300
2310
2320

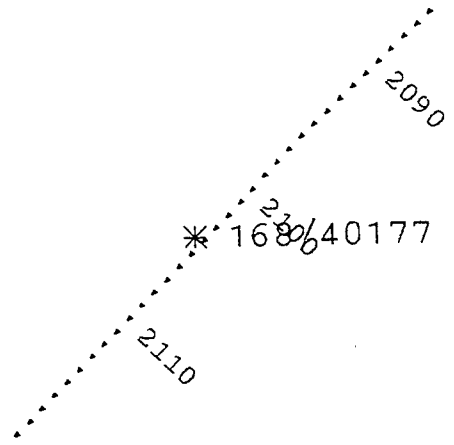
168/40177
2090
2100
2110

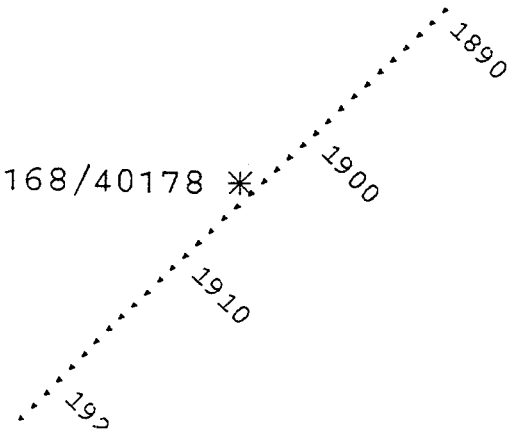
168/40178
1890
1900
1910
192

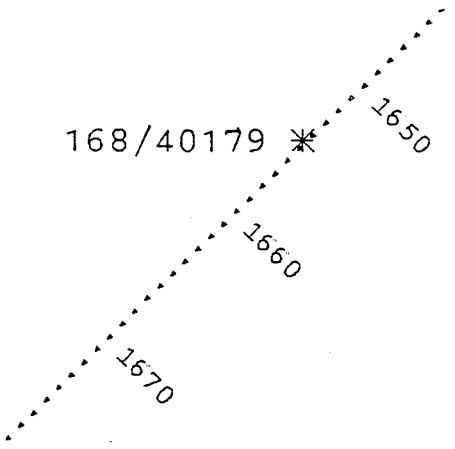
168/40179
1650
1660
1670

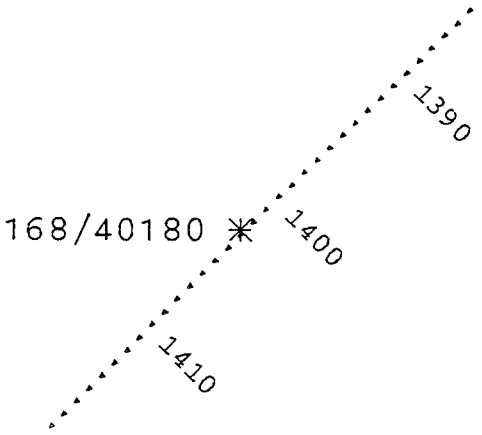
168/40180
1390
1400
1410

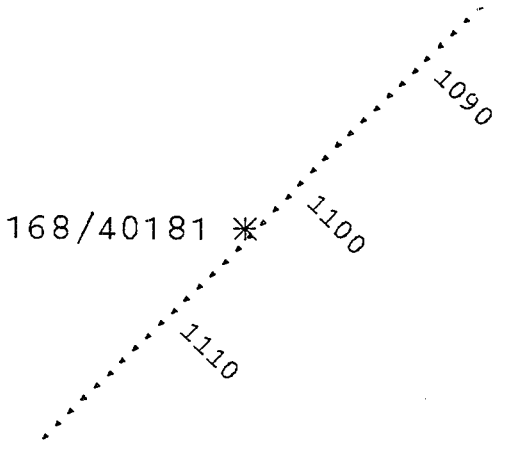
168/40181
1090
1100
1110

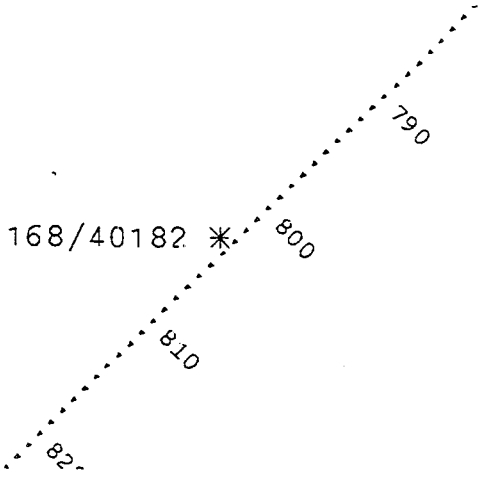
168/40182
790
800
810
82

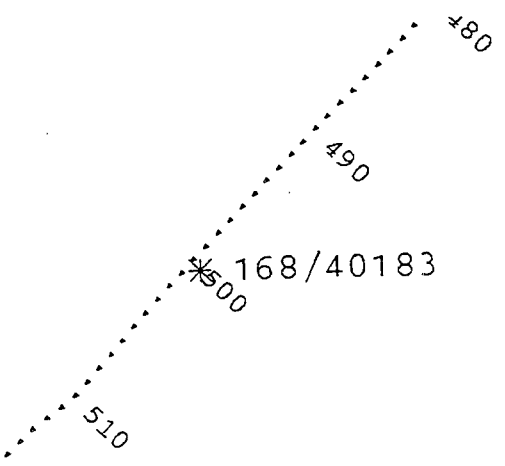
168/40183
480
490
500
510

Appendix 5 - Plots of Inversion Results: OBS Clock Correction

The plots represent a scaled version of Figure 7, such that when dcdw = 0 the clock correction has zero slope between t3 (2 h post-deployment) and t6 (post-recovery). The dashed lines represent dcdw values in increments of 0.05 from 0.0 to 0.5 during the period of data acquisition. In all cases the input value of dcdw was 0.0, as seen from the graphs. The square plotted near the intersection of the dashed lines indicates the secondary clock correction, being the offset from the initial clock correction line, and given in **Table 17** below.

Table 17 - Clock correction and drift rate

OBS	sec cc (s)	final cc (s)	final drift (s/day)
69	-0.020	0.505	0.06551
70	-0.001	1.135	0.19926
71	-0.022	1.613	0.36587
72	-0.010	1.019	0.28930
73	-0.040	1.017	0.26029
74	-0.001	0.598	0.18687
75	-0.011	0.997	0.25700
76	-0.014	0.872	0.48971
77	-0.014	1.276	0.30329
78	-0.016	1.283	0.29402
79	-0.011	0.907	0.30756
80	-0.010	0.837	0.20210
81	-0.015	0.804	0.35510
82	-0.002	0.667	0.22589
83	-0.019	0.727	0.22613

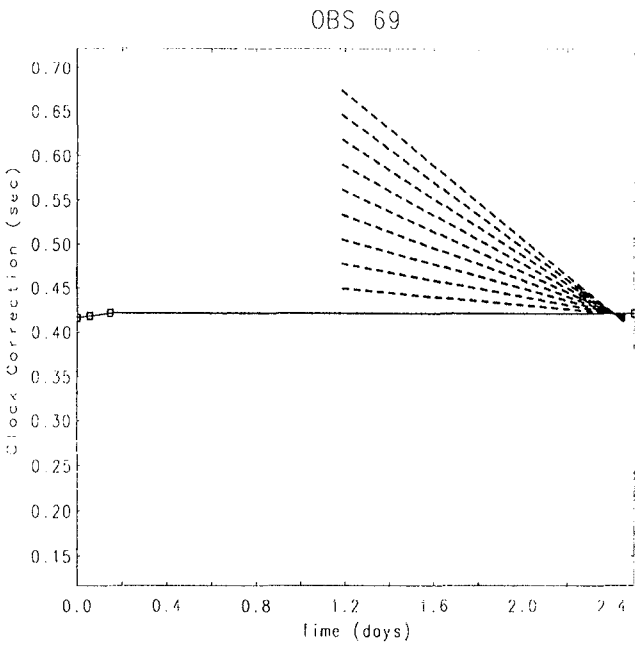
OBS 69
Clock Correction (sec)
0.70
0.65
0.60
0.55
0.50
0.45
0.40
0.35
0.30
0.25
0.20
0.15
0.0
0.4
0.8
1.2
1.6
2.0
2.4
Time (days)

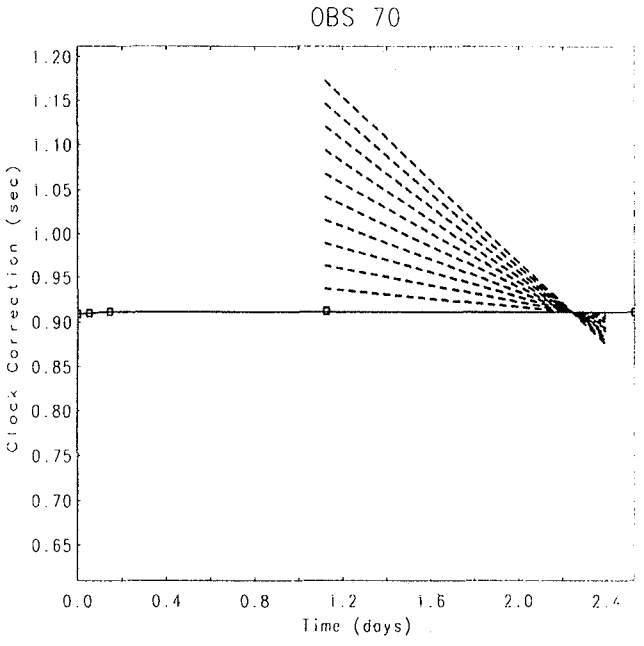
OBS 70
Clock Correction (sec)
1.20
1.15
1.10
1.05
1.00
0.95
0.90
0.85
0.80
0.75
0.70
0.65
0.0
0.4
0.8
1.2
1.6
2.0
2.4
Time (days)

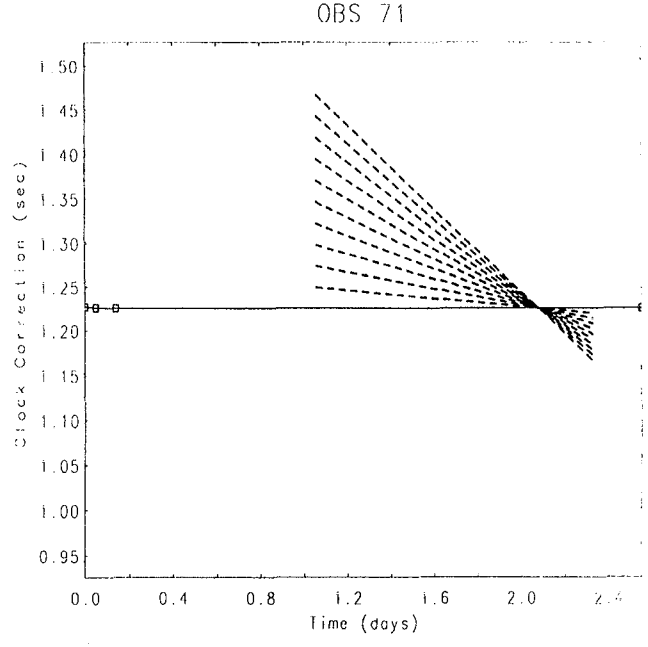
OBS 71
Clock Correction (sec)
1.50
1.45
1.40
1.35
1.30
1.25
1.20
1.15
1.10
1.05
1.00
0.95
0.0
0.4
0.8
1.2
1.6
2.0
Time (days)

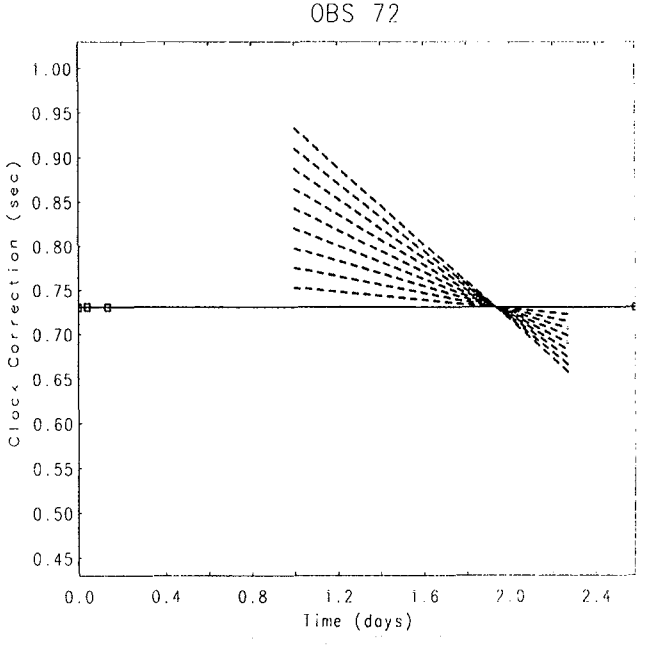
OBS 72
Clock Correction (sec)
1.00
0.95
0.90
0.85
0.80
0.75
0.70
0.65
0.60
0.55
0.50
0.45
0.0
0.4
0.8
1.2
1.6
2.0
2.4
Time (days)

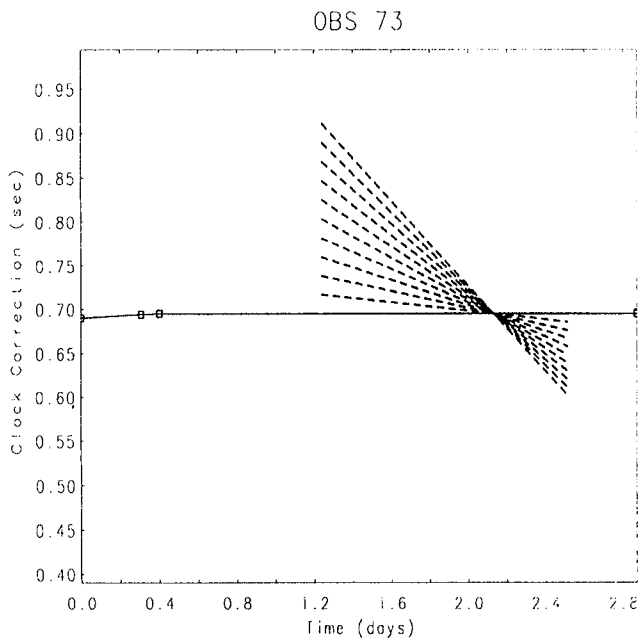
OBS 73
Clock Correction (sec)
0.95
0.90
0.85
0.80
0.75
0.70
0.65
0.60
0.55
0.50
0.45
0.40
0.0
0.4
0.8
1.2
1.6
2.0
2.4
Time (days)

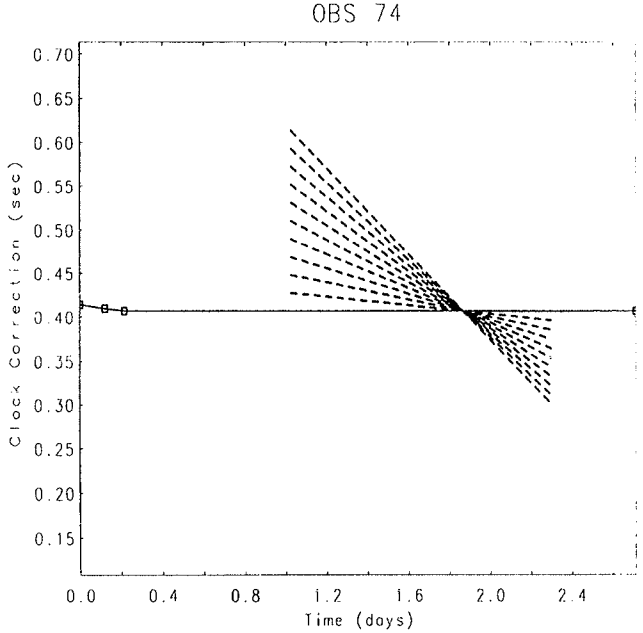
OBS 74
Clock Correction (sec)
0.70
0.65
0.60
0.55
0.50
0.45
0.40
0.35
0.30
0.25
0.20
0.15
0.0
0.4
0.8
1.2
1.6
2.0
2.4
Time (days)

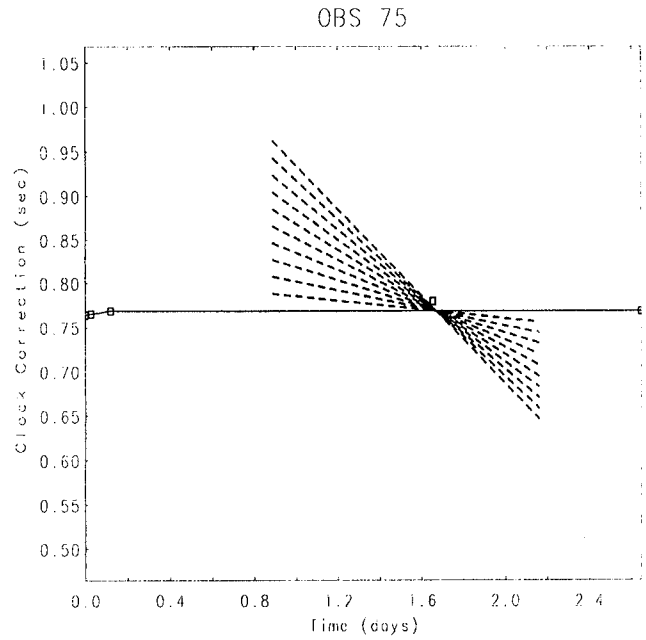
OBS 75
Clock Correction (sec)
1.05
1.00
0.95
0.90
0.85
0.80
0.75
0.70
0.65
0.60
0.55
0.50
0.0
0.4
0.8
1.2
1.6
2.0
2.4
Time (days)

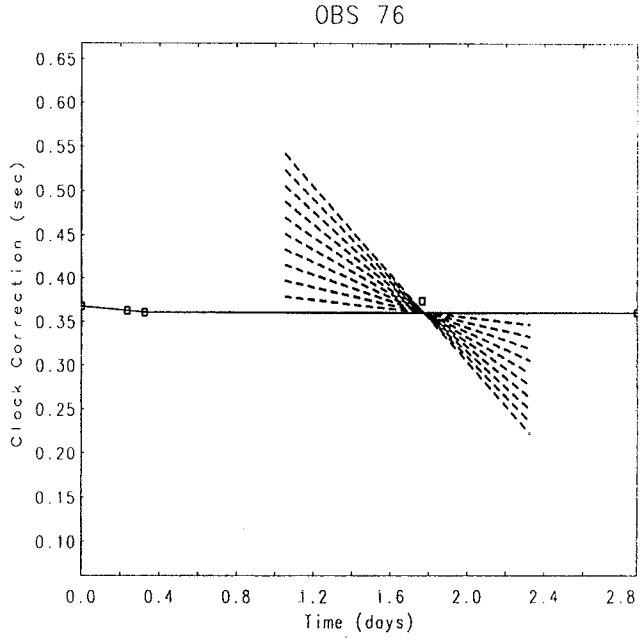
OBS 76
Clock Correction (sec)
0.65
0.60
0.55
0.50
0.45
0.40
0.35
0.30
0.25
0.20
0.15
0.10
0.0
0.4
0.8
1.2
1.6
2.0
2.4
2.8
Time (days)

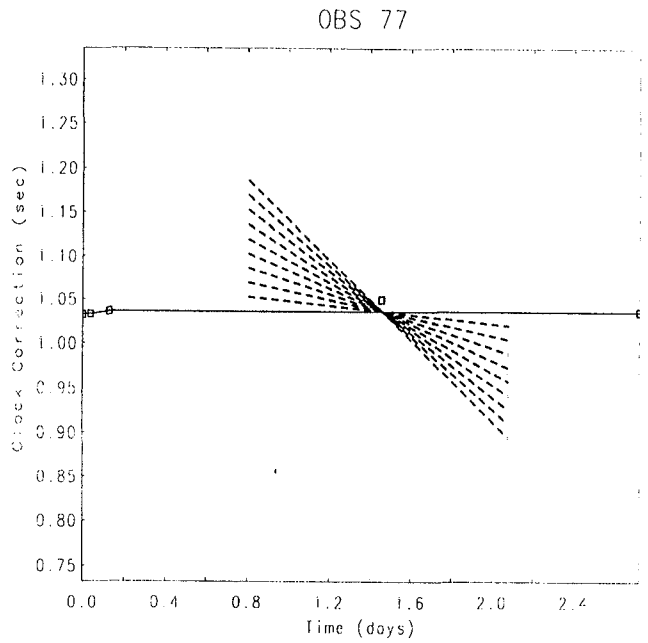
OBS 77
Clock Correction (sec)
1.30
1.25
1.20
1.15
1.10
1.05
1.00
0.95
0.90
0.85
0.80
0.75
0.0
0.4
0.8
1.2
1.6
2.0
2.4
Time (days)

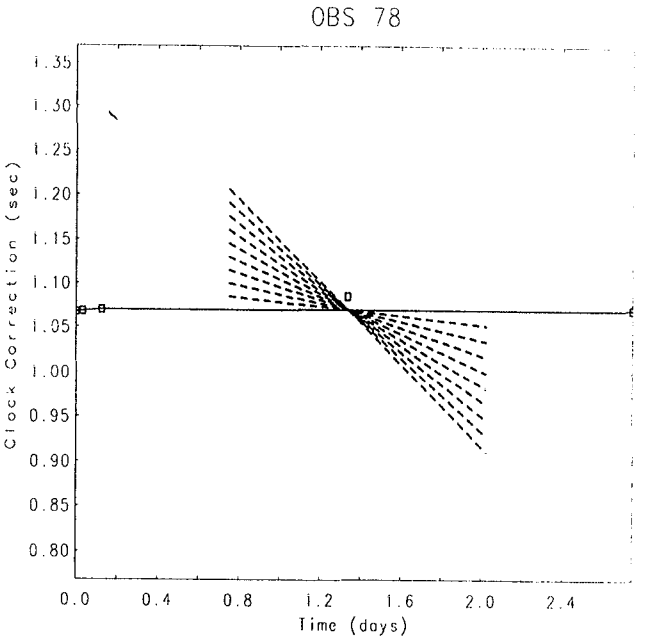
OBS 78
Clock Correction (sec)
1.35
1.30
1.25
1.20
1.15
1.10
1.05
1.00
0.95
0.90
0.85
0.80
0.0
0.4
0.8
1.2
1.6
2.0
2.4
Time (days)

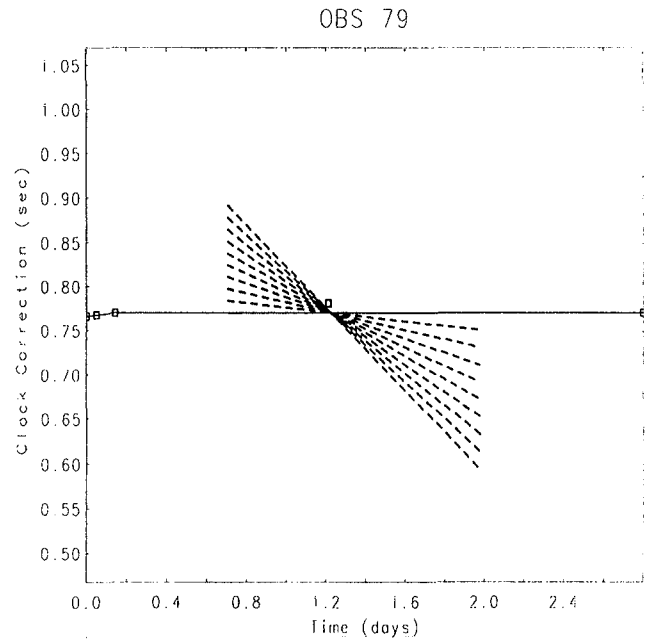
OBS 79
Clock Correction (sec)
1.05
1.00
0.95
0.90
0.85
0.80
0.75
0.70
0.65
0.60
0.55
0.50
0.0
0.4
0.8
1.2
1.6
2.0
2.4
Time (days)

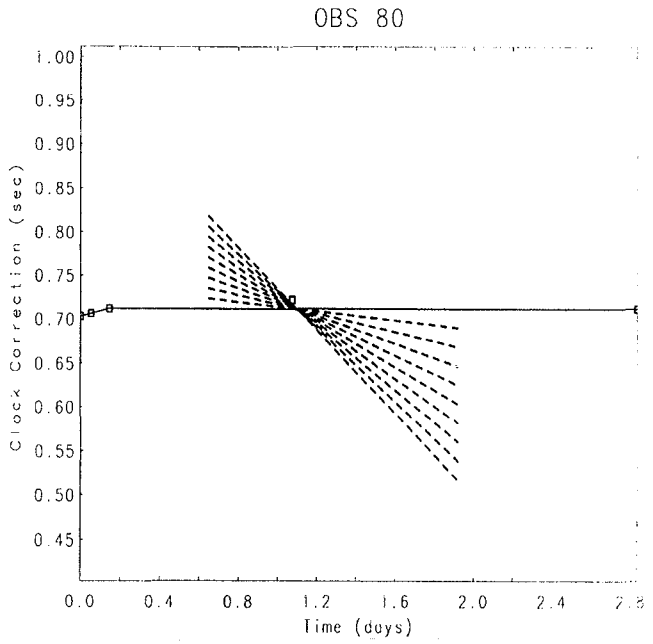
OBS 80
Clock Correction (sec)
1.00
0.95
0.90
0.85
0.80
0.75
0.70
0.65
0.60
0.55
0.50
0.45
0.0
0.4
0.8
1.2
1.6
2.0
2.4
Time (days)

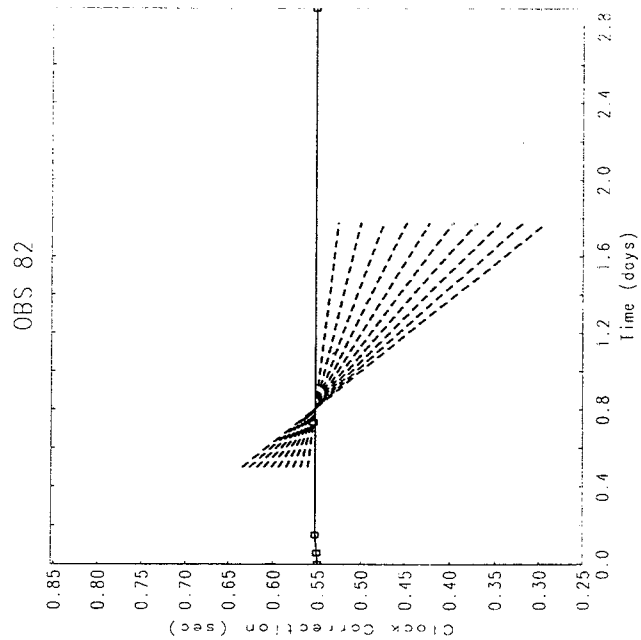

Appendix 5

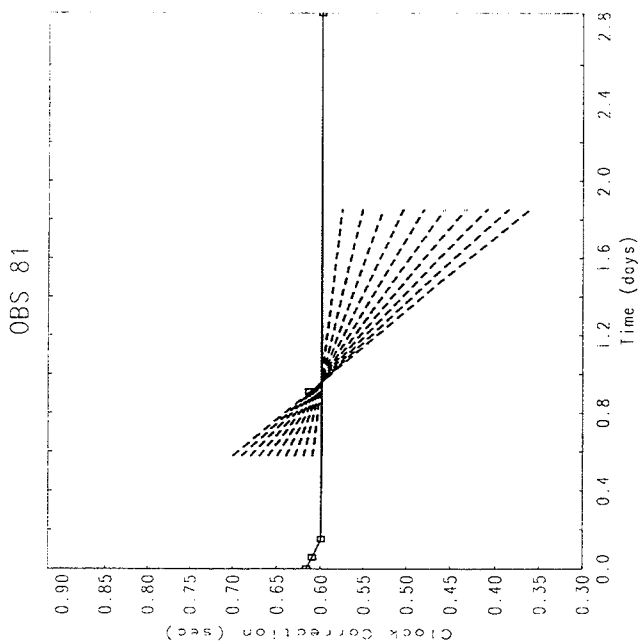

Appendix 5

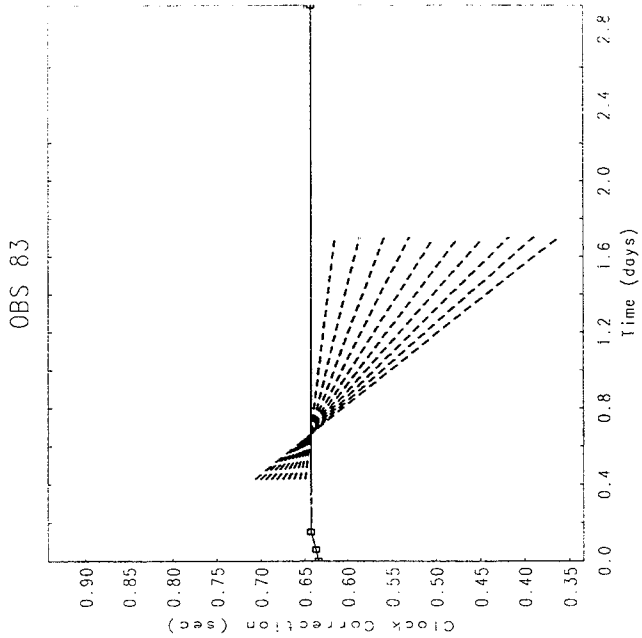

Appendix 6 - Plots of Inversion Results: OBS Orientation

The inversion algorithm generally gave poor results for OBS orientation, due to the shallow water and few water wave first arrivals. The plots depict the horizontal polarisation angle vs distance from the OBS (open circles), together with the computed horizontal polarisation after inversion for OBS orientation (solid line). Table 18 summarises the results.

The horizontal polarisation at point P is the difference between the OBS azimuth (bearing of H1 component) and the bearing of the OBS from P. A polarisation of zero at P means that the H1 component vector has the same direction as the vector from P to the OBS. The physical significance of this instance is that all of the energy from a wave emanating from P will be represented in the H1 component. See Christeson (1995, p24) for an alternative explanation of the method of computing the horizontal polarisation.

Table 18 - OBS azimuth

OBS	Azimuth	RMS error
69	146.5	35.3
70	320.9	28.6
71	18.8	43.1
72	323.4	28.7
73	208.0	32.4
74	233.4	25.3
75	144.2	40.6
76	345.9	20.0
77	201.8	55.0
78	156.1	40.9
79	351.3	44.9
80	126.2	38.0
81	153.1	40.9
82	133.6	20.8
83	202.0	52.1

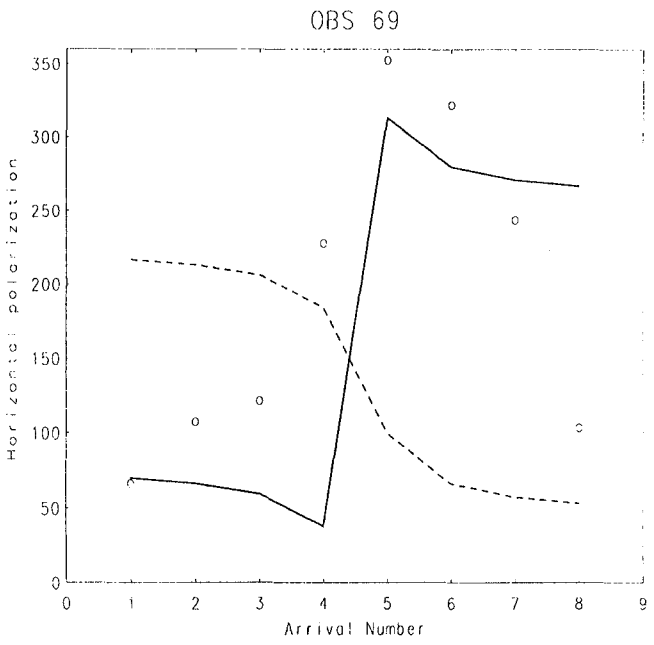
OBS 69
Horizontal polarization
Arrival Number

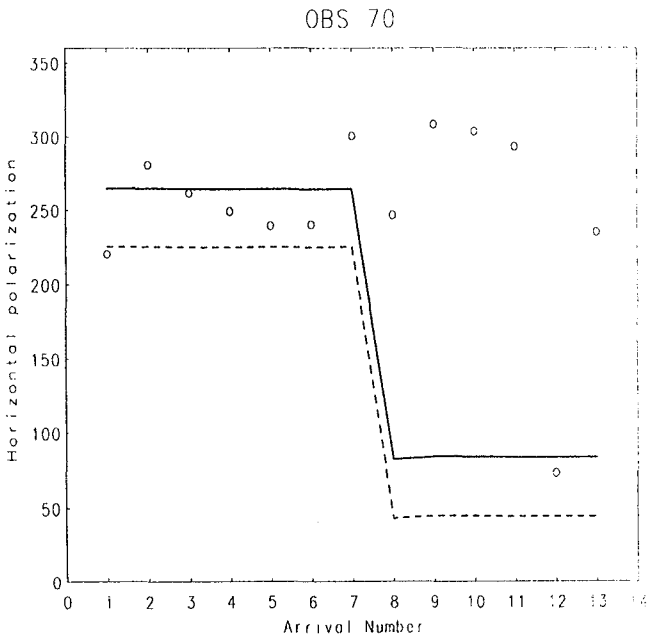
OBS 70
Horizontal polarization
Arrival Number

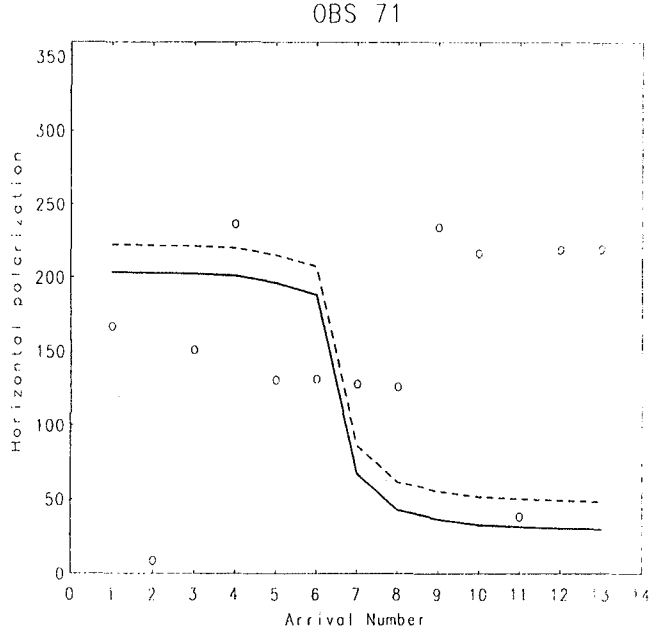
OBS 71
Horizontal polarization
Arrival Number

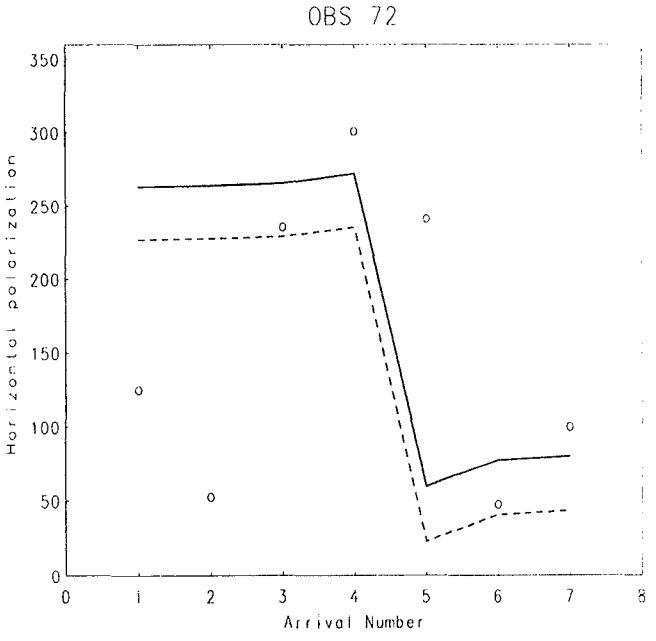
OBS 72
Horizontal polarization
Arrival Number

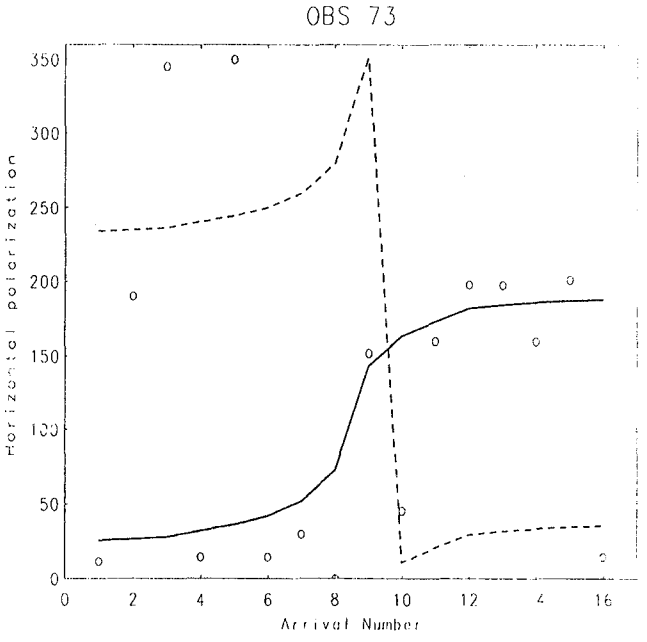
OBS 73
Horizontal polarization
Arrival Number

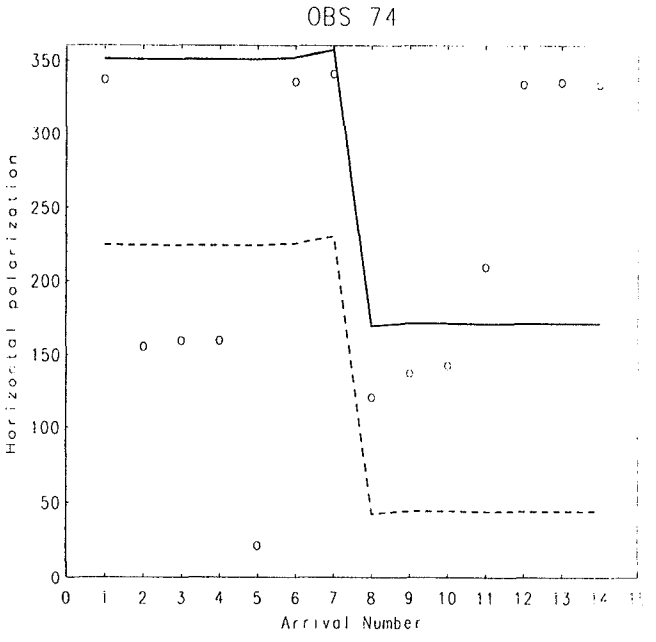
OBS 74
Horizontal polarization
Arrival Number

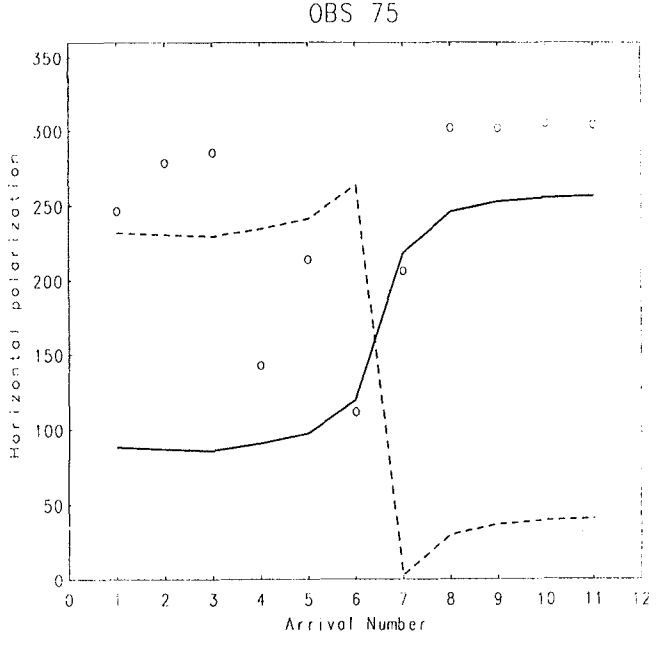
OBS 75
Horizontal polarization
Arrival Number

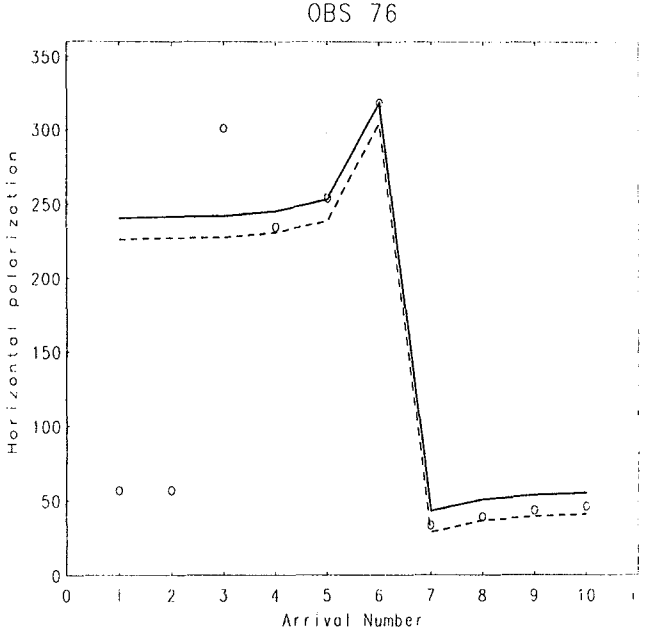
OBS 76
Horizontal polarization
Arrival Number

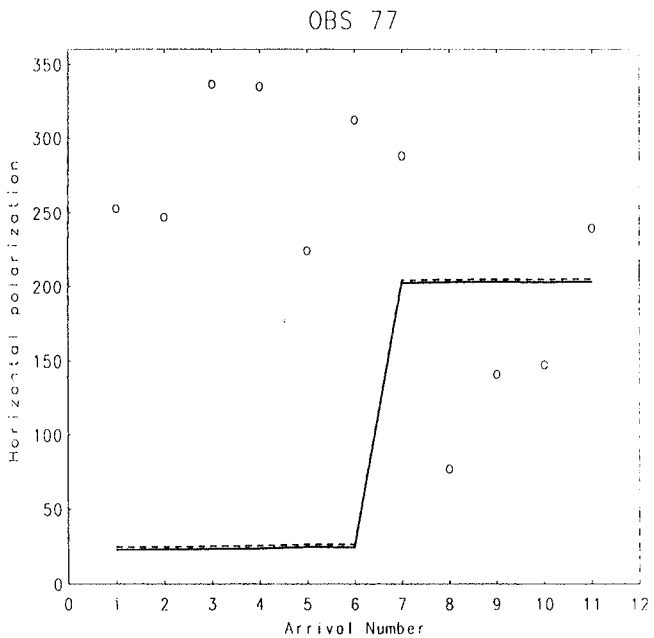
OBS 77
Horizontal polarization
Arrival Number

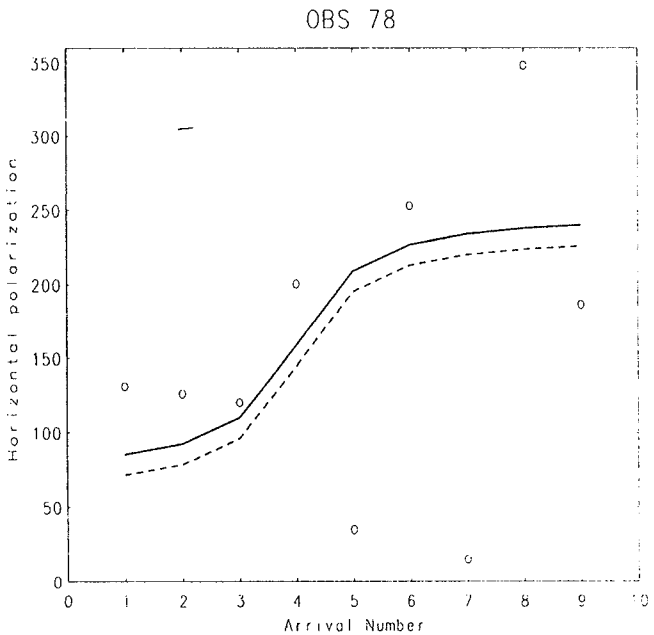
OBS 78
Horizontal polarization
Arrival Number

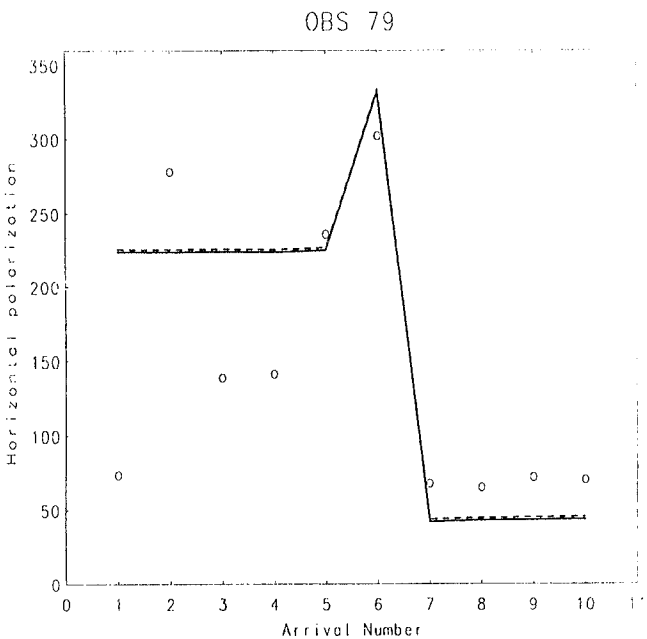
OBS 79
Horizontal polarization
Arrival Number

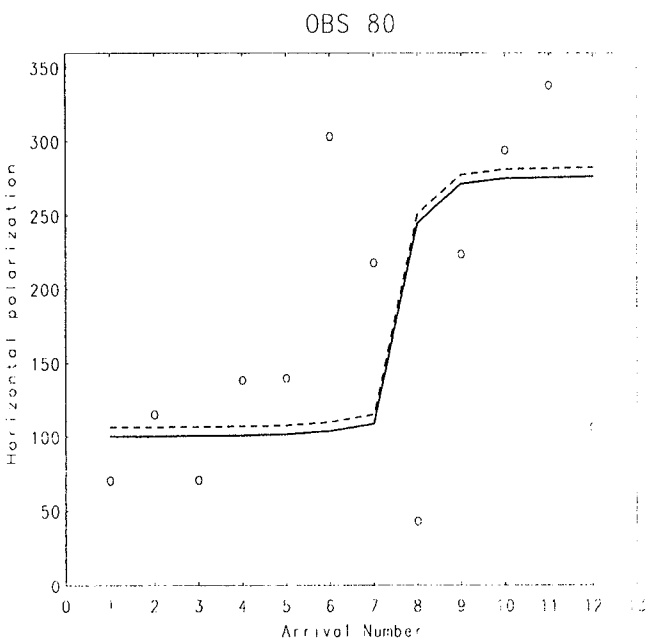
OBS 80
Horizontal polarization
Arrival Number

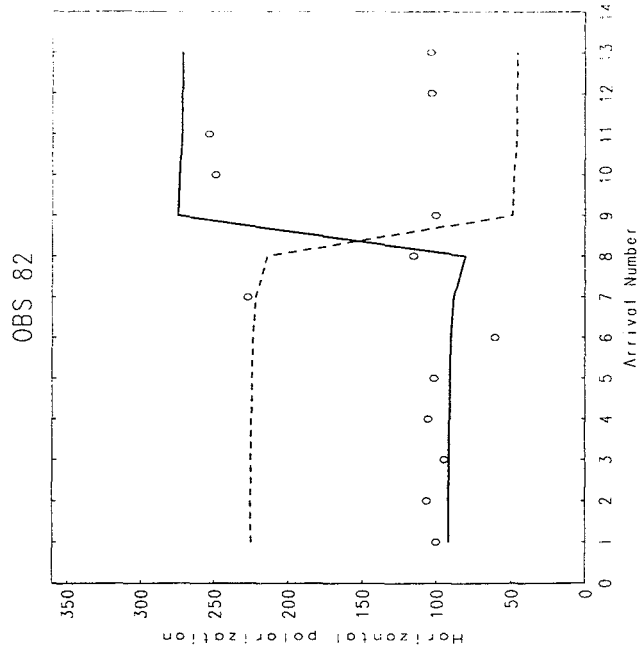

Appendix 6

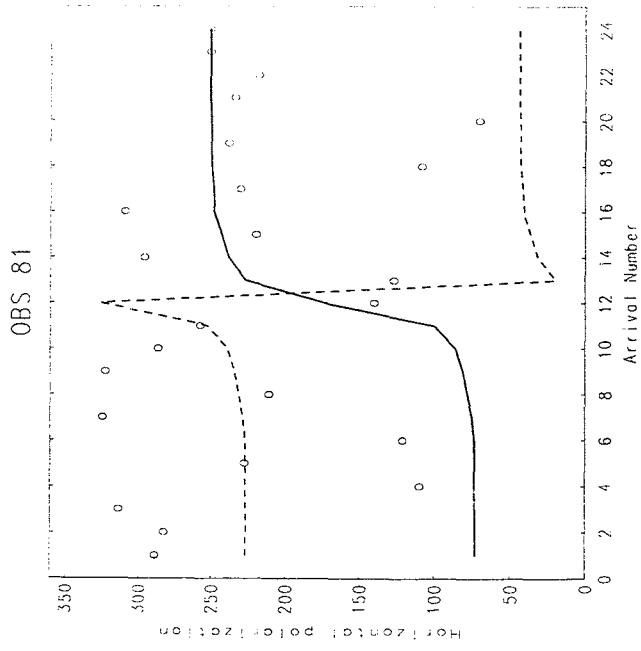

Appendix 6

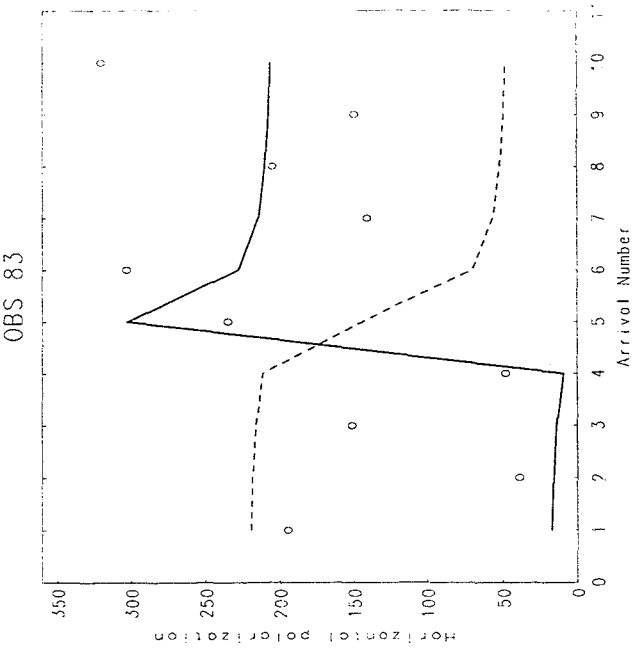

Appendix 7 - Plots of Inversion Results: Travel Times for Starting and Final Model

The diagrams depict the water wave arrival times (circles), the computed arrival times for the starting model (dashed line) and the computed arrival times for the final model (solid line) reported by the inversion program.

In all instances the inversion algorithm was for position and clock correction. Table 19 summarises the RMS error for each graph.

Table 19 - Travel time RMS error for inititial and final OBS position

OBS	Initial mean error	Final mean error
69	0.003	0.003
70	0.024	0.018
71	0.018	0.005
72	0.036	0.001
73	0.042	0.010
74	0.044	0.009
75	0.011	0.002
76	0.012	0.006
77	0.028	0.002
78	0.004	0.001
79	0.031	0.001
80	0.010	0.002
81	0.016	0.004
82	0.081	0.009
83	0.017	0.005

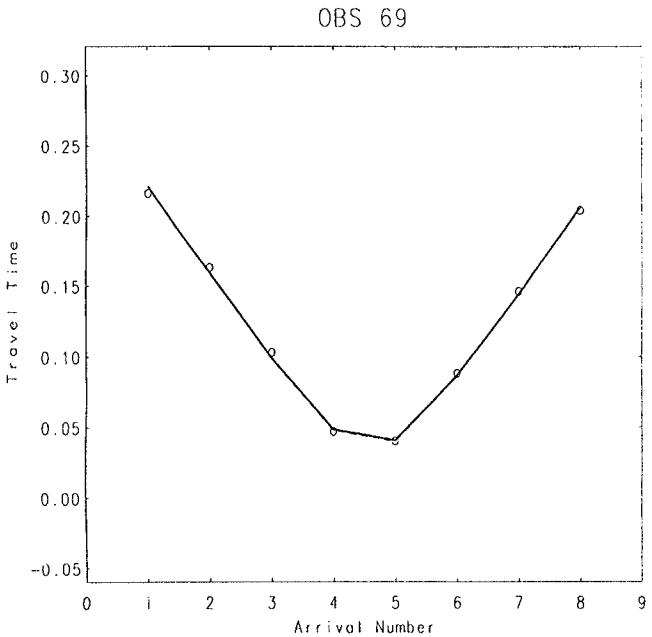
OBS 69
Travel Time
Arrival Number

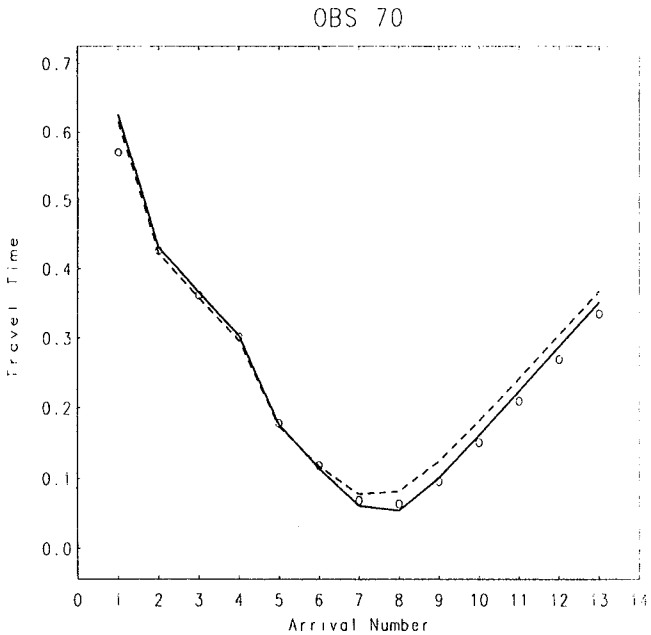
OBS 70
Travel Time
Arrival Number

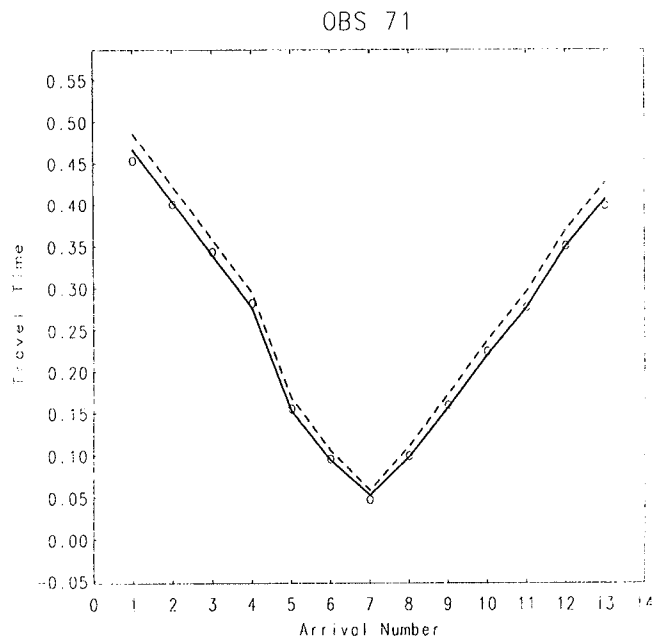
OBS 71
Travel Time
Arrival Number

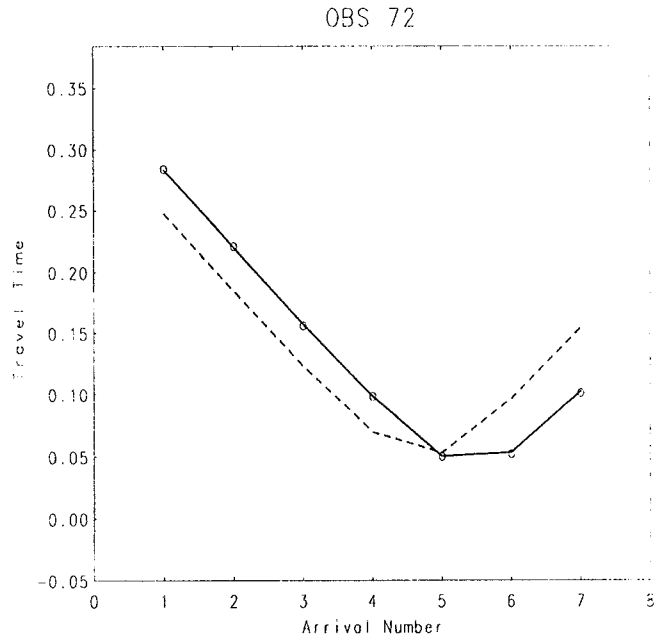
OBS 72
Travel Time
Arrival Number

Appendix 7

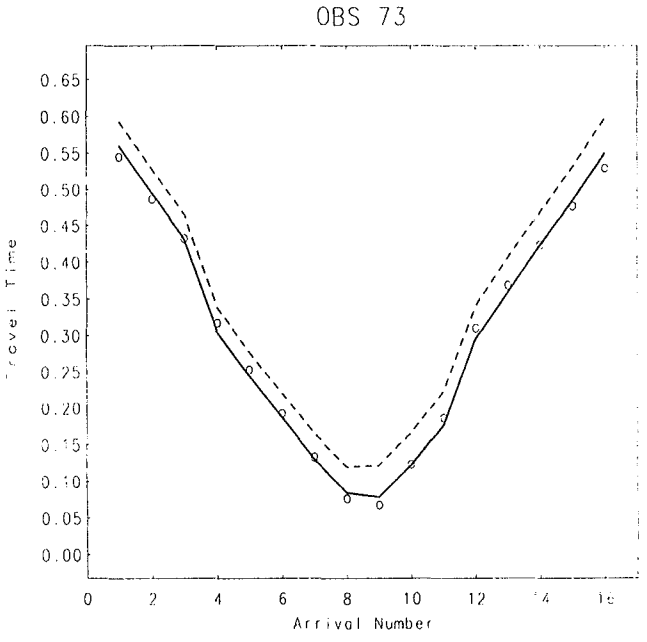
OBS 73
Travel Time
Arrival Number

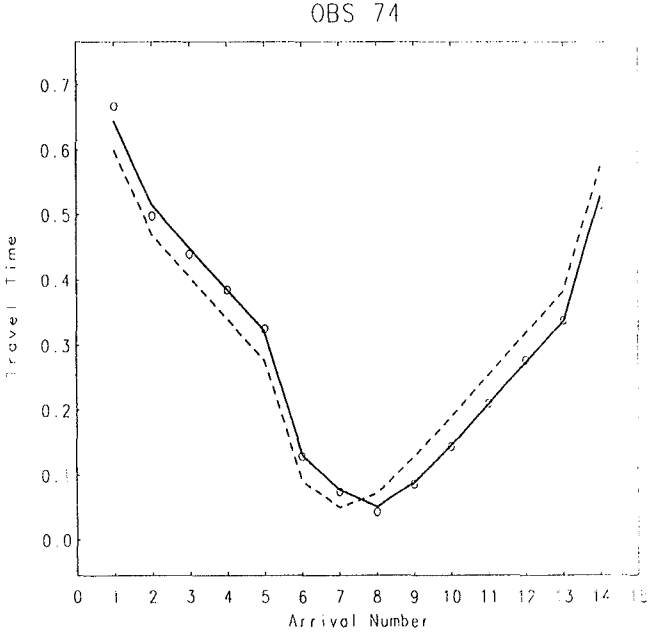
OBS 74
Travel Time
Arrival Number

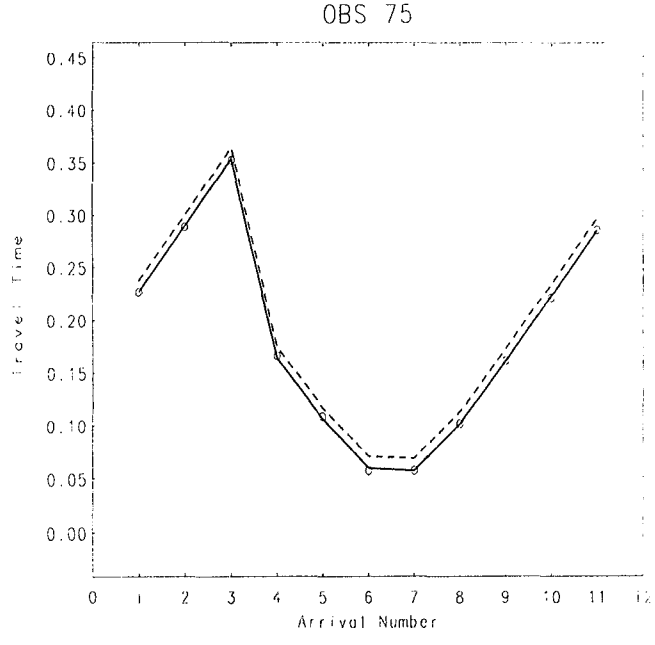
OBS 75
Travel Time
Arrival Number

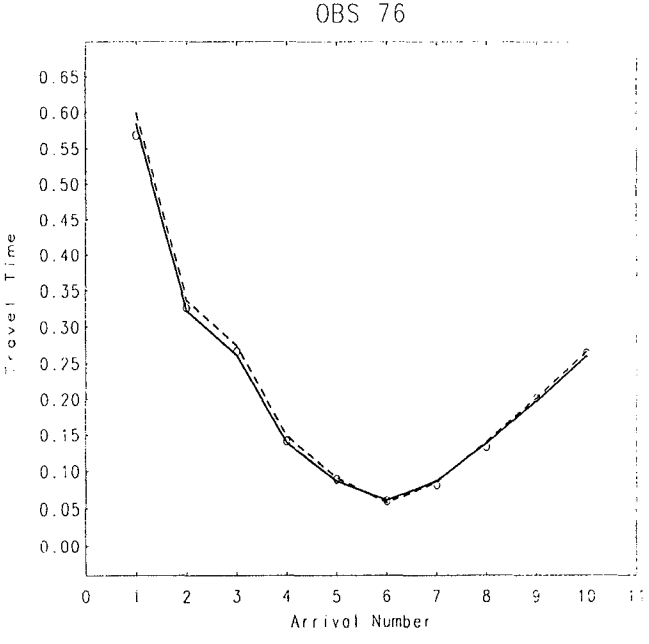
OBS 76
Travel Time
Arrival Number

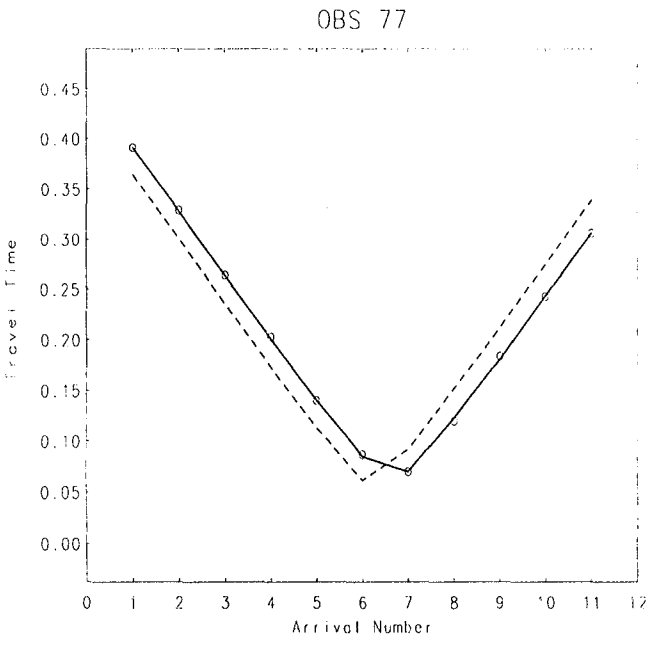
OBS 77
Travel Time
Arrival Number

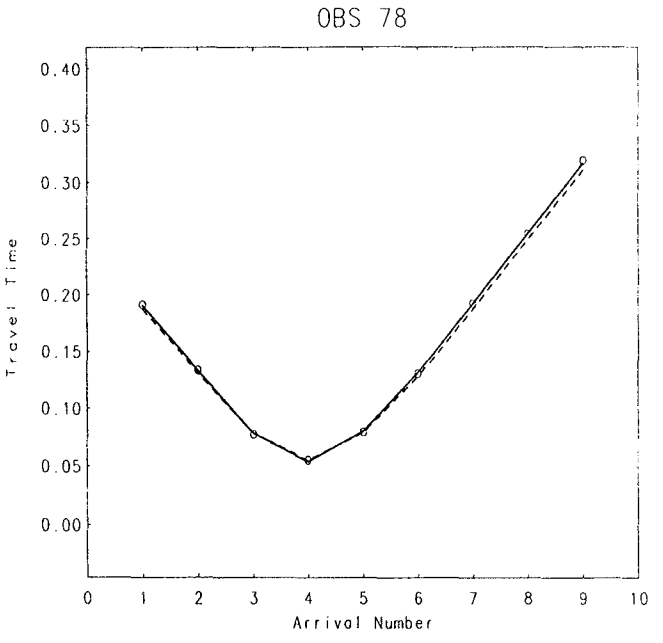
OBS 78
Travel Time
Arrival Number

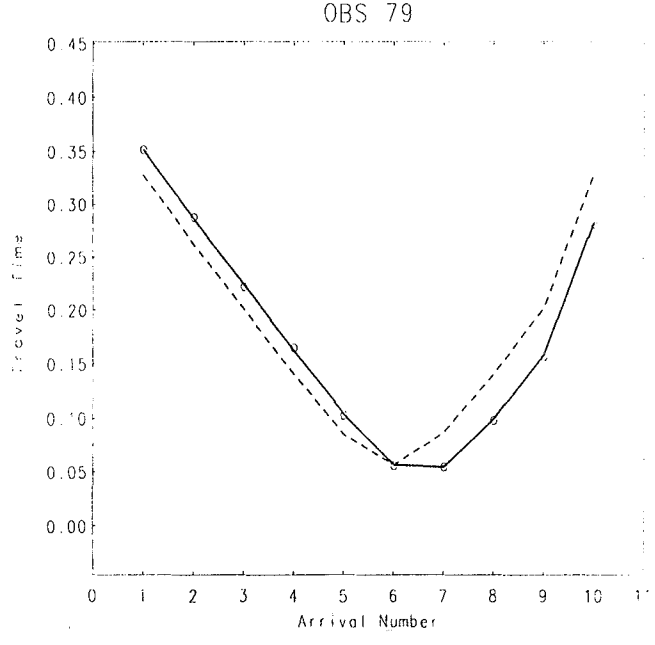
OBS 79
Travel Time
Arrival Number

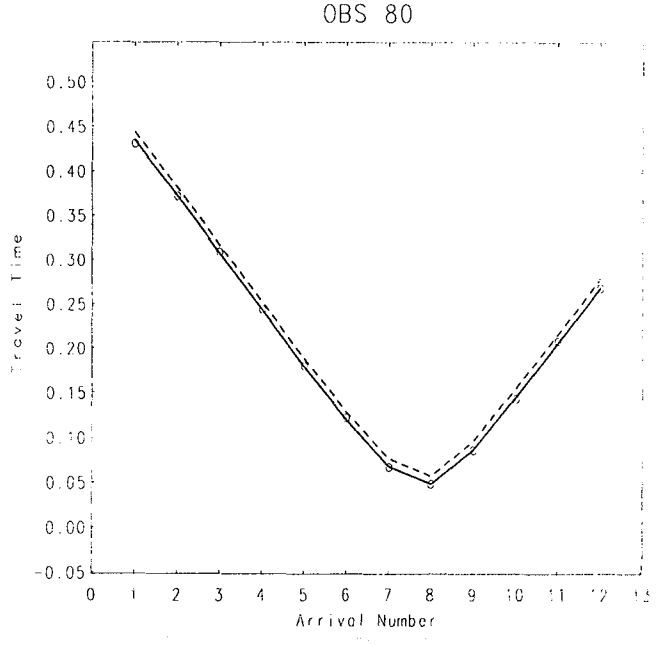
OBS 80
Travel Time
Arrival Number

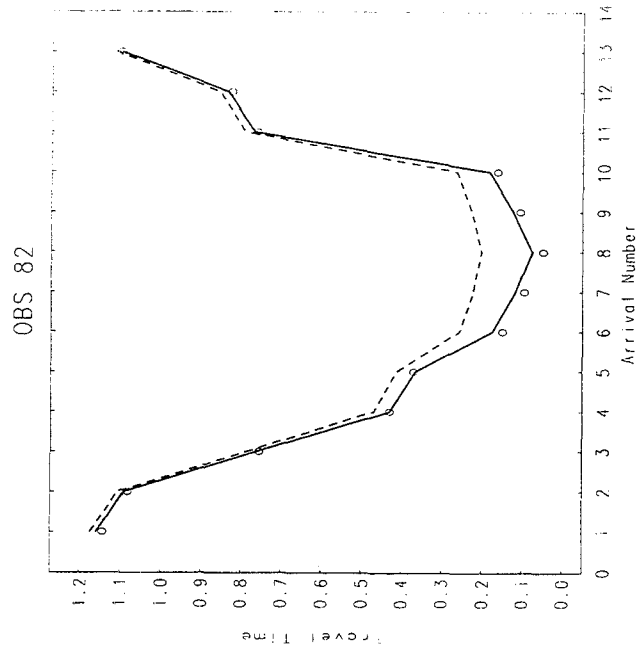

Appendix 7

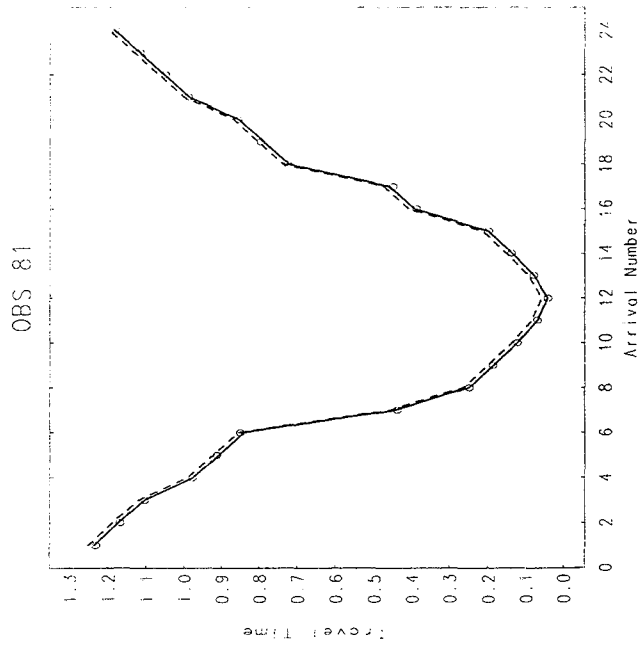

Appendix 7

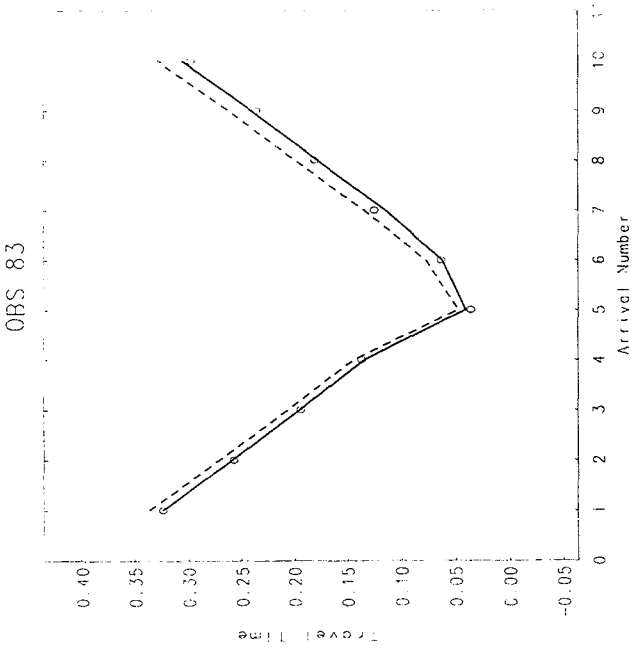

Appendix 8

Plots of Water Temperature Measurements

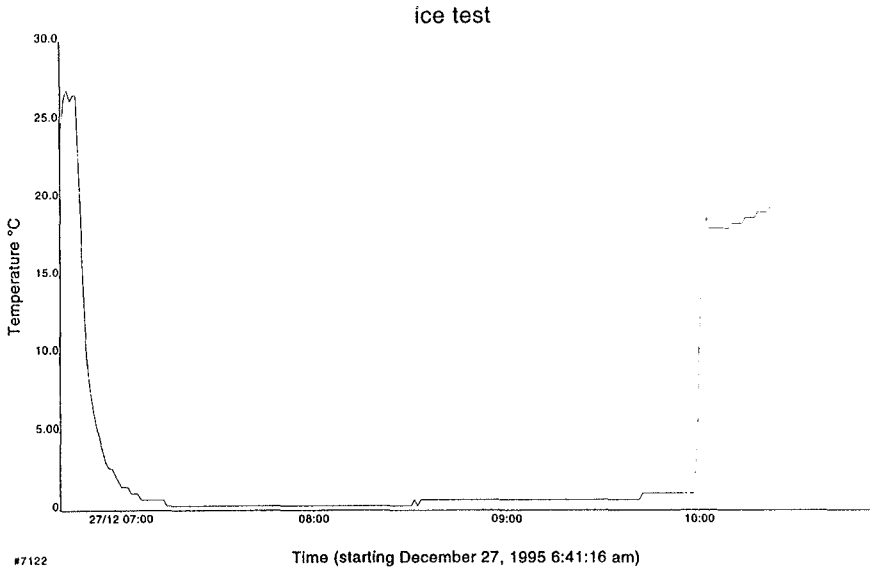
ice test
30.0
25.0
20.0
15.0
10.0
5.00
0
Temperature °C
27/12 07:00
08:00
09:00
10:00
#7122
Time (starting December 27, 1995 6:41:16 am)

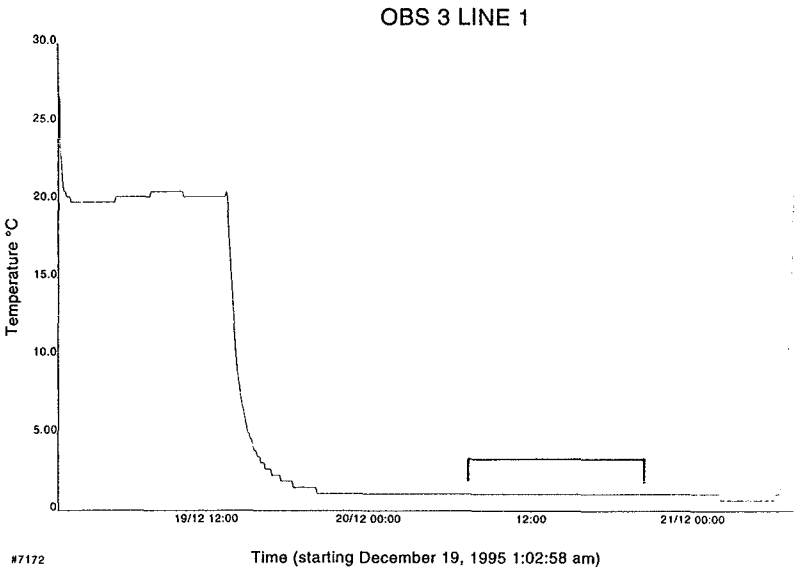
OBS 3 LINE 1
30.0
25.0
20.0
15.0
10.0
5.00
0
Temperature °C
19/12 12:00
20/12 00:00
12:00
21/12 00:00
#7172
Time (starting December 19, 1995 1:02:58 am)

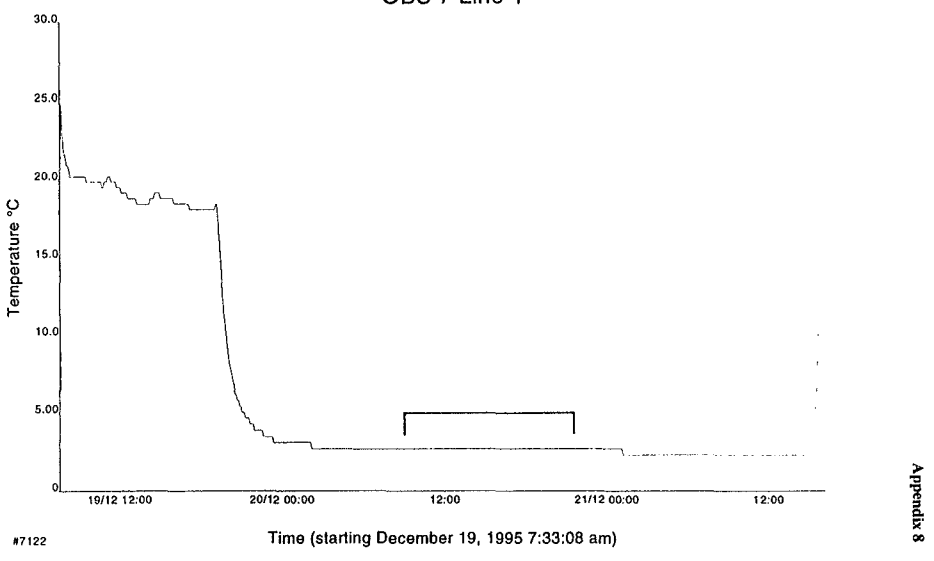
OBS 7 Line 1
30.0
25.0
20.0
15.0
10.0
5.00
0
Temperature °C
19/12 12:00
20/12 00:00
12:00
21/12 00:00
12:00
#7122
Time (starting December 19, 1995 7:33:08 am)

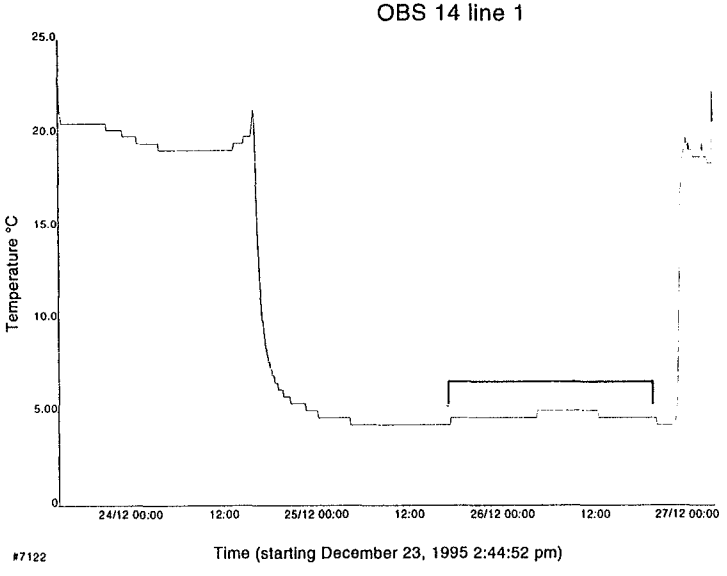
OBS 14 line 1
25.0
20.0
15.0
10.0
5.00
0
Temperature °C
24/12 00:00
12:00
25/12 00:00
12:00
26/12 00:00
12:00
27/12 00:00
#7122
Time (starting December 23, 1995 2:44:52 pm)

OBS 22 LINE 1

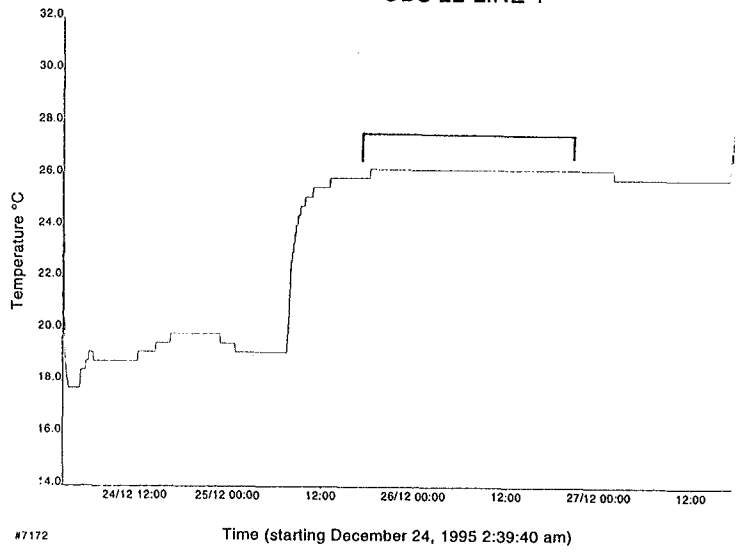

Appendix 8

OBS 30 line 2

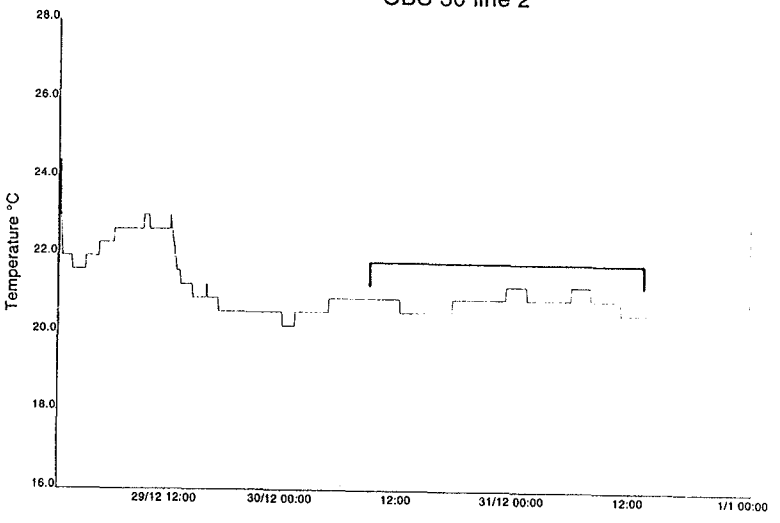

Appendix 8

OBS 34 Line 2

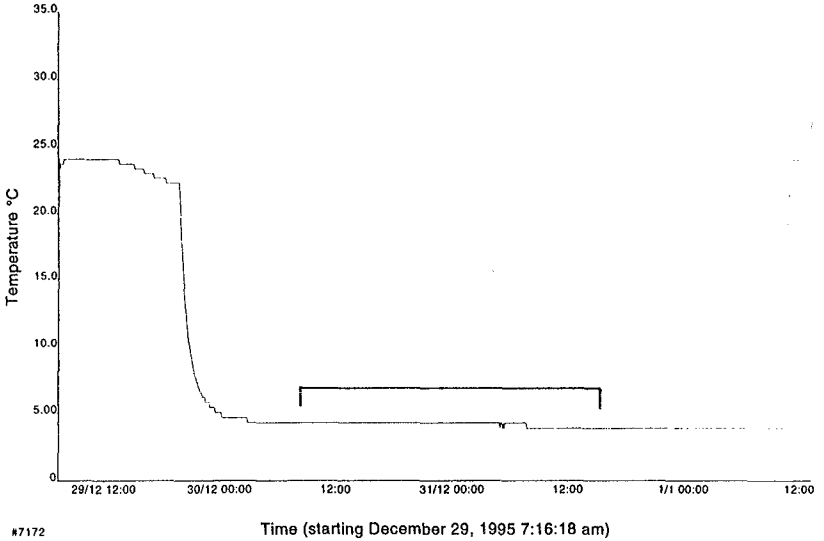

Appendix 8

OBS 42 line 2

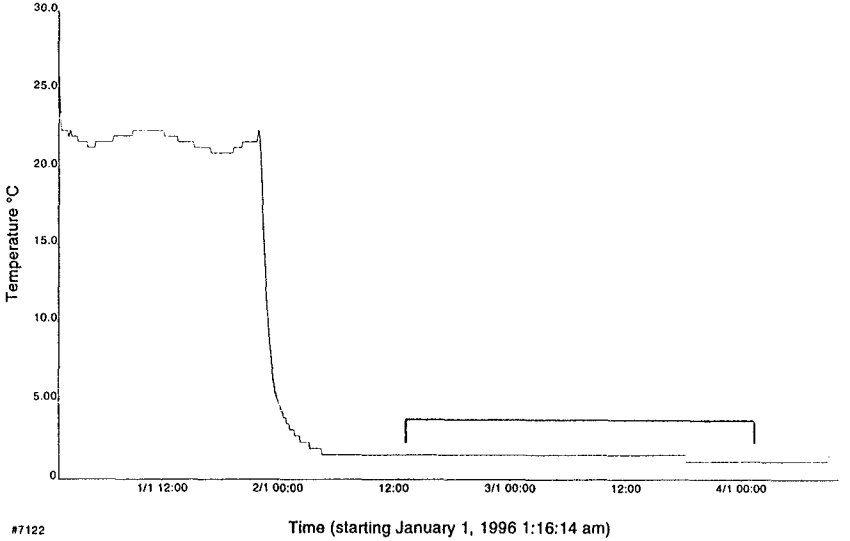

Appendix 8

OBS 53 LINE 3

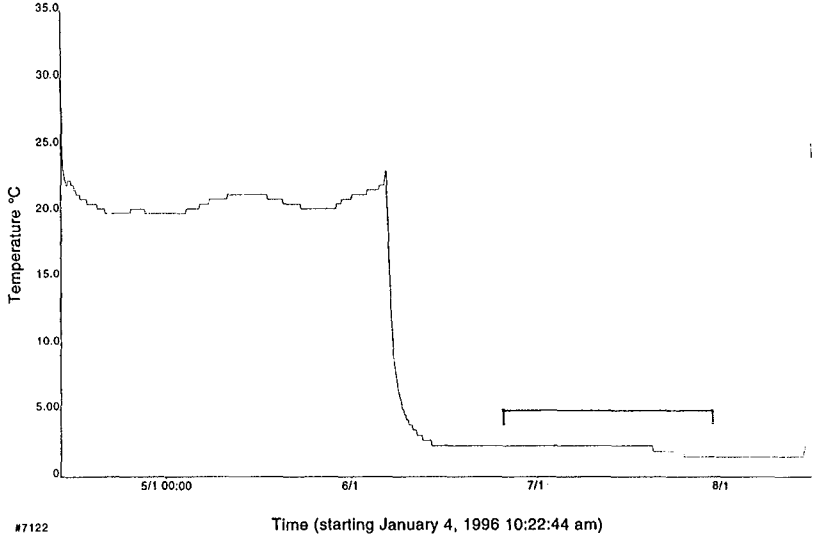

obs 63 line 3

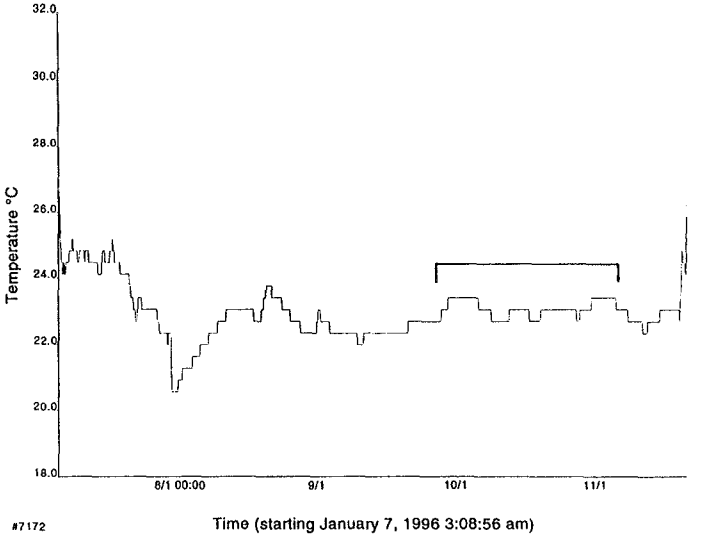

OBS 71 LINE 4

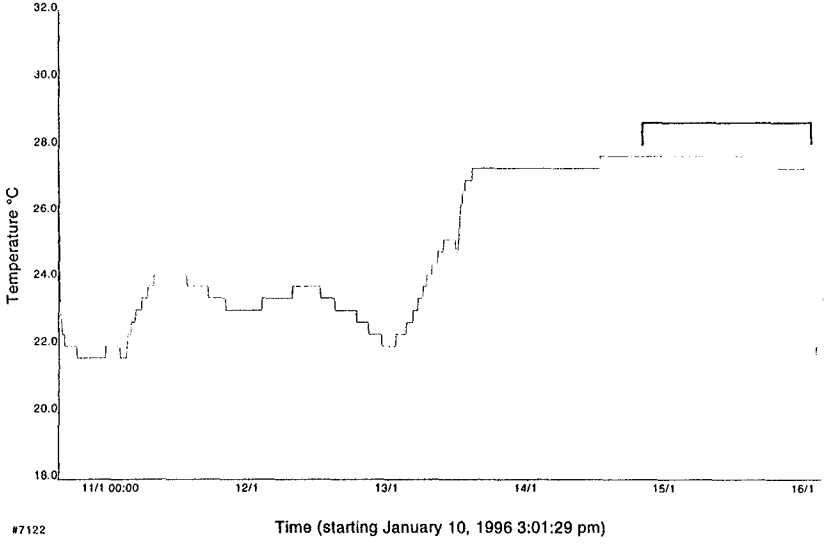

obs 76 line 4

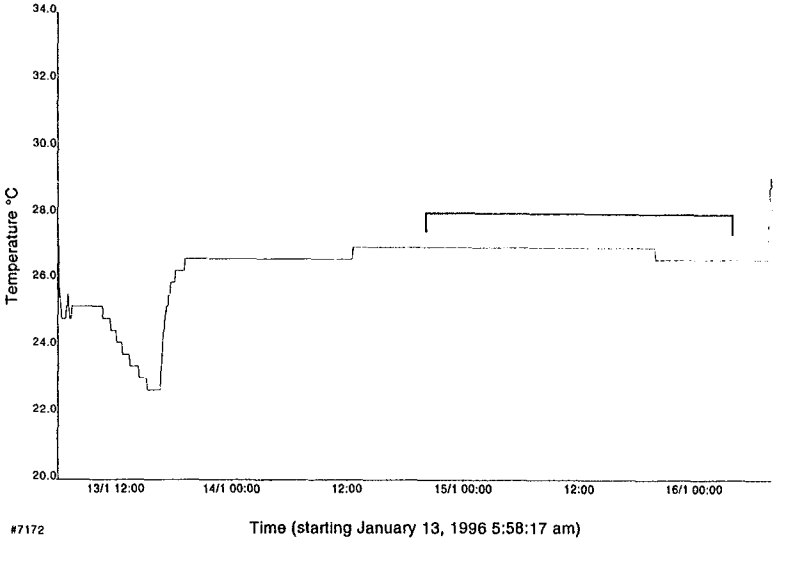

OBS 88 LINE 5

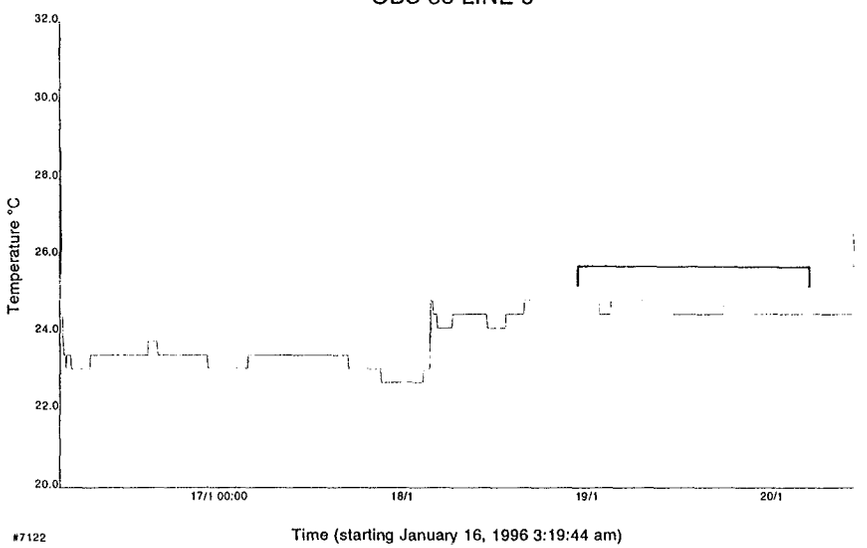

obs 93 line 5

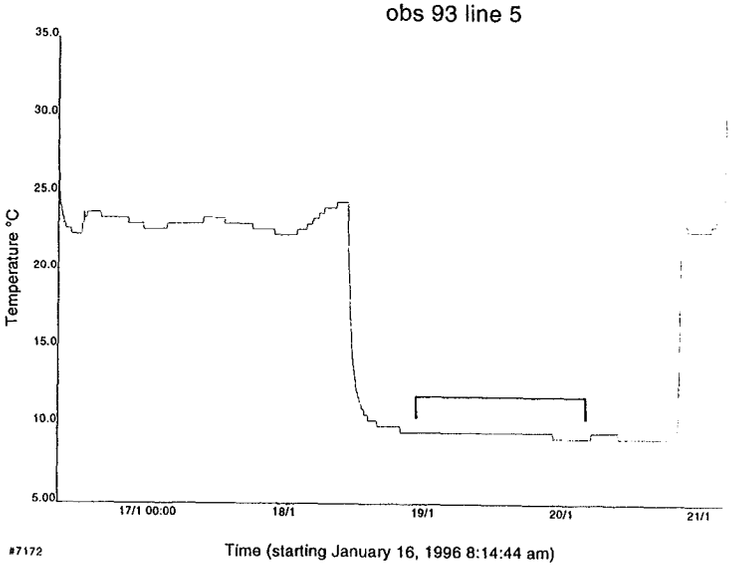

Appendix 9 - Listing of Typical DISCO Job File: Station 77

```
** DISCO BANDPASS FILTER AND PLOT JOB
**
*JOB    S168    401     ppetkovi
**
**------ READ SEG-Y DATA ------------------------------------------------
-
*CALL   GIN     12000   4       1       cdp     INCR    SEGY
TAPEOPT /tapefile="/export/mpsr/nsp0/s168/401/obsdata.77.segy.final.c1"
DENSITY 6250
REEL    sgydisk 100     3581
LIST
**
** ---- PATCH MUTED TRACES BY COMPUTING MEAN --------------------------
*CALL   PATCH           SHOT    10
TRACES
0       1499    104     103     105     104     103
0       1499    114     113     115     114     113
0       1499    124     123     125     124     123
0       1499    134     133     135     134     133
1111    12000   144     143     145     144     143
6919    12000   154     153     155     154     153
0       1499    155     154     156     155     154
0       1499    165     164     166     165     164
0       1499    175     174     176     175     174
3022    12000   185     184     186     185     184
9557    12000   195     194     196     195     194
0       1499    196     195     197     196     195
0       1499    206     205     207     206     205
10880   12000   215     214     216     215     214
0       1499    216     215     217     216     215
.
.
.
4597    12000   3515    3514    3516    3515    3514
8514    12000   3525    3524    3526    3525    3524
0       1499    3526    3525    3527    3526    3525
0       1499    3536    3535    3537    3536    3535
2582    12000   3546    3545    3547    3546    3545
0       1499    3557    3556    3558    3557    3556
0       1499    3567    3566    3568    3567    3566
4633    12000   3577    3576    3578    3577    3576
0       1499    3578    3577    3579    3578    3577
**
**----- write station number to shot number header for Sigma compatibility-
-
** *CALL   HDRMATH
** HCMUL   ffid    0       temp
** HCADD   temp    77      ffid
**
**------ COLLECT ALL TRACES TO MIMIC 1 SHOT INTO 3481 CHANNELS ----------
-
*CALL   COLLECT 3481
**
**------ FILTER ---------------------------------------------------------
-
*CALL   FILTER  shot                            MINIMUM
KEYDEF  1
BANDSL  BP      OCTSL
1               5       24      10      40
*IF
RANGE   shot    100     1140
**
**----- STACK TRACES ----------------------------------------------------
-
*CALL   RUNMIX  3
WEIGHTS
1       2       1
*RESET
```

```
*IF
RANGE    shot     3080     3581
*CALL    RUNMIX   3
WEIGHTS
1        2        1
*RESET
**
**----- EQUALISE TRACE AMPLITUDES ----------------------------------------
-
** *call         balance
*CALL    AGC      1500
**
**------ DISPLAY DATA ----------------------------------------------------
-
*CALL    SECPLOT RL       VA       40       1.181    1        0
SETAMP   CONSTANT1.33e8                    1
XPLOT    offset  5000     0.01     100
PLOTOPT  /name=sec0
LABEL    offset  5        1        shot     20
LABELSZ  0.09    0.075
TITLE    168/401.77 (5-10 Hz) Vertical Component
TRANGE   0        12000
TITLE2         Runmix 3 traces (1,2,1)
*CALL    SIDELBL 0.5
HISTORY  ALLCALL 2        8
PLOTOPT  /segment=every/pos=(after,sec0)
**
**----- WRITE OUTPUT FILE -----------------------------------------------
-
*CALL    GOUT
DENSITY  6250
REEL     SGYDISK
TAPEOPT  /tapefile="/export/mpsr/obs2/401/obs77.sgy"
*END
```

Appendix 10

Refraction Data Display after Bandpass Filter

168/401.69 (5-10 Hz) Vertical Component

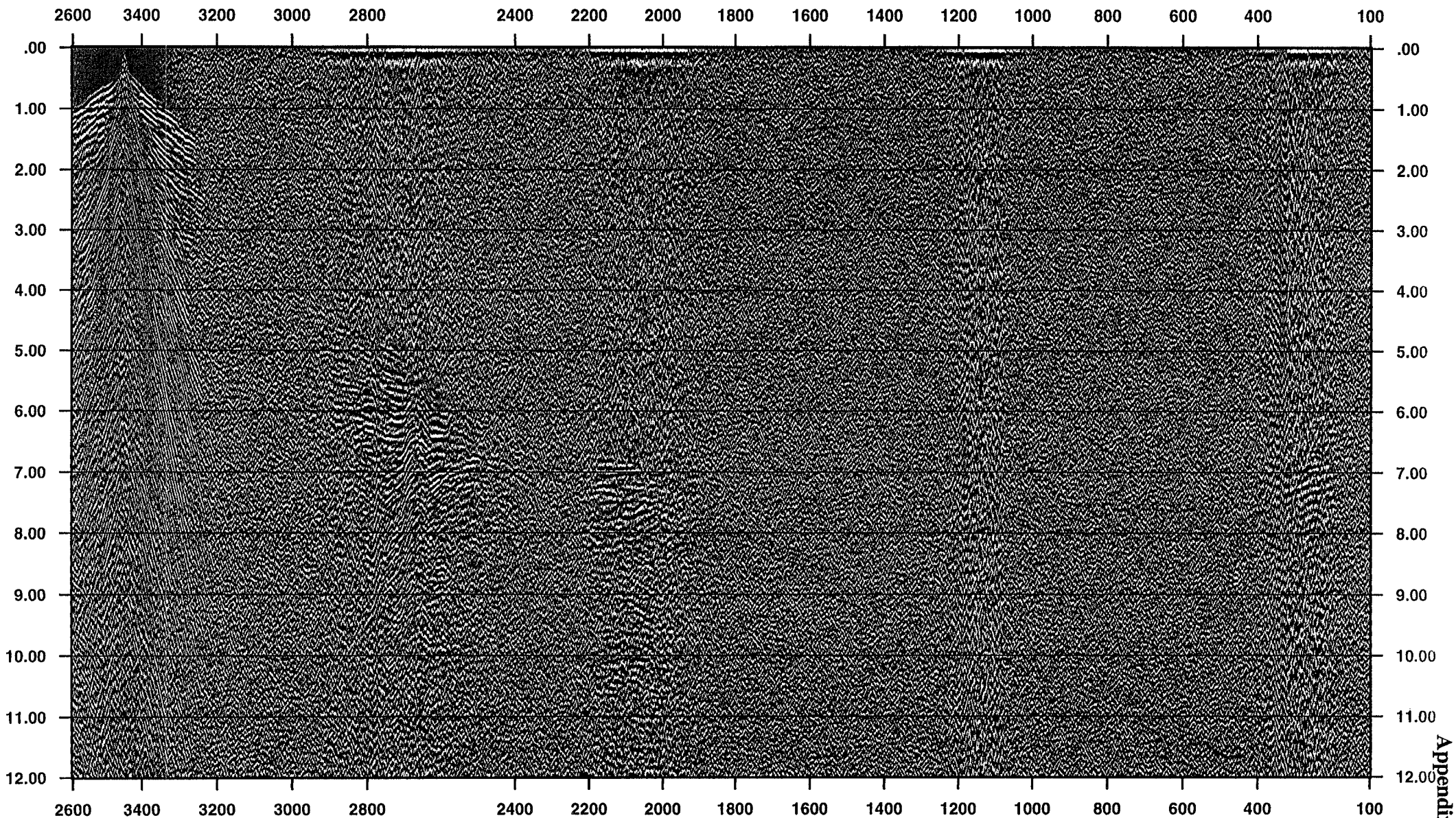

Appendix 10

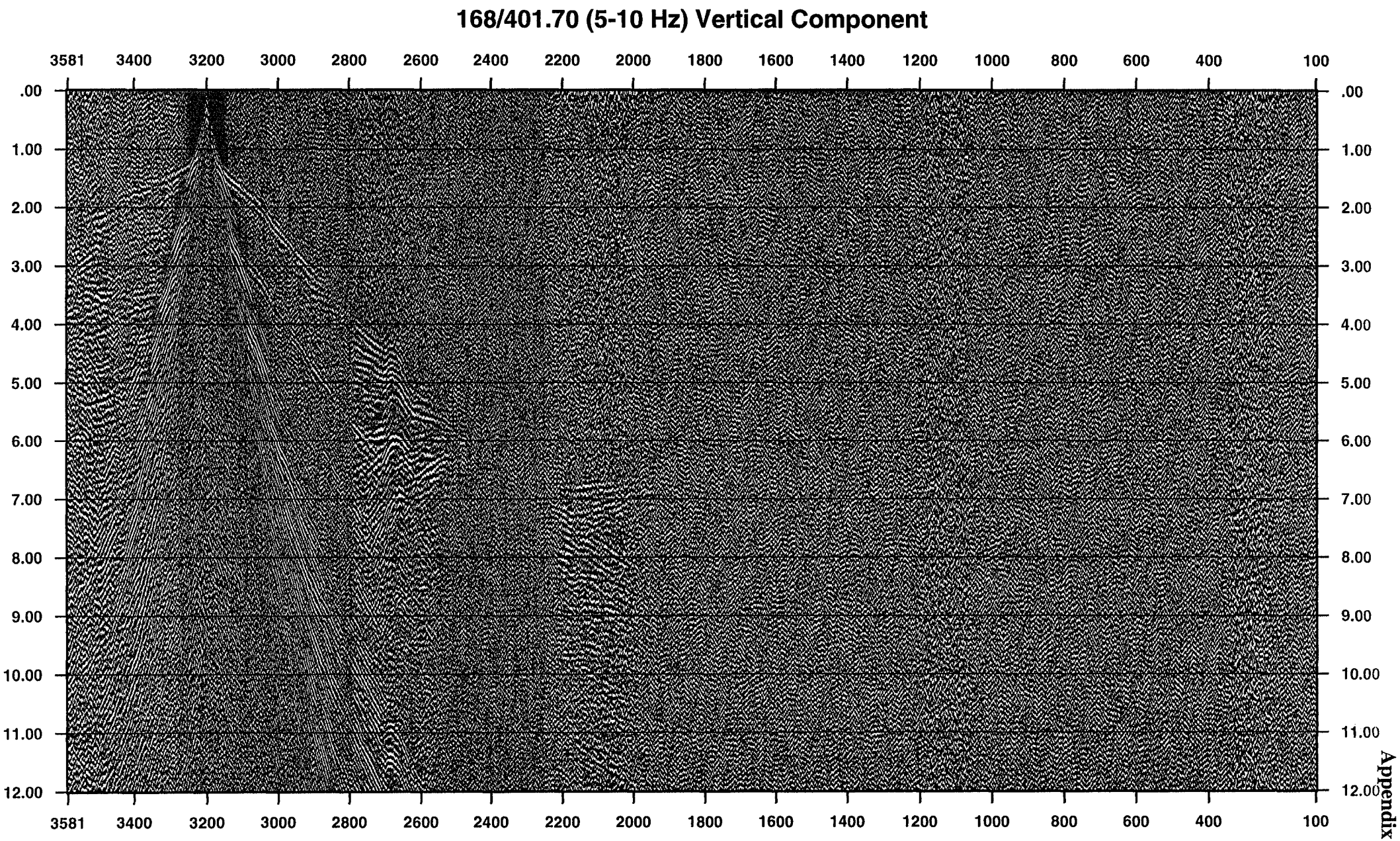
168/401.70 (5-10 Hz) Vertical Component
3581 3400 3200 3000 2800 2600 2400 2200 2000 1800 1600 1400 1200 1000 800 600 400 100
.00 1.00 2.00 3.00 4.00 5.00 6.00 7.00 8.00 9.00 10.00 11.00 12.00

Appendix 10

168/401.71 (5-10 Hz) Vertical Component

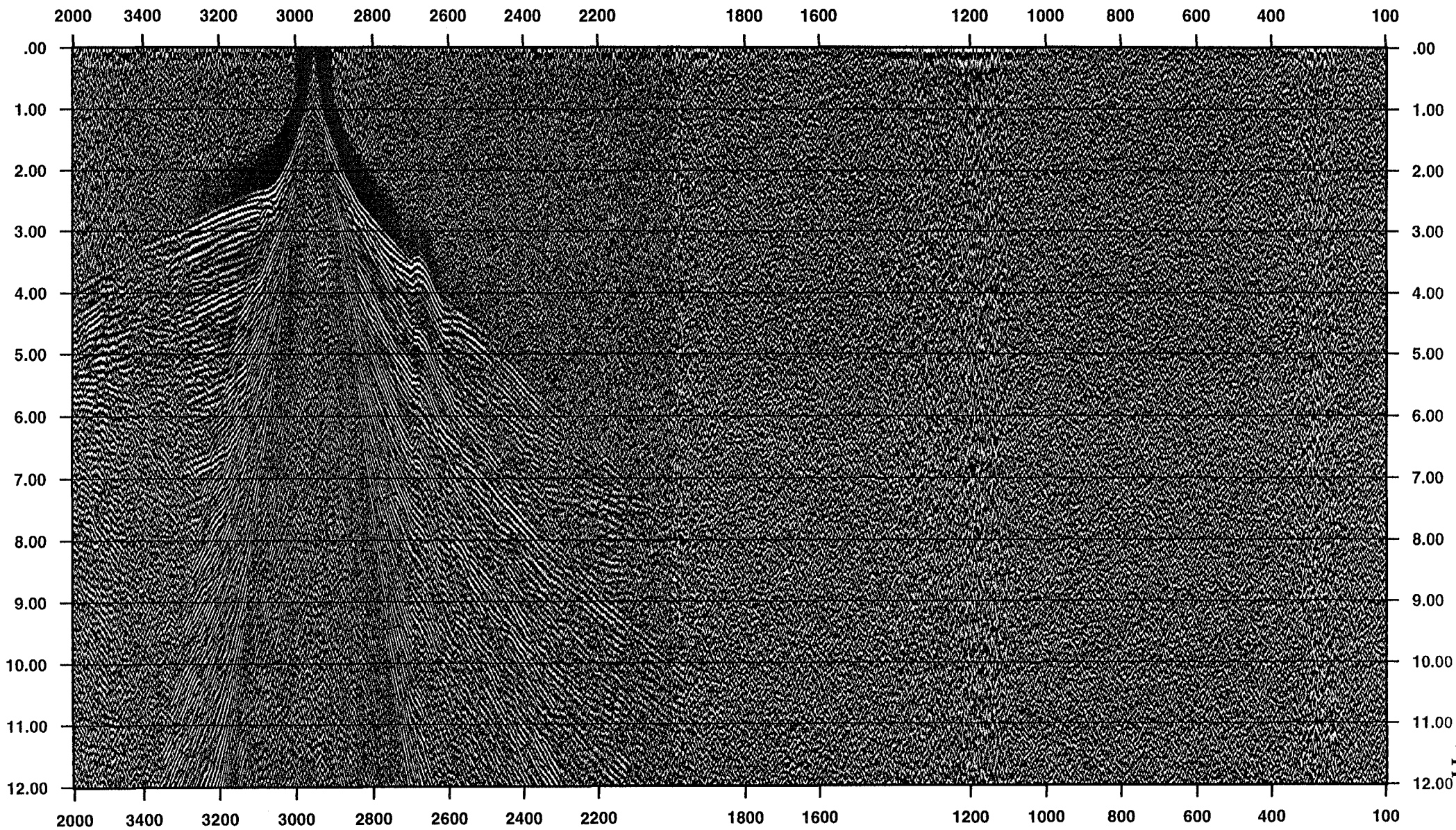

Appendix 10

168/401.72 (5-10 Hz) Vertical Component

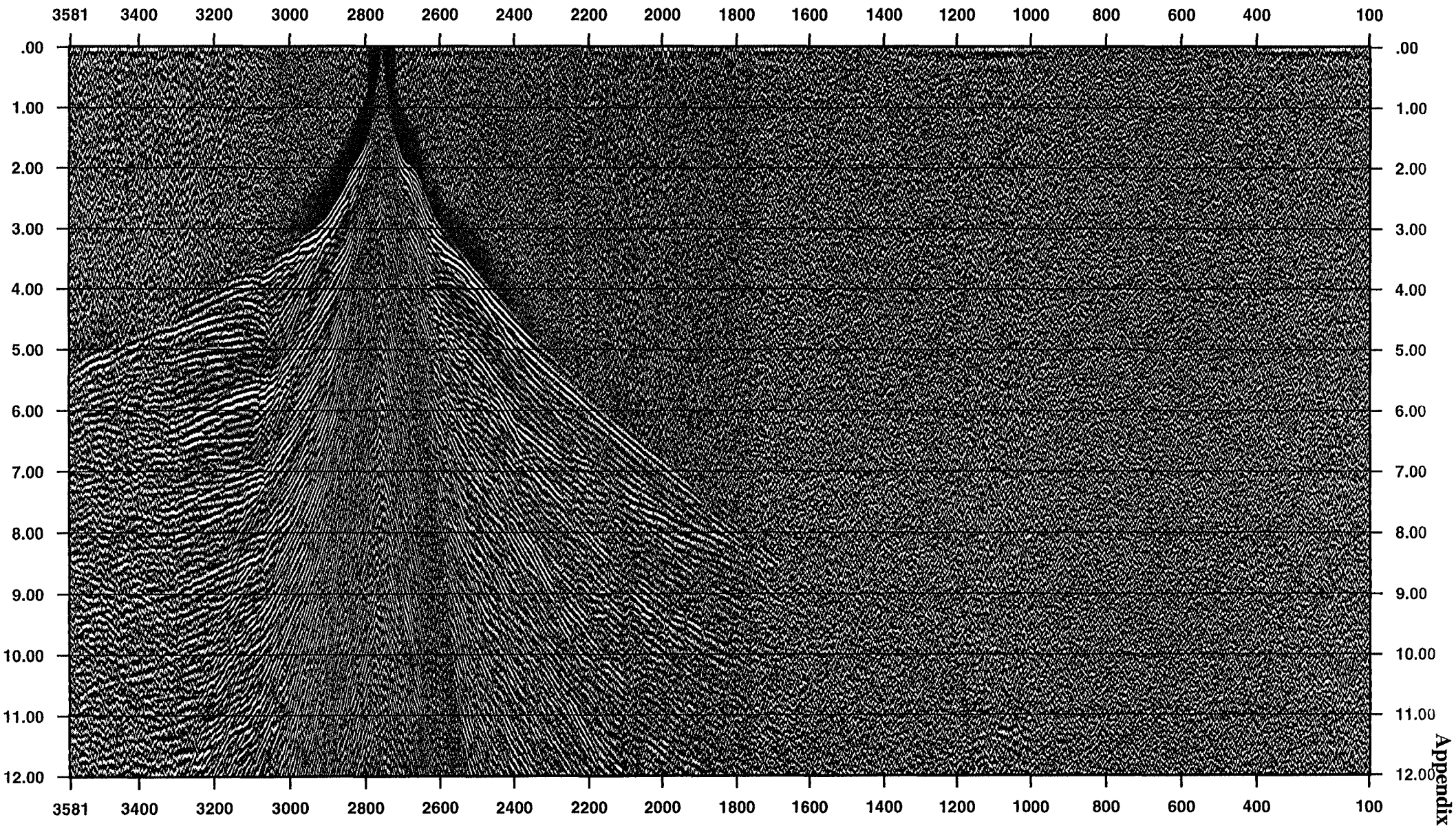

Appendix 10

168/401.73 (5-10 Hz) Vertical Component

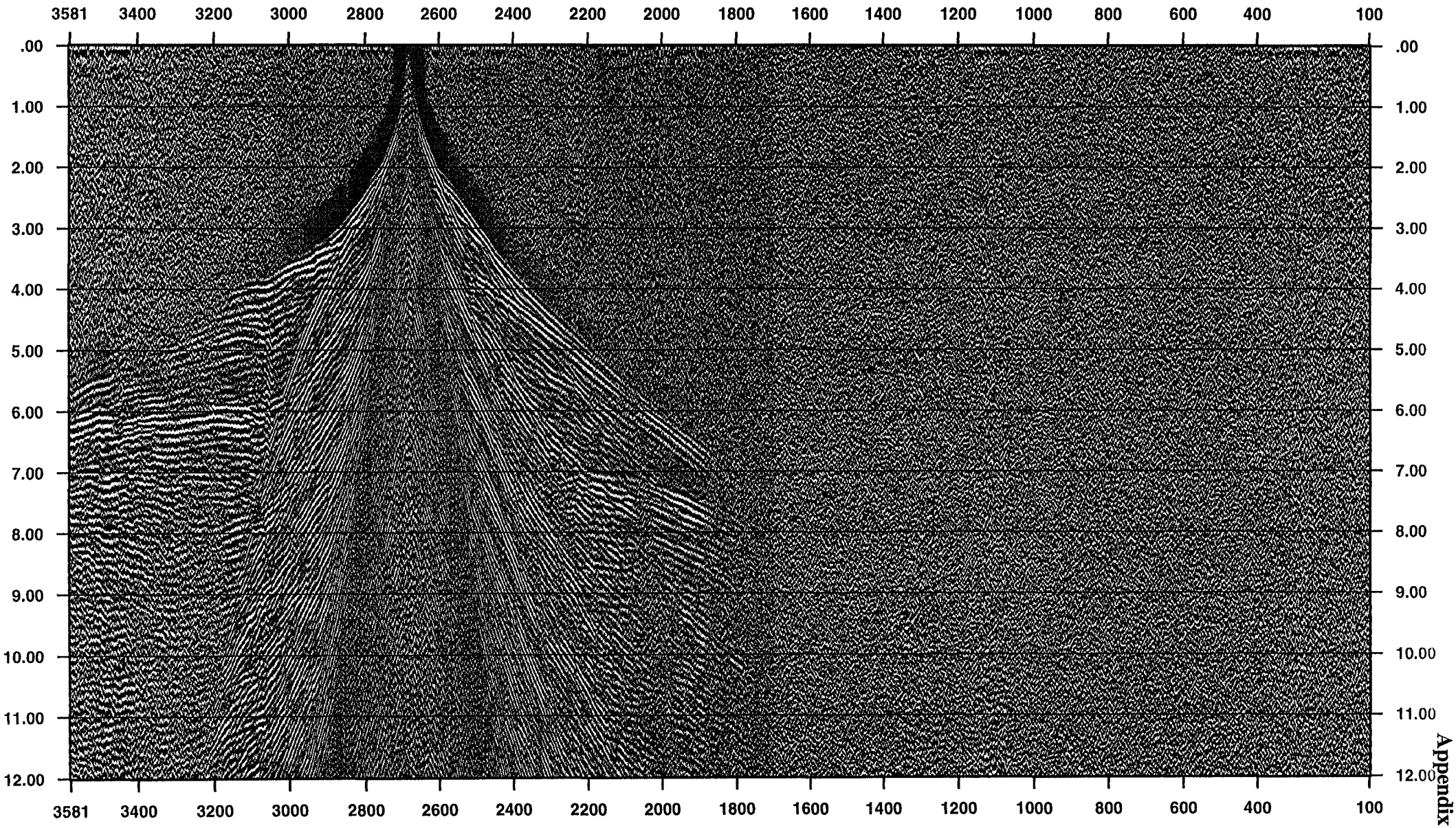

Appendix 10

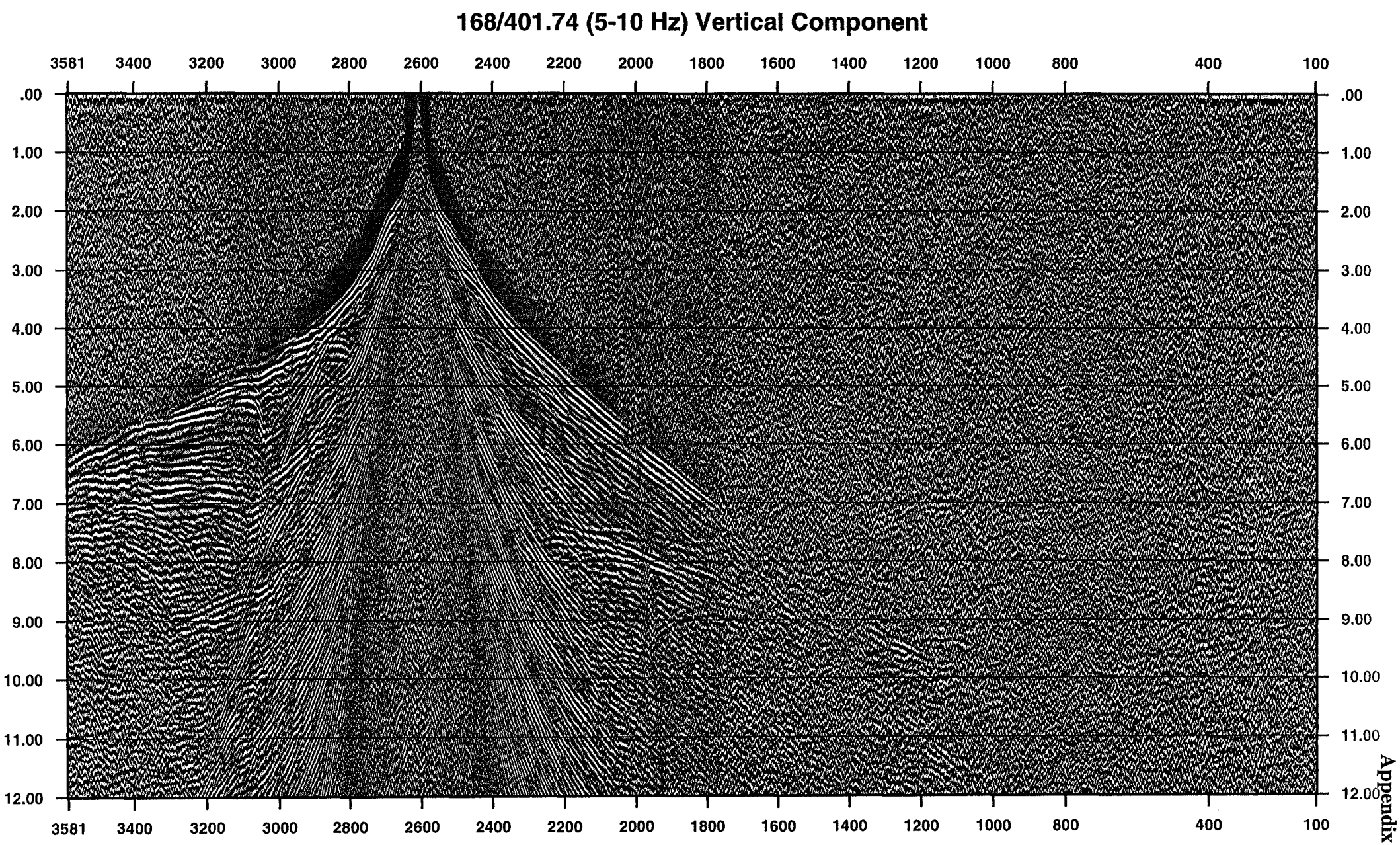
168/401.74 (5-10 Hz) Vertical Component
3581
3400
3200
3000
2800
2600
2400
2200
2000
1800
1600
1400
1200
1000
800
400
100
.00
1.00
2.00
3.00
4.00
5.00
6.00
7.00
8.00
9.00
10.00
11.00
12.00

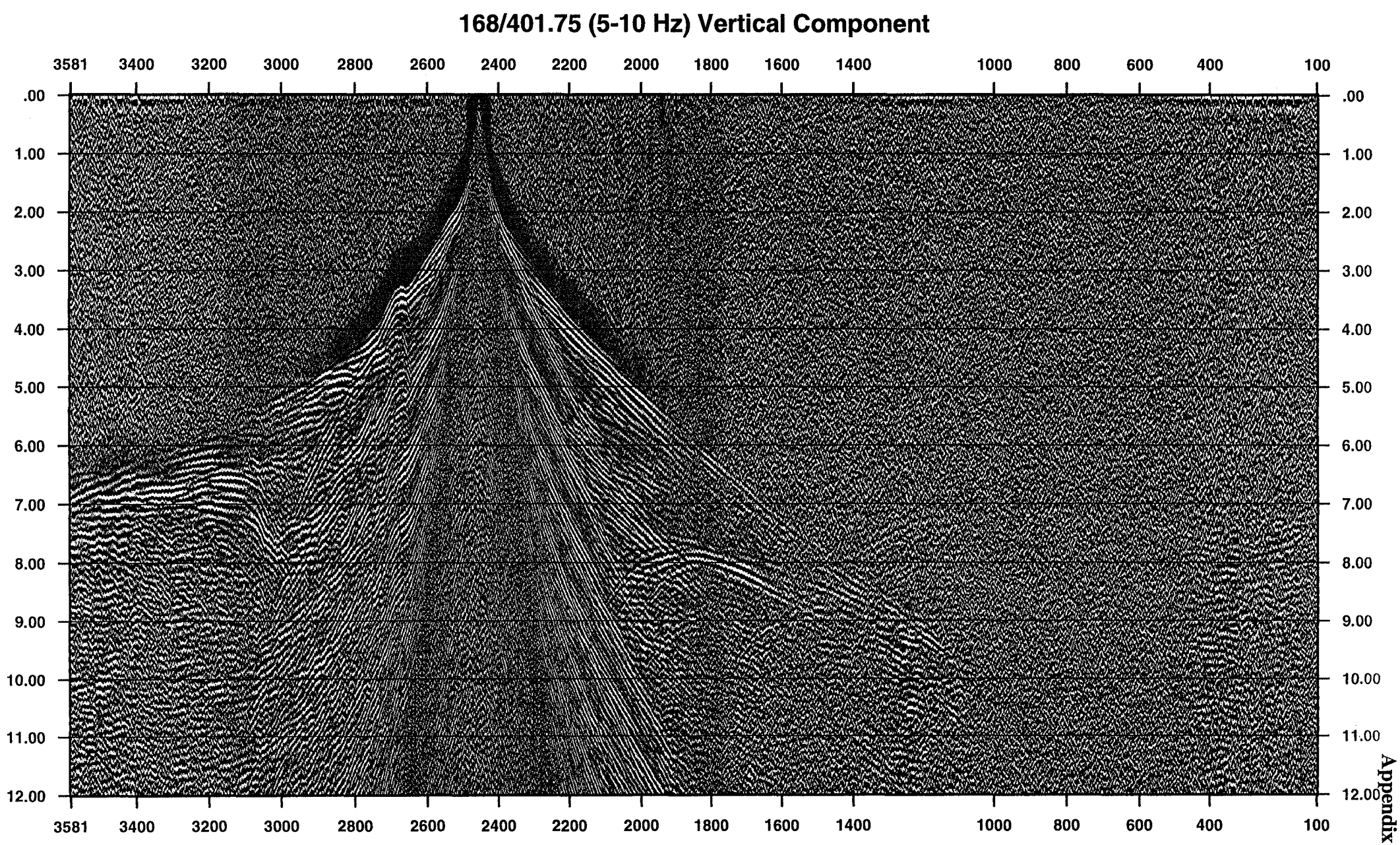
168/401.75 (5-10 Hz) Vertical Component
3581 3400 3200 3000 2800 2600 2400 2200 2000 1800 1600 1400 1000 800 600 400 100
.00 1.00 2.00 3.00 4.00 5.00 6.00 7.00 8.00 9.00 10.00 11.00 12.00

Appendix 10

168/401.76 (5-10 Hz) Vertical Component

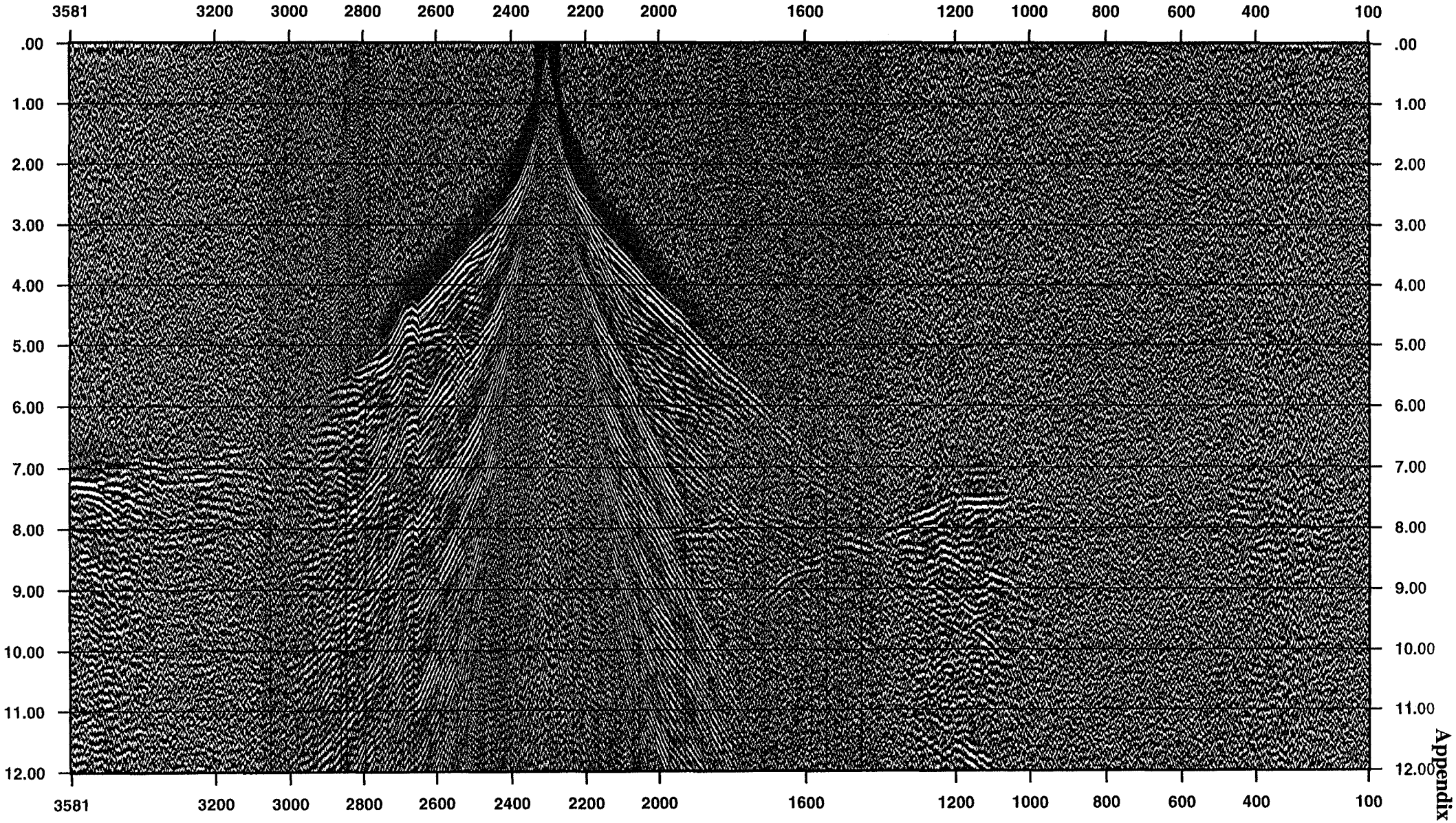

Appendix 10

168/401.77 (5-10 Hz) Vertical Component

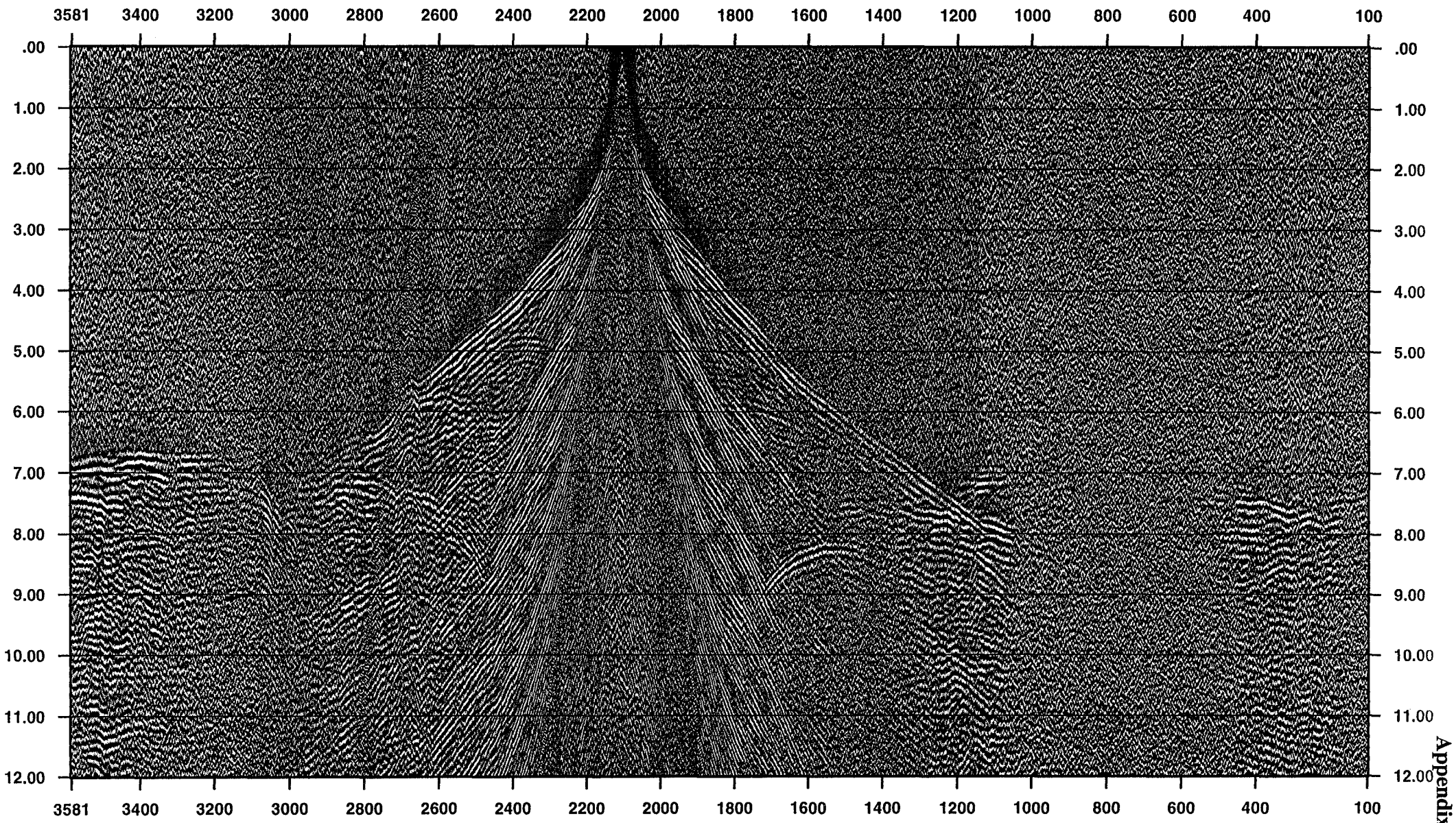

Appendix 10

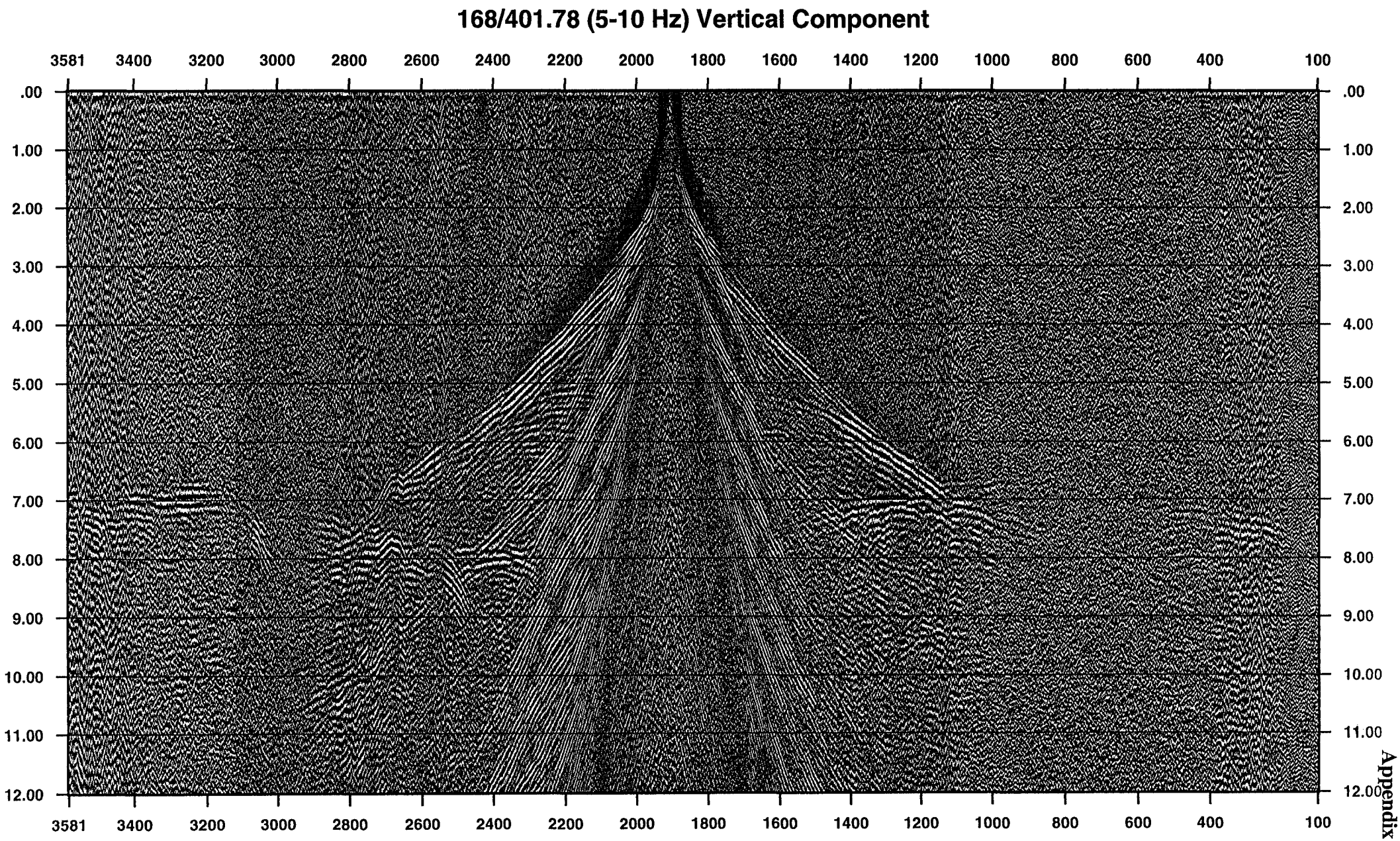
168/401.78 (5-10 Hz) Vertical Component
3581 3400 3200 3000 2800 2600 2400 2200 2000 1800 1600 1400 1200 1000 800 600 400 100
.00 1.00 2.00 3.00 4.00 5.00 6.00 7.00 8.00 9.00 10.00 11.00 12.00

Appendix 10

168/401.79 (5-10 Hz) Vertical Component

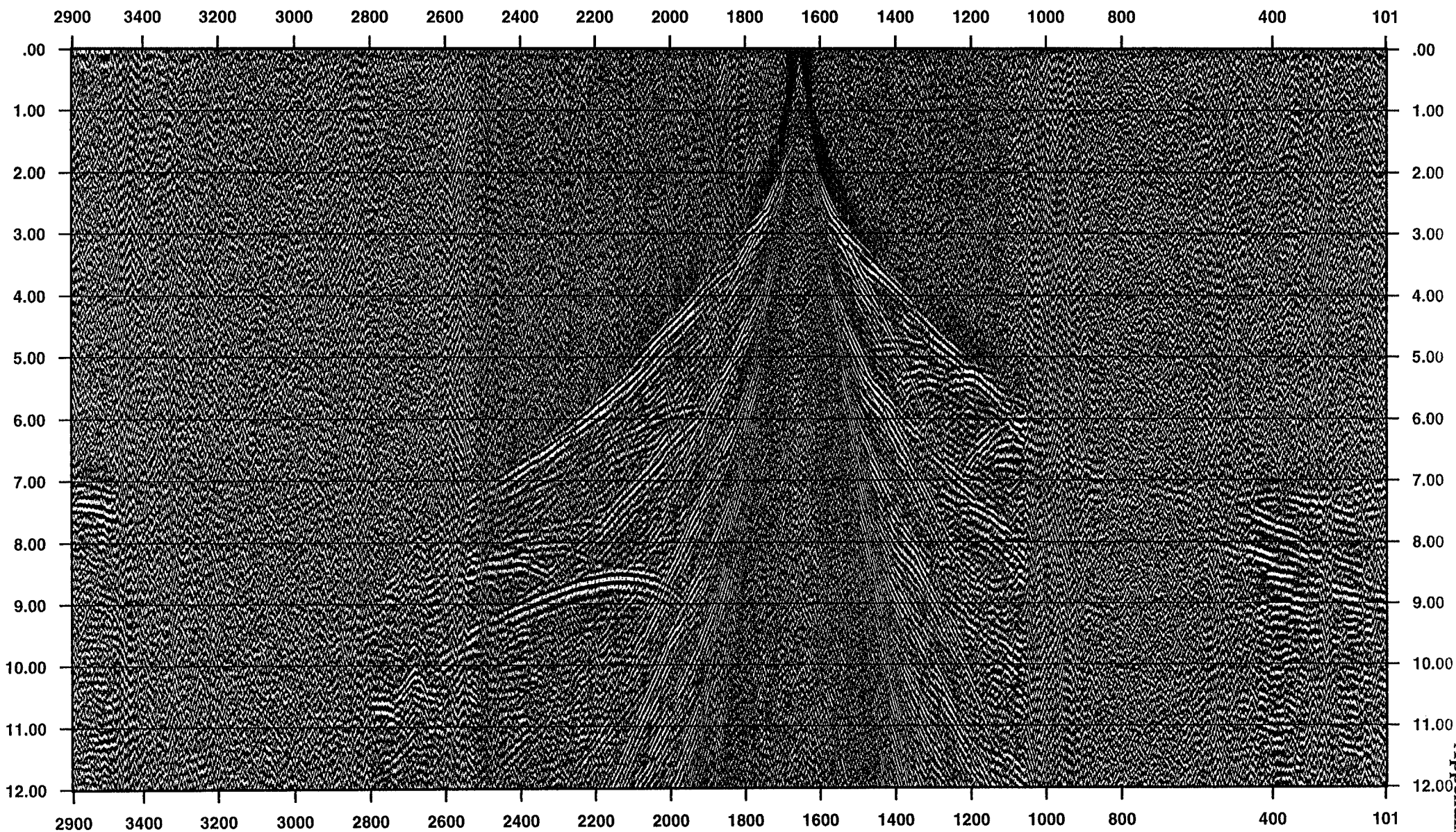

Appendix 10

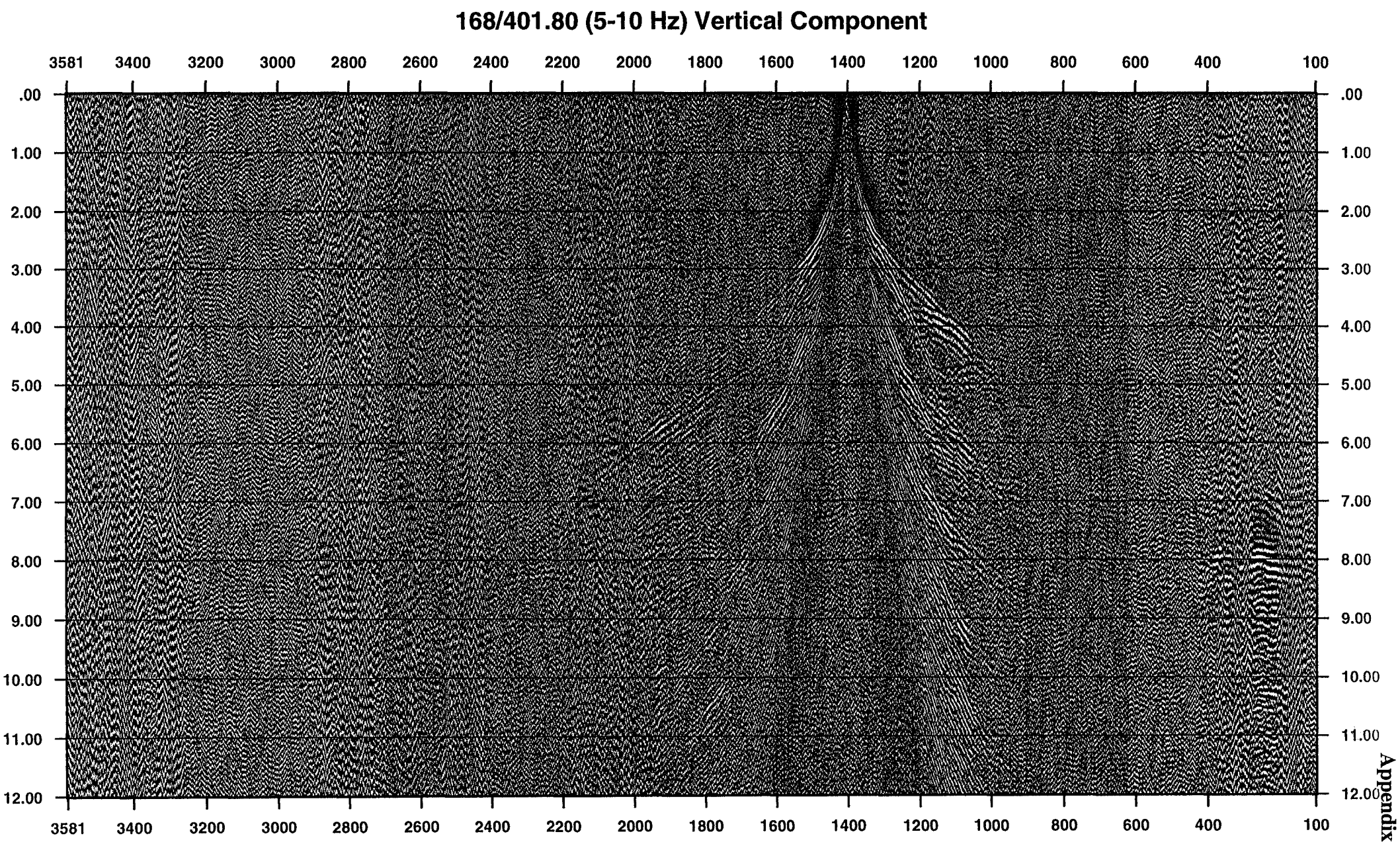
168/401.80 (5-10 Hz) Vertical Component
3581 3400 3200 3000 2800 2600 2400 2200 2000 1800 1600 1400 1200 1000 800 600 400 100
.00 1.00 2.00 3.00 4.00 5.00 6.00 7.00 8.00 9.00 10.00 11.00 12.00

168/401.81 (5-10 Hz) Vertical Component

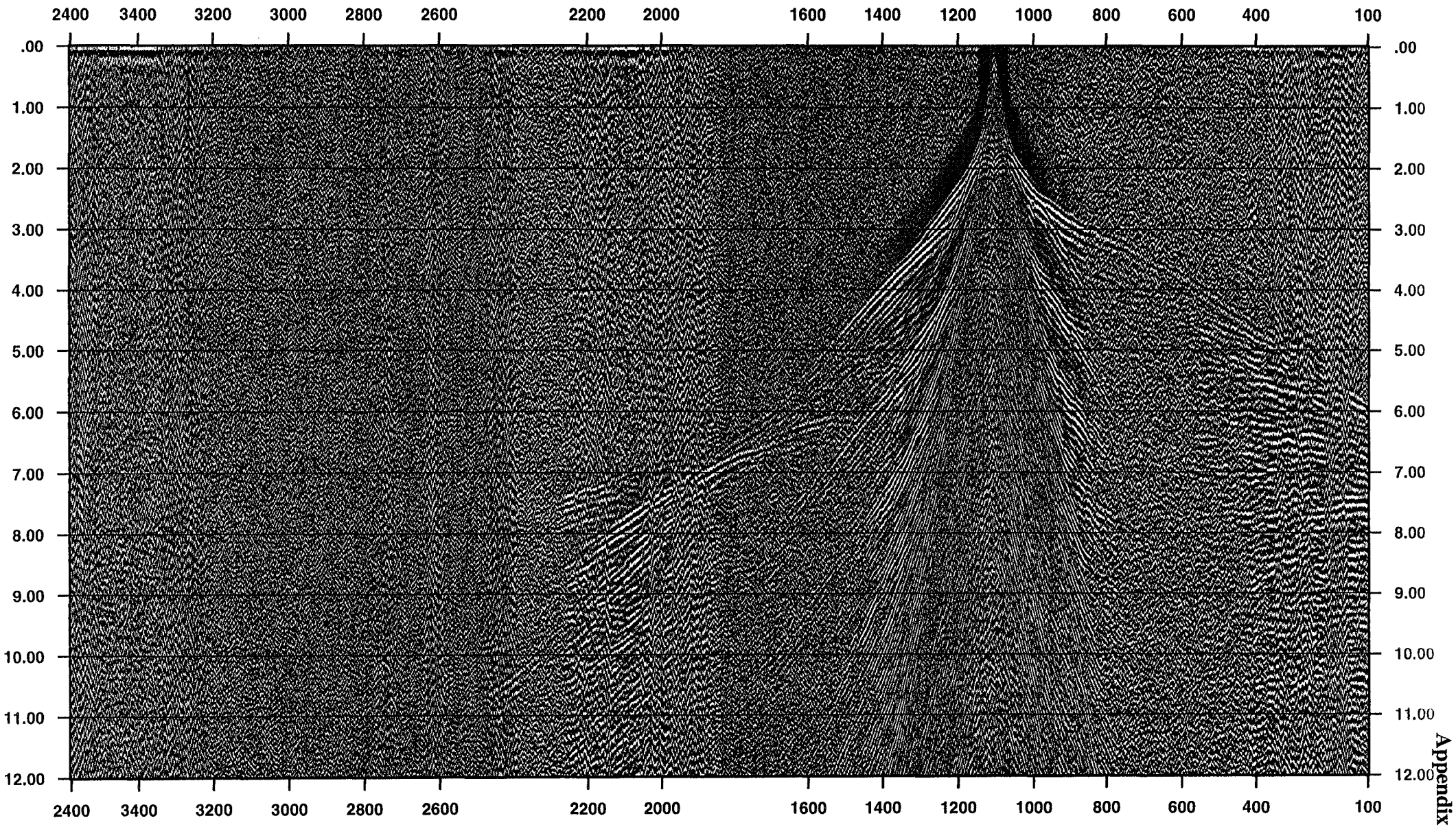

Appendix 10

168/401.82 (5-10 Hz) Vertical Component

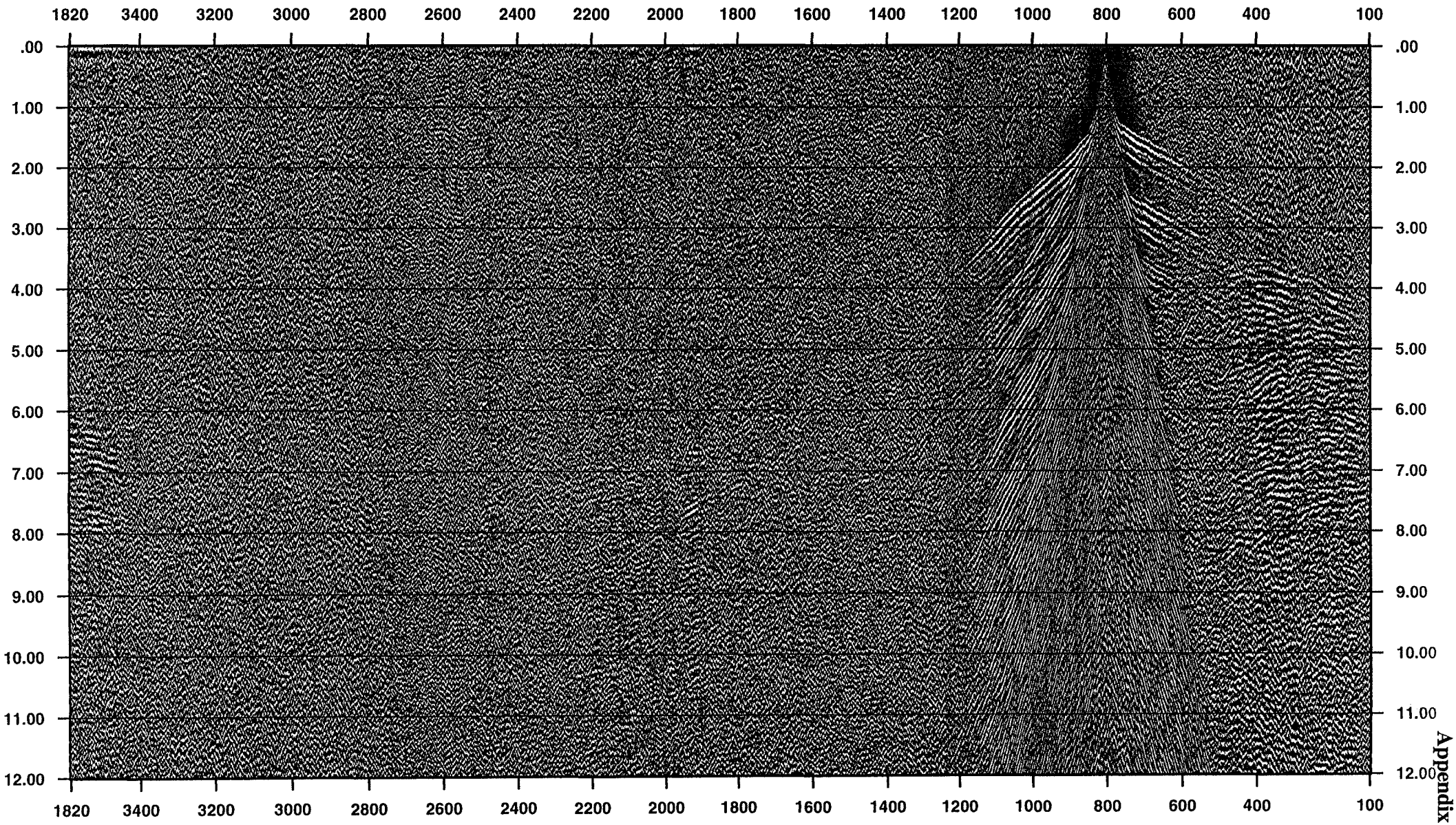

Appendix 10

168/401.83 (5-10 Hz) Vertical Component

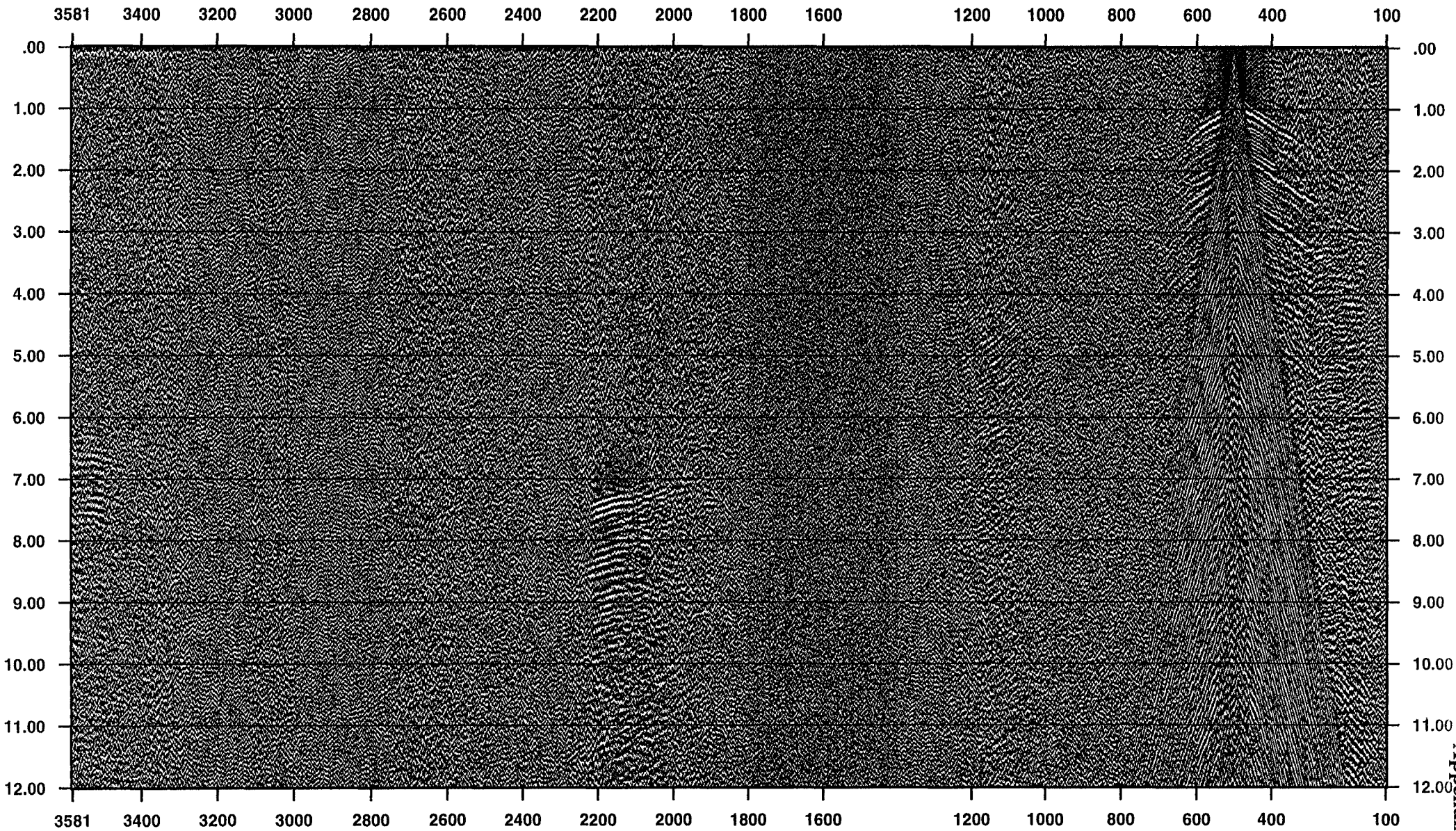

Appendix 10

Appendix 11

Comparison of arrivals picked before and after FK filtering

Comparison of arrivals picked before and after FK filtering
OBS 69

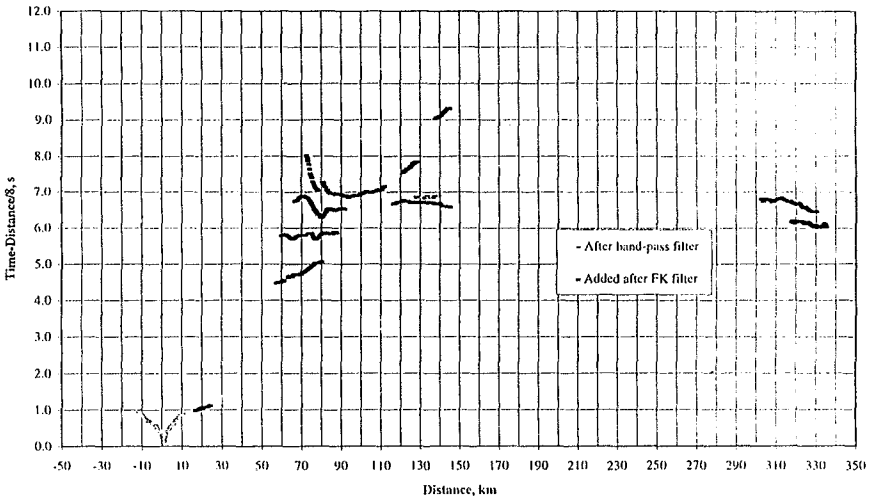

Comparison of arrivals picked before and after FK filtering
OBS 70

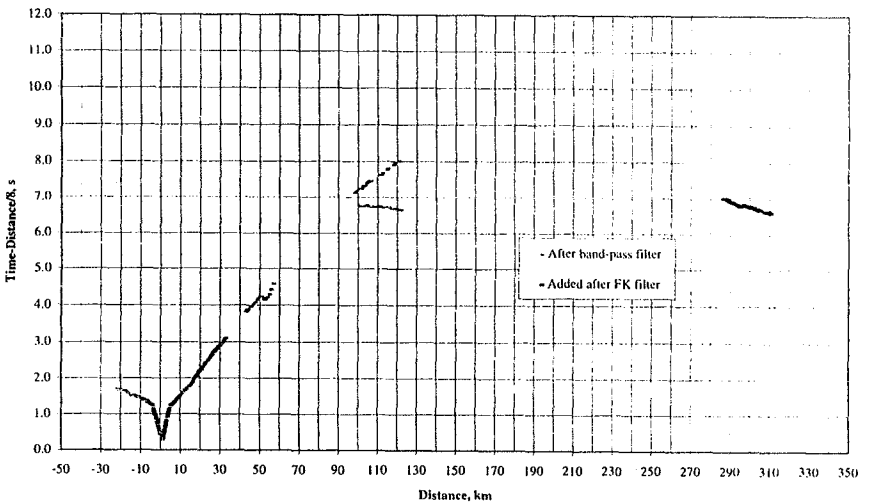

Comparison of arrivals picked before and after FK filtering
OBS 71

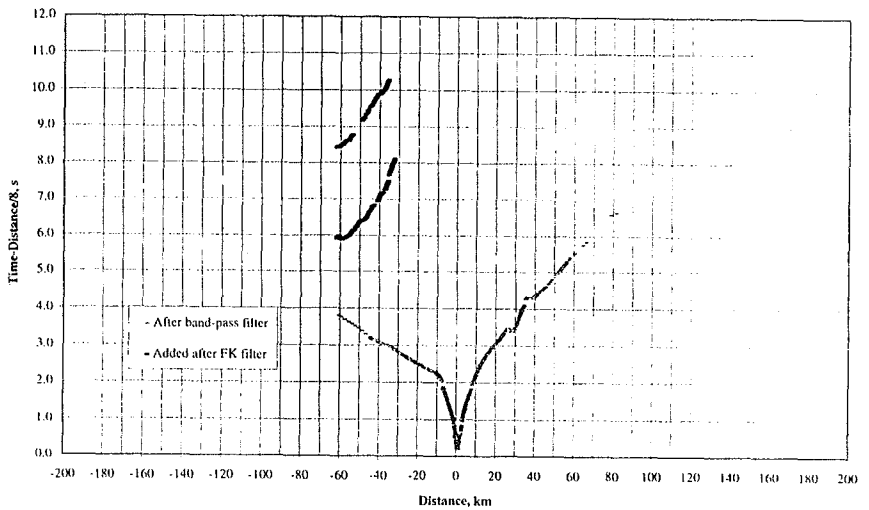

Comparison of arrivals picked before and after FK filtering
OBS 72

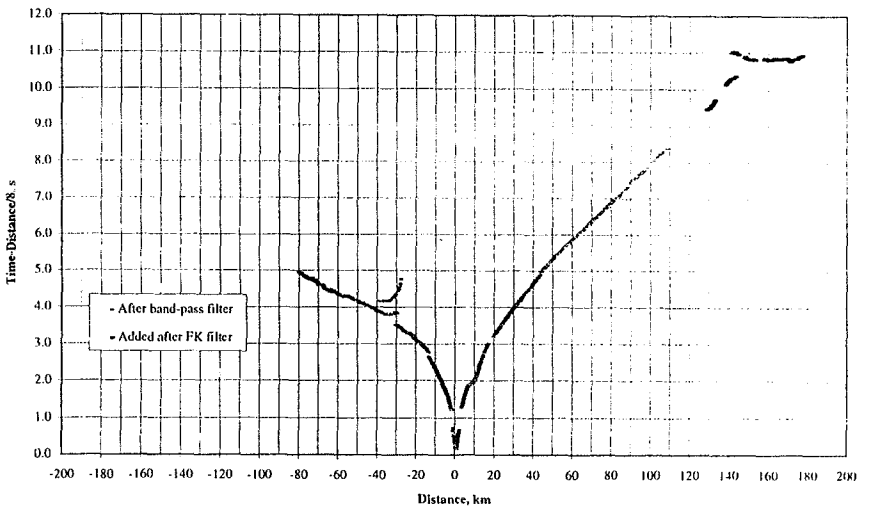

Comparison of arrivals picked before and after FK filtering
OBS 73

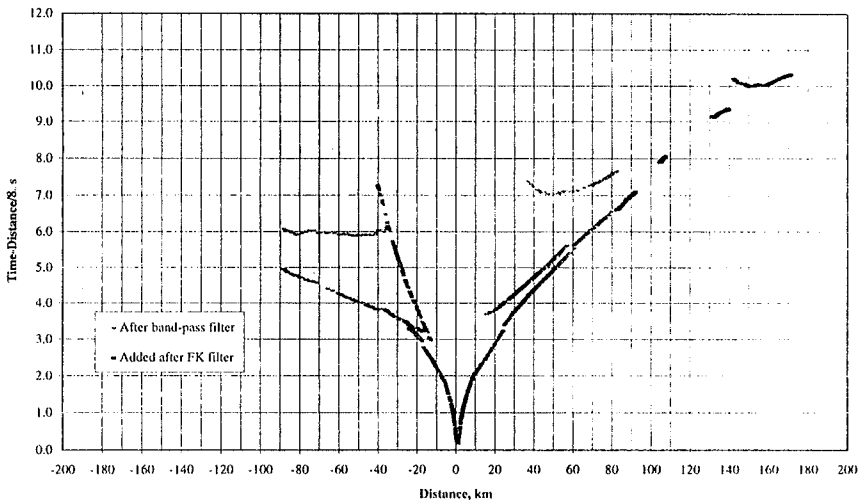

Comparison of arrivals picked before and after FK filtering
OBS 78

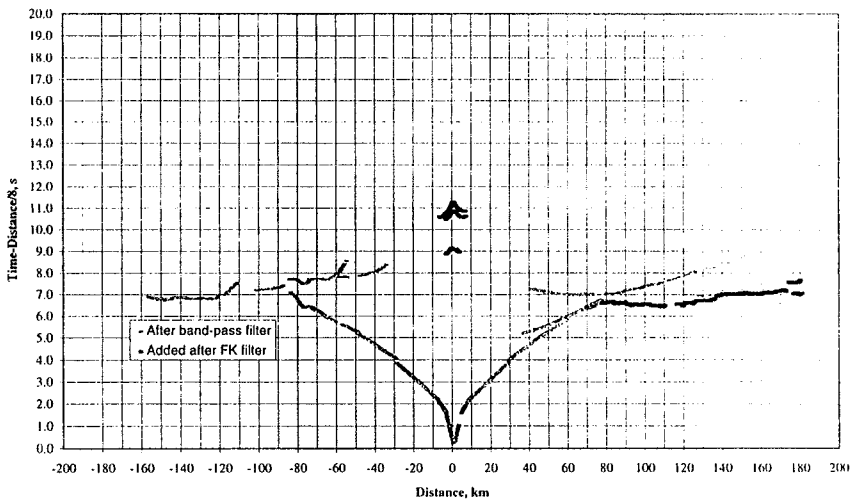

Comparison of arrivals picked before and after FK filtering
OBS 79

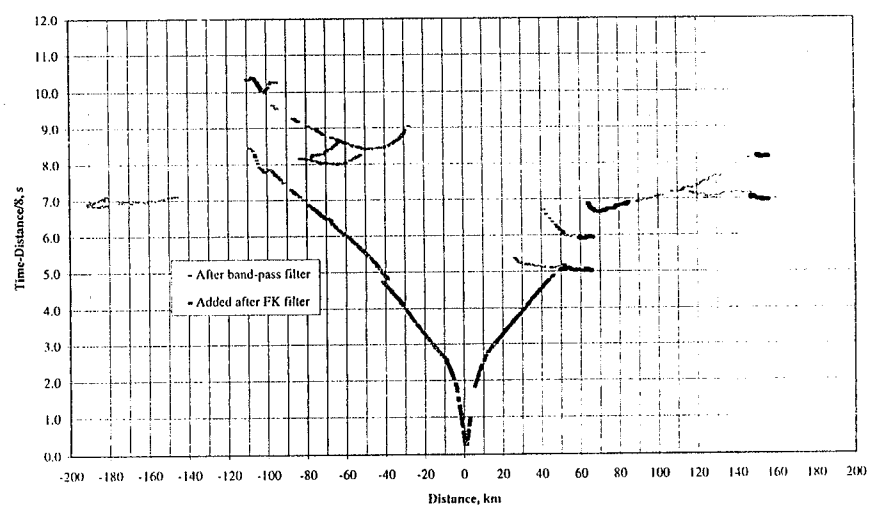

Comparison of arrivals picked before and after FK filtering
OBS 80

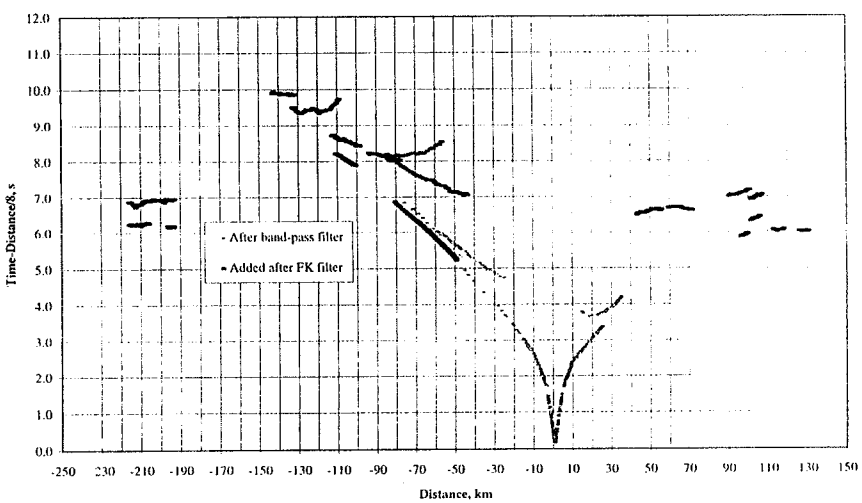

Comparison of arrivals picked before and after FK filtering
OBS 81

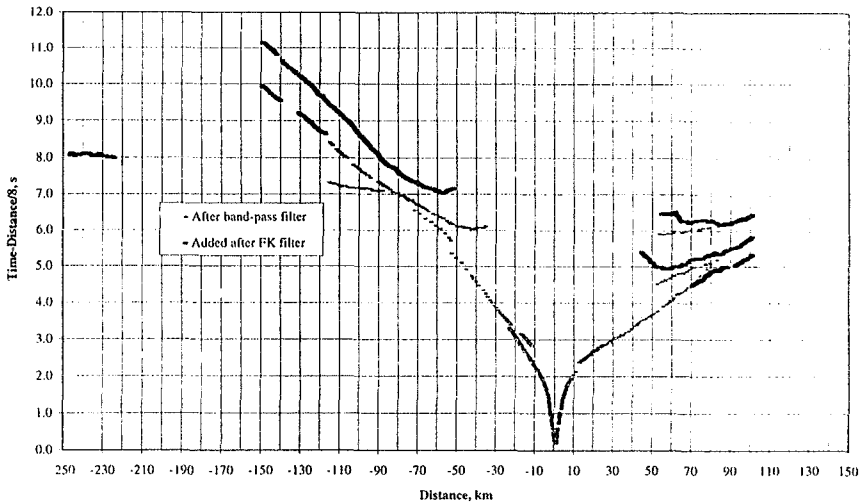

Comparison of arrivals picked before and after FK filtering
OBS 82

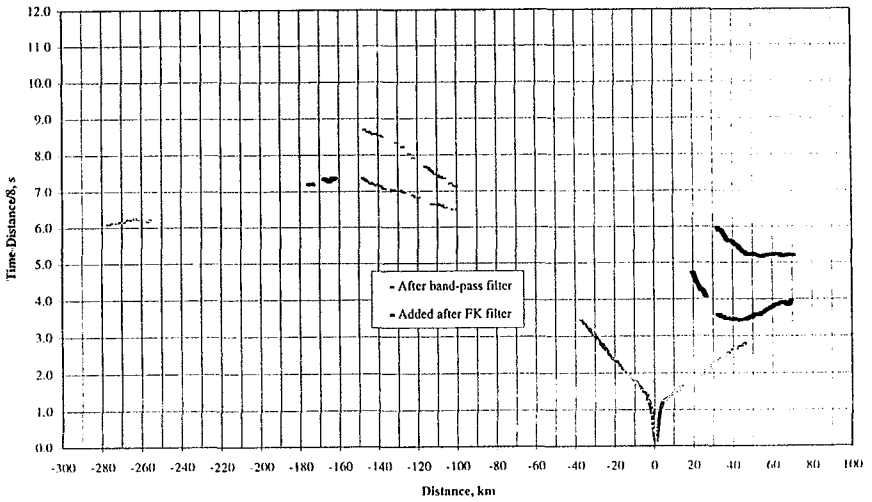

Comparison of arrivals picked before and after FK filtering
OBS 83